

PRODUCTION, CHARACTERIZATION, AND ELUCIDATION OF
STRUCTURE-FUNCTION RELATIONSHIP OF LACTOFERRICIN AND OTHER
PEPTIDES DERIVED FROM FOOD-GRADE BOVINE LACTOFERRIN

by

JUDY CHUK KWAN CHAN

B. Sc., The University of British Columbia, 1997

M. Sc., The University of British Columbia, 1999

A THESIS SUBMITTED IN PARTIAL FULFILMENT OF THE REQUIREMENTS FOR
THE DEGREE OF

DOCTOR OF PHILOSOPHY

in

THE FACULTY OF GRADUATE STUDIES

(Food Science)

THE UNIVERSITY OF BRITISH COLUMBIA

September 2006

© Judy Chuk Kwan Chan, 2006

Abstract

Lactoferricin (Lfcin), a cationic antimicrobial peptide, was purified by peptic digestion of food grade bovine lactoferrin (LF) followed by fractionation on an industrial grade cation exchange resin with stepwise salt gradient elution. A 2-step process using competitive displacement cation exchange chromatography led to 35% recovery of peptides with masses of 3124 and 3196 Da corresponding to Lfcin. Other cationic peptides produced concurrently with Lfcin were tentatively identified. Varying iron saturation levels of LF had no effect on the production of Lfcin. Two approaches were used to understand how Lfcin acts as an antimicrobial agent. Homology Similarity Analysis (HSA) was used to evaluate the impact of peptide pattern similarities of various Lfcin derivatives on their effects as antimicrobial agents. Helical property of residues 4-9 in the Lfcin sequence was the most important in determining the antimicrobial activity of Lfcin against *Escherichia coli*, followed by cationic charge pattern of residues 4-9 and residues 1-3. Raman spectroscopy in the C-H stretching ($2800-3000\text{ cm}^{-1}$) region was used to study interactions between Lfcin and bacterial membrane models. Presence of Lfcin in 1,2-dipalmitoyl-*sn*-glycerol-3-phosphocholine (DPPC) multilamellar liposomes restricted the lateral chain-chain interaction along the acyl chain throughout the temperature range examined, and increased the main transition temperature (T_m) from 38-40 °C. Lfcin had little effect on 1,2-dipalmitoyl-*sn*-glycerol-3-[phosphor-*rac*-(1-glycerol)] (DPPG) liposomes at temperatures below the T_m . In contrast, mobility of the acyl chains in 1,2-dipalmitoyl-*sn*-glycerol-3-phosphoethanolamine (DPPE) was increased in the presence of Lfcin at temperatures below 32 °C. Although Lfcin had little effect on the zwitterionic unsaturated phospholipids, 1-palmitoyl-2-oleoyl-*sn*-glycerol-3-phosphocholine (POPC) and 1-palmitoyl-2-oleoyl-*sn*-glycerol-3-phosphoethanolamine (POPE), Lfcin lowered the lateral chain-chain interaction along the acyl chains of negatively charged 1-palmitoyl-2-oleoyl-*sn*-glycerol-3-[phosphor-*rac*-(1-glycerol)] (POPG). Raman spectral analyses also showed that the removal of arginine promoted interactions of Lfcin derivatives with hydrophobic acyl chains and methyl ends of negatively charged DPPG liposomes. Furthermore, addition of two extra tryptophan residues in Lfcin derivatives stabilized acyl chains and methyl ends in DPPE liposomes. HSA and Raman spectroscopy are two useful tools for understanding the antimicrobial mechanisms of Lfcin and will facilitate the application and utilization of Lfcin as a naturally occurring antimicrobial agent.

Table of Contents

Abstract	ii
Table of Contents	iii
List of Tables	vii
List of Figures	ix
List of Abbreviations	xi
Acknowledgements	xii
Dedication	xiii
Co-Authorship Statements	xiv
CHAPTER 1. GENERAL INTRODUCTION AND LITERATURE REVIEW.....	1
1.1. Lactoferrin	1
1.1.1. Sources of Lactoferrin	1
1.1.2. Structure of Lactoferrin.....	1
1.1.3. Biological Functions of Lactoferrin	2
1.1.3.1. Antimicrobial Properties of Lactoferrin.....	2
1.1.3.2. Antiviral Functions of Lactoferrin	3
1.1.3.3. Other Biological Functions of Lactoferrin.....	3
1.1.3.4. Other Functions of Lactoferrin	4
1.2. Lactoferricin & Its Derivatives	5
1.2.1. Production and Purification of Lactoferricin and Related Peptides.....	5
1.2.1.1. Discovering Lactoferricin	5
1.2.1.2. Identifying Lactoferricin.....	5
1.2.1.3. Production and Purification Strategies	6
1.2.2. Antimicrobial Spectrum of Lactoferricin and Related Peptides.....	8
1.2.3. Structure – Function Relationship Analysis of Lactoferricin and Its Derivatives	8
1.2.3.1. Basic Structural Properties of Bovine Lactoferricin	8
1.2.3.2. Roles of Secondary Structure.....	9
1.2.3.3. Roles of Basic Amino Acids.....	10
1.2.3.4. Roles of Hydrophobic Amino Acids	11
1.3. Cationic Antimicrobial Peptides	12
1.3.1. Structures and Modes of Action of Other Cationic Antimicrobial Peptides.....	12
1.3.2. Proposed Antimicrobial Mechanisms of Lactoferricin	13
1.4. Phospholipid Bilayer	14
1.5. Raman Spectroscopy	15
1.5.1. Raman Spectroscopy: Structure – Function Relationship of Proteins.....	15
1.5.2. Raman Spectroscopy: Structure – Function Relationship of Peptides and Phospholipid Bilayers.....	16
1.6. Multivariate Data Analysis Techniques	17
1.6.1. Principal Component Analysis	18
1.6.2. Partial Least Square Regression	18
1.6.3. Principal Component Similarity Analysis.....	18

1.6.4.	Multivariate Data Analysis: Structure – Function Relationship of Lactoferricin and Its Derivatives.....	20
1.7.	Hypotheses.....	22
1.8.	Objectives.....	22
1.9.	References.....	30
CHAPTER 2. PRODUCTION OF LACTOFERRICIN AND OTHER CATIONIC PEPTIDES FROM FOOD GRADE BOVINE LACTOFERRIN WITH VARYING IRON SATURATION LEVELS		39
2.1.	Introduction.....	39
2.2.	Materials and Methods.....	40
2.2.1.	Preparation of Lactoferrin with Varying Iron Saturation Levels.....	40
2.2.2.	Digestion of Lactoferrin	40
2.2.3.	Purification of Lactoferricin and Other Peptides.....	40
2.2.4.	Peptide Mass Analysis	41
2.2.5.	Identification of Peptide Sequences.....	41
2.2.6.	Iron Content in Lactoferrins.....	41
2.2.7.	Protein Structure by Raman Spectroscopy.....	41
2.3.	Results.....	42
2.3.1.	Production of Lactoferricin and Other Cationic Peptides from Lactoferrin.....	42
2.3.2.	A Two-Step Process for Lactoferricin Isolation.....	42
2.3.3.	The Identification of Lactoferricin and Other Cationic Peptides.....	43
2.3.4.	Effects of Iron Saturation Levels of Lactoferrin.....	44
2.4.	Discussion.....	44
2.4.1.	Production of Lactoferricin and Other Cationic Peptides from Lactoferrin.....	44
2.4.2.	Identification of Other Cationic Bioactive Peptides	46
2.4.3.	Effects of Iron Saturation Levels of Lactoferrin.....	47
2.5.	References.....	60
CHAPTER 3. HOMOLOGY SIMILARITY ANALYSIS OF SEQUENCES OF LACTOFERRICIN AND ITS DERIVATIVES.....		62
3.1.	Introduction.....	62
3.2.	Materials and Methods.....	63
3.2.1.	Lactoferricin Sequences.....	63
3.2.2.	Peptide Property Scales.....	63
3.2.3.	Homology Similarity Analysis (HSA).....	63
3.2.4.	Principal Component Similarity (PCS) Analysis.....	64
3.2.5.	Artificial Neural Networks (ANN).....	64
3.3.	Results.....	64
3.3.1.	Homology Similarity Analysis of Lactoferricin Sequences.....	64

3.3.2.	Principal Component Similarity Analysis.....	65
3.3.3.	Regression Analysis Using Artificial Neural Networks.....	66
3.4.	Discussion.....	66
3.5.	References.....	81
CHAPTER 4. RAMAN SPECTROSCOPIC STUDY OF THE EFFECTS OF LACTOFERRICIN ON THERMAL TRANSITIONS OF PHOSPHOLIPIDS IN LIPOSOMES.....		83
4.1.	Introduction.....	83
4.2.	Materials and Methods.....	84
4.2.1.	Materials.....	84
4.2.2.	Preparation of Liposomes.....	85
4.2.3.	Raman Spectroscopy.....	85
4.2.4.	Raman Spectral Analysis.....	85
4.3.	Results.....	86
4.4.	Discussion.....	88
4.4.1.	Temperature-induced Changes in Raman Spectra of Model Membranes.....	88
4.4.2.	Effects of Lactoferricin on Model Membranes.....	91
4.5.	References.....	98
CHAPTER 5. RAMAN SPECTROSCOPIC STUDY OF THE EFFECTS OF LACTOFERRICIN DERIVATIVES ON PHOSPHOLIPID LIPOSOMES.....		101
5.1.	Introduction.....	101
5.2.	Materials and Methods.....	102
5.2.1.	Materials.....	102
5.2.2.	Preparation of Liposomes.....	103
5.2.3.	Raman Spectroscopy.....	103
5.2.4.	Raman Spectral Analysis.....	103
5.2.5.	Properties of Lactoferricin Derivatives.....	103
5.3.	Results.....	103
5.3.1.	Effects of Lactoferricin Derivatives on DPPC Liposomes.....	103
5.3.2.	Effects of Lactoferricin Derivatives on DPPG Liposomes.....	104
5.3.3.	Effects of Lactoferricin Derivatives on DPPE Liposomes.....	105
5.4.	Discussion.....	106
5.4.1.	Effects of Arginine on Lactoferricin on the Thermal Behaviour of Phospholipid Liposomes.....	106
5.4.2.	Effects of Tryptophan on the Thermal Behaviour of Lactoferricin of Phospholipid Liposomes.....	107
5.4.3.	Effects of Peptide Length on the Thermal Behaviour of Lactoferricin of Phospholipid Liposomes.....	109
5.4.4.	Proposed Antimicrobial Actions.....	110

5.5. References.....	117
CHAPTER 6. CONCLUSION.....	120
6.1. Review of Results as Related to Working Hypotheses	120
6.2. Strengths and Significance of Results to the Field of Study.....	121
6.3. Recommendations for Future Studies	121
6.4. References.....	123

List of Tables

Table 1.1. Percentage of phosphatidylcholine (PC), phosphatidylethanolamine (PE), phosphatidylglycerol (PG), and 1,3-bis(sn-3-phosphatidyl)-sn-glycerol (cardiolipin, CL) in bacterial membranes.....	29
Table 2.1. Possible cationic peptides produced from the peptic digestion of bovine lactoferrin at 37 °C for 4 hours at pH 2.0. Cationic amino acids are indicated in bold.	58
Table 2. 2. Secondary structure of bovine lactoferrin preparations (LF) at pH 2.0 as determined using Raman spectroscopy in this study and human lactoferrin (LFH) as reported in the literature.	59
Table 3.1. Homology similarity coefficient and average property values for helix (Hx), charge (Ch), hydrophobicity (Hp) and bulkiness (Bk) calculated for three segments in the sequences of Group I lactoferricin derivatives, with minimum inhibitory concentrations (MIC) against <i>E. coli</i> as reported in the literature. Segment I = position 1-3, Segment II = position 4-9, and Segment III = position 10-15 in the reference (Peptide 13) with 15-amino acid sequence identical to bovine lactoferricin. Shaded zones in the sequences represent regions with high similarity to the reference peptide, while the shading of Hx II indicates the high similarity coefficient for helix propensity in Segment II for Group I derivatives. Peptide #13 was used as the reference peptide and its values were shaded for easy comparison.....	69
Table 3.2. Homology similarity coefficient and average property values for helix (Hx), charge (Ch), hydrophobicity (Hp) and bulkiness (Bk) calculated for three segments in the sequences of Group II lactoferricin derivatives, with minimum inhibitory concentrations (MIC) against <i>E. coli</i> as reported in the literature. Segment I = position 1-3, Segment II = position 4-9, and Segment III = position 10-15 in the reference (Peptide 13) with 15-amino acid sequence identical to bovine lactoferricin. Shaded zones in the sequences represent regions with high similarity to the reference peptide, while the shading of Ch I indicates the high average values for charge in Segment I characteristic of Group II derivatives.	71
Table 3.3. Homology similarity coefficient and average property values for helix (Hx), charge (Ch), hydrophobicity (Hp) and bulkiness (Bk) calculated for three segments in the sequences of Group III lactoferricin derivatives, with minimum inhibitory concentrations (MIC) against <i>E. coli</i> as reported in the literature. Segment I = position 1-3, Segment II = position 4-9, and Segment III = position 10-15 in the reference (Peptide 13) with 15-amino acid sequence identical to bovine lactoferricin. Shaded zones in the sequences represent regions with high similarity to the reference peptide. Group III derivatives included exceptional cases with unexplained high or low MIC values.	72
Table 3.4. Homology similarity coefficient and average propensity values for helix (Hx), charge (Ch), hydrophobicity (Hp) and bulkiness (Bk) calculated for three segments in the sequences of Group IV lactoferricin derivatives, with minimum inhibitory concentrations (MIC) against <i>E. coli</i> as reported in the literature. Segment I = position 1-3, Segment II = position 4-9, and Segment III = position 10-15 in the reference (Peptide 13) with 15-amino acid sequence identical to bovine lactoferricin. Shaded zones in the sequences represent regions with high similarity to the reference peptide, while the shading of Ch II indicates low similarity coefficient and average values of charge in Segment II of Group IV derivatives.....	73
Table 3.5. Homology similarity coefficient and average property values for helix (Hx), charge (Ch), hydrophobicity (Hp) and bulkiness (Bk) calculated for three segments in the sequences of Group V lactoferricin derivatives, with minimum inhibitory concentrations	

(MIC) against *E. coli* as reported in the literature. Segment I = position 1-3, Segment II = position 4-9, and Segment III = position 10-15 in the reference (Peptide 13) with 15-amino acid sequence identical to bovine lactoferricin. Shaded zones in the sequences represent regions with high similarity to the reference peptide, while the shading of HxII indicates low similarity coefficient values for helix propensity in Segment II of Group V derivatives. 75

Table 3.6. Amino acid structural propensity values used for Homology Similarity Analysis (HSA). 77

Table 3.7. Loadings of input variables, homology similarity constant (SimCnst, determined using homology similarity analysis, HSA) and Average (Ave) of Helical Propensity in position 4 to 9, charge in position 4 to 9, charge in position 1 to 3, and charge in position 10 to 15, determined by Principal Component Analysis (PCA). 78

Table 5.1. Structural properties of lactoferricin derivatives used in the study. 116

List of Figures

Figure 1.1. Primary amino acid sequence (single letter code) of bovine lactoferrin. * denotes residues 17 to 42, representing the antimicrobial peptide, lactoferricin. + denotes the major contributors to one of the two iron-binding sites, and ^ denotes the major contributors to the second iron-binding site (adapted from Pierce et al., 1991).	23
Figure 1.2. Three-dimensional structure of diferric bovine lactoferrin at 2.8 Å resolution where the arrows indicate the location of bound iron (Reprinted from Moore et al., 1997, Copyright 1997, with permission from Elsevier).	24
Figure 1.3. Antimicrobial peptide fragments isolated from bovine lactoferrin as reported in the literature; Peptides I, II, III are from Dionysius and Milne (1997) and Peptides, 1a, 1b, 2, and 3 are from Hoek et al. (1997).	25
Figure 1.4. Hydrophobic (a), hydrophilic (b), and positive (c) side chains along the β-strands of bovine lactoferricin. The backbone of all residues is shown in gray, while the highlighted side chains are in black (Reprinted from Hwang et al., 1998, Copyright 1998, with permission from American Chemical Society).	26
Figure 1.5. Structural representation of the arrangement of phospholipids. Arrangement of the head group and fatty acid domains of phospholipids in the fluid liquid crystalline state (L _α), the ordered gel state (L _β), and the reversed hexagonal state (H _{II}) (Reprinted from Dowhan, 1997, Copyright 1997, with permission from the Annual Reviews www.annualreviews.org).	27
Figure 1.6. Raman spectra of dipalmitoylphosphatidylglycerol (DPPG) in the C-H stretching mode region (2800-3000 cm ⁻¹) between 25 and 55 °C (a). Peak height intensity ratios (b): I ₂₈₅₀ /I ₂₈₈₀ (A) and I ₂₉₃₅ /I ₂₈₈₀ (B) (adapted from Vincent et al., 1993).	28
Figure 2.1. MALDI-ToF mass spectrum of lactoferrin digest produced by peptic digestion for 4 hours at 37 °C at pH 2.0.	50
Figure 2.2. Purolite C-106 cation exchange chromatography of peptic LF digest (Solid line, Absorbance at 280nm; dotted line, conductivity). The supernatant of a 0.5 g of peptic LF digest was loaded onto a 10 mL column and eluted with 50 mM sodium phosphate buffer (pH 6.5) containing 0, 0.2, 0.5, 0.8, 1.0, and 2.0 M of NaCl at a flow rate of 1.0 mL per minute. Fraction peaks were collected and further analyzed.	51
Figure 2.3. MALDI-ToF mass spectra of LF digest fractions eluted from a 10 mL cation exchange column with Purolite C-106 resin using 50 mL phosphate buffer at pH 6.5 containing no NaCl (a), 0.2 M NaCl (b), 0.5 M NaCl (c), 0.8 M NaCl (d), 1.0 M NaCl (e), and 2.0 M NaCl (f).	52
Figure 2.4. Purolite C-106 cation exchange chromatography in competitive displacement mode of peptic LF digest (a: Solid line, Absorbance at 280nm; dotted line, conductivity). The supernatant of a 5.0 g of peptic LF digest was loaded onto a 5.0 mL column and eluted with 50 mM sodium phosphate buffer (pH 6.5) containing 0, 1.0, and 2.0 M NaCl (a). Fraction peaks were collected and further analyzed by MALDI-ToF (b, i: fraction collected after sample loading was completed; ii: 1.0 M NaCl fraction; iii: 2.0 M NaCl fraction.)	53
Figure 2.5. MALDI-ToF post source decay mass spectrum of peak with mass of 3196 Da (a) and possible peptides that were resulted from the post source decay (b).	54
Figure 2.6. MALDI-ToF mass spectra of lactoferrin digest resulting from peptic digestion of apo-LF (a) and holo-LF (b).	55
Figure 2.7. MALDI-ToF mass spectra of 1.0 M NaCl fractions resulting from peptic digestion of apo-LF (a) and holo-LF (b).	56

Figure 2.8. MALDI-ToF mass spectra of 2.0 M NaCl fractions resulting from peptic digestion of apo-LF (a) and holo-LF (b).	57
Figure 3.1. Principal component similarity (PCS) scattergram of lactoferricin derivatives using data obtained from homology similarity analysis (HSA). Group I-V are listed in Tables 3.1 – 3.5.	79
Figure 3.2. Plots of predicted values vs. observed values by artificial neural network: (a) Log MIC and (b) Reciprocal MIC.	80
Figure 4.1. Raman spectra of dipalmitoylphosphatidylcholine (DPPC) liposomes in the presence of lactoferricin showing changes in the major peaks near 2850, 2880, and 2935 cm^{-1} as a function of temperature.	94
Figure 4.2. I_{2850}/I_{2880} ratio of DPPC (a), I_{2935}/I_{2880} ratio of DPPC (b), I_{2850}/I_{2880} ratio of POPC (c), and I_{2935}/I_{2880} ratio of POPC (d) in the absence (\diamond) or presence (\blacksquare) of Lfcin measured between -10 °C and 70 °C by Raman spectroscopy.	95
Figure 4.3. I_{2850}/I_{2880} ratio of DPPG (a), I_{2935}/I_{2880} ratio of DPPG (b), I_{2850}/I_{2880} ratio of POPG (c), and I_{2935}/I_{2880} ratio of POPG (d) in the absence (\diamond) or presence (\blacksquare) of Lfcin measured between -10 °C and 70 °C by Raman spectroscopy.	96
Figure 4.4. I_{2850}/I_{2880} ratio of DPPE (a), I_{2935}/I_{2880} ratio of DPPE (b), I_{2850}/I_{2880} ratio of POPE (c), and I_{2935}/I_{2880} ratio of POPE (d) in the absence (\diamond) or presence (\blacksquare) of Lfcin measured between -10 °C and 70 °C by Raman spectroscopy.	97
Figure 5.1. Thermal behaviours of DPPC as indicated by I_{2850}/I_{2880} (a) and I_{2935}/I_{2880} (b) in the absence of lactoferricin (Lfcin, \square), the presence of Lfcin ₁₅ (i, \blacksquare), Lfcin ₁₅ R- (ii, \blacklozenge), Lfcin ₁₅ W- (iii, \blacktriangle), Lfcin ₁₅ W+ (iv, \blacktimes), and LfcinCore (v, \blackstar) measured between -10 °C and 70 °C by Raman spectroscopy.	113
Figure 5.2. Thermal behaviours of DPPG as indicated by I_{2850}/I_{2880} (a) and I_{2935}/I_{2880} (b) in the absence of lactoferricin (Lfcin, \diamond), the presence of Lfcin ₁₅ (i, \blacksquare), Lfcin ₁₅ R- (ii, \bullet), Lfcin ₁₅ W- (iii, \blacktriangle), Lfcin ₁₅ W+ (iv, \blacktimes), and LfcinCore (v, \blackstar) measured between -10 °C and 70 °C by Raman spectroscopy.	114
Figure 5.3. Thermal behaviours of DPPE as indicated by I_{2850}/I_{2880} (a) and I_{2935}/I_{2880} (b) in the absence of lactoferricin (Lfcin, \circ), the presence of Lfcin ₁₅ (i, \blacksquare), Lfcin ₁₅ R- (ii, \blacklozenge), Lfcin ₁₅ W- (iii, \blacktriangle), Lfcin ₁₅ W+ (iv, \blacktimes), and LfcinCore (v, \blackstar) measured between -10 °C and 70 °C by Raman spectroscopy.	115

List of Abbreviations

ANN	Artificial Neural Network
CAP	Cationic Antimicrobial Peptide
DPPC	1,2-dipalmitoyl- <i>sn</i> -glycerol-3-phosphocholine
DPPE	1,2-dipalmitoyl- <i>sn</i> -glycerol-3-phosphoethanolamine
DPPG	1,2-dipalmitoyl- <i>sn</i> -glycerol-3-[phospho- <i>rac</i> -(1-glycerol)]
HSA	Homology Similarity Analysis
LF	Lactoferrin from Bovine, unless otherwise stated
LFB	Lactoferrin from Bovine
Lfcin	Lactoferricin from Bovine, unless otherwise stated
Lfcin ₁₅	Lactoferricin derivative with the following sequence: FKCRR WQWRM KKLGA
Lfcin ₁₅ R-	Lactoferricin derivative with the following sequence: FKCAA WQWAM KKLGA
Lfcin ₁₅ W-	Lactoferricin derivative with the following sequence: FKCRR AQARM KKLGA
Lfcin ₁₅ W+	Lactoferricin derivative with the following sequence: FKCWR WQWRW KKLGA
LfcinB	Lactoferricin from Bovine
LfcinCore	Lactoferricin derivative with the following sequence: RRWQW R-NH ₂
LfcinH	Lactoferricin from Human
LFH	Lactoferrin from Human
MIC	Minimum Inhibitory Concentration
PCA	Principal Component Analysis
PCS	Principal Component Similarity
PLS	Partial Least Square
POPC	1-palmitoyl-2-oleoyl- <i>sn</i> -glycerol-3-phosphocholine
POPE	1-palmitoyl-2-oleoyl- <i>sn</i> -glycerol-3-phosphoethanolamine
POPG	1-palmitoyl-2-oleoyl- <i>sn</i> -glycerol-3-[phospho- <i>rac</i> -(1-glycerol)]

Acknowledgements

Many, many thanks go to many people who worked with me in the Department. They listened when I faced hurdles during my research progress; they cheered when I made important breakthroughs. They know who they are and they understand why they are not named here.

Sincere thanks go to my supervisor, Dr. Eunice Li-Chan, who is knowledgeable, dedicated, and caring. It is a true joy to be her student.

Funding for this research was provided by the Dairy Farmers of Canada and the Natural Sciences and Engineering Research Council of Canada. JCKC was the recipient of the University Graduate Fellowship provided by the University of the British Columbia.

Dedication

This thesis is dedicated to:

Dad who encourages me to follow my dreams
Mom who makes sure that I study hard so that I can follow my dreams

Dennis who is always there with me when I follow my dreams

Co-Authorship Statements

Part of the work presented in Chapter 2 was submitted for publication in the Journal of Agricultural and Food Chemistry, titled "Production of lactoferricin and other cationic peptides from food grade bovine lactoferrin with varying iron saturation levels". JCK Chan, the thesis author, was the principal author who identified and designed the research program, performed the research, analyzed data, and prepared the manuscript. ECY Li-Chan, JCK Chan's supervisor, was the co-author and provided close guidance on the above research.

Part of the work presented in Chapter 3 was published in the Journal of Agricultural and Food Chemistry, 2003: 51, 1215-1223, titled "Homology similarity analysis of sequences of lactoferricin and its derivatives". S Nakai, member of JCK's supervisory committee, was the principal author who identified and designed the research program. JCK Chan, the thesis author, assisted in data collection, verified data analyses, and aided in manuscript preparation. J Dou, co-author of the study, developed the computer programs used in the study. ECY Li-Chan and M Ogawa, co-authors of the study, provided guidance on the design of the research program and manuscript preparation.

Part of the work presented in Chapter 4 will be submitted for publication in Biochimica et Biophysica Acta (BBA) – Biomembranes, titled "Raman spectroscopic study of the effects of lactoferricin on thermal transitions of phospholipids in liposomes". JCK Chan, the thesis author, was the principal author who identified and designed the research program, performed the research, analyzed data, and prepared the manuscript. ECY Li-Chan, JCK Chan's supervisor, was the co-author and provided close guidance on the above research.

Part of the work presented in Chapter 5 will be submitted for publication in Biochimica et Biophysica Acta (BBA) – Biomembranes, titled "Raman spectroscopic study of the effects of lactoferricin derivatives on phospholipid liposomes". JCK Chan, the thesis author, was the principal author who identified and designed the research program, performed the research, analyzed data, and prepared the manuscript. ECY Li-Chan, JCK Chan's supervisor, was the co-author and provided close guidance on the above research.

JCK Chan

ECY Li-Chan

CHAPTER 1. GENERAL INTRODUCTION AND LITERATURE REVIEW

Lactoferrin (LF) is an iron-binding protein in bovine whey, with a broad spectrum of antimicrobial activity (Bellamy et al., 1992b). Studies have shown that pepsin digestion of bovine LF yields a peptide fragment that has more potent activity than undigested LF (Tomita et al., 1991). This fragment is named bovine lactoferricin (Lfcin) and is a 25-amino acid peptide corresponding to residues 17-41 from the N-terminal loop region of LF with the sequence FKCRRWQWRM KKLGA PSITC VRRAF (Bellamy et al., 1992b). This 25-amino acid peptide includes 8 basic amino acids that contribute to a net charge of +6.85 at pH 7 and forms an anti-parallel, amphipathic, β -sheet structure (Rekdal et al., 1999; Hwang et al., 1998). Lfcin has been the subject of intense research in past decades in regard to its antimicrobial and immunomodulatory activities, as well as its inhibitory effects on carcinomas and tumor metastasis (Gifford et al., 2005; Mader et al., 2005).

1.1. Lactoferrin

1.1.1. Sources of Lactoferrin

Lactoferrin (LF), a member of the transferrin family of iron-binding proteins, was first reported in bovine milk in 1939 (Sørensen and Sørensen, 1939). Since then, LF has been found in and isolated from various mammalian milks including human (LFH) (Johansson, 1960), bovine (LFB) (Groves, 1960), and camel (Kappeler et al., 1999; Masson and Heremans, 1971). LF levels in milks depend on the species, as well as the lactation period. The amount of LF is 5 to 7 mg \cdot mL⁻¹ in human colostrum and 1 to 3 mg \cdot mL⁻¹ in mature milk (Hennart et al., 1991), while the content of LF in bovine milk is markedly lower at 0.8 mg \cdot mL⁻¹ in the colostrum and 0.1 to 0.4 mg \cdot mL⁻¹ in mature milk (Sánchez et al., 1988). In addition to mammalian milks, LF has also been found in various exocrine secretions such as tears, seminal fluid, cervical mucus, and saliva (Levay and Viljoen, 1995). Furthermore, LF was detected in the lymphatic system (Beljaars et al., 2002).

1.1.2. Structure of Lactoferrin

Bovine lactoferrin consists of a single polypeptide chain of 689 amino acids with a molecular weight of 76,000 Da (**Figure 1.1**) (Pierce et al., 1991). Crystallographic analyses have revealed that both bovine (Moore et al., 1997) and human (Anderson et al., 1987 and 1989) lactoferrins are composed of two globular lobes of similar size which are connected by a single short bridging peptide (**Figure 1.2**). These studies demonstrated that LFB is an α/β protein containing approximately 41% α -helix and 24% β -sheet. Results from Fourier transform infrared (FTIR) spectroscopic analysis of LFH also showed similar results; the secondary

structural content of LFH was estimated to be approximately 44% α -helix, 28% β -sheet, and 21% turns (Hadden et al., 1994).

Crystallographic studies indicated that each lobe of the LF consists of two domains that form a cleft enclosing the binding site for a metal ion (Moore et al., 1997). Hence, each LF molecule has the ability to bind reversibly two ferric ions (Fe^{3+}) per molecule (Moore et al., 1997). In addition to these specific iron binding sites, it has been reported that LFB was capable of binding 700 times the amount of iron that could be bound to the specific binding sites (Nagasako et al., 1993). It was postulated that LFB binds iron at sites other than the specific binding sites, possibly on the surface of the globular protein (Nagasako et al., 1993).

The binding of iron to lactoferrin is an important factor in the thermal stability of its structure. Paulsson et al. (1993) reported that iron-saturated (holo-) bovine lactoferrin was more resistant to heat-induced changes than was the iron-depleted (apo-) LF. Results from differential scanning calorimetry demonstrated that lactoferrin isolated from human milk had a maximum peak temperature at 67.0 °C, and transition enthalpy, and activation energy of 2276 kJ • mol⁻¹, and 275.5 kJ • mol⁻¹, respectively, while holo-lactoferrin saturated with iron had a maximum peak temperature at 90.6 °C, a transition enthalpy of 3209 kJ • mol⁻¹, and an activation energy of 387.6 kJ • mol⁻¹ (Mata et al., 1998). Although results from a FTIR spectroscopy study showed that iron status in LF did not affect the secondary structural content, i.e. α -helix, β -sheet, and turns, of LFH, removal of iron from LFH led to increases in the extent of ¹H-²H exchange (Hadden et al., 1994). Hadden et al. (1994) postulated a "loosening" of LF upon iron removal. This could explain the lower heat stability demonstrated by apo-lactoferrin.

Bovine LF possesses five N-linked glycosylation sites at Asn-233, -281, -368, -476, and -545 (Pierce et al., 1991). The carbohydrate moieties of bovine LF consist of complex and high-mannose type glycans and the relative proportions of these glycans vary with the lactation period (Hutchens et al., 1994). It was reported that the structures of these glycans are highly heterogeneous (Wei et al., 2000).

1.1.3. Biological Functions of Lactoferrin

1.1.3.1. Antimicrobial Properties of Lactoferrin

A physiologically diverse range of pathogenic Gram-positive and Gram-negative bacteria was reported to be susceptible to inhibition and inactivation by bovine lactoferrin (Antonini et al., 1997; Bellamy et al., 1992a and 1992b; Ellison and Giehl, 1991; Tomita et al., 1991 and 1994; Yamauchi et al., 1993; Yamazaki et al., 1997). In addition, LF was used to enhance the effectiveness of antifungal agents against various *Candida* species (Wakabayashi

et al., 1996 and 1998). LF also inhibited *Trichophyton mentagrophytes* in a guinea pig model with dermatophytosis (Wakabayashi et al., 2000).

Several early studies demonstrated that the antimicrobial property of LF is iron dependent. Nonnecke and Smith (1984) reported that the addition of ferric iron to the assay system diminished the inhibitory activity of apo-LF. The antibacterial effect of LF on enterotoxigenic *Escherichia coli* was also affected by the iron status of the LF. The presence of $1.0 \text{ mg} \cdot \text{mL}^{-1}$ of holo-LF did not inhibit the growth of any of the 19 *E. coli* strains tested. On the contrary, the presence of apo-LF acted against all strains tested (Dionysius and Milne, 1997). Hence, the strong iron-binding capacity of LF could be responsible for the antimicrobial actions of LF simply by removing iron from the environment and thus limiting microbial growth (Bullen et al., 1972). Nevertheless, increasing evidence has suggested that additional mechanisms are involved in the antimicrobial actions of LF. For instance, bactericidal effects exhibited by apo-LF could not be reversed by the addition of exogenous iron in excess of its chelating capacity and such antimicrobial effects could not be reproduced by exposing the microorganisms to iron-deficient medium alone (Arnold et al., 1980 and 1982). Furthermore, immunofluorescence studies have shown that LF bound directly to the surface of microorganisms, causing damage to the outer membrane and the release of lipopolysaccharides (Ellison et al., 1988; Ellison and Giehl, 1991).

1.1.3.2. Antiviral Functions of Lactoferrin

Lactoferrin is capable of inhibiting replication of a wide range of viruses, namely, hepatitis C (Ikeda et al., 1998, 2000), rotavirus (Superti et al., 1997), poliovirus (Marchetti et al., 1999), human immunodeficiency virus (HIV) (Harmsen et al., 1995; Puddu et al., 1998), and β -herpes virus (Andersen et al., 2001). Evidence has shown that LF prevents viral infection of the target cell by direct binding to either the virus particles or the viral receptors of the host cell that the virus uses for cell entry. Furthermore, LF could indirectly exert its antiviral mode of action through the upregulation of the antiviral response of the immune system (van der Strate et al., 2001).

1.1.3.3. Other Biological Functions of Lactoferrin

Besides milk, lactoferrin can be found in various body fluids and it is therefore postulated to have significant roles in immunoregulation. The release of LF in the body is activated by the presence of neutrophils. LF in the body is believed to play several significant roles in the host defense system including the regulations of the growth and differentiation of various immune cells, as an anti-inflammatory agent, prevention of oxidative tissue damage, and regulation of iron availability (Brock, 1995).

Bovine LF exerted at least a 87% inhibitory effect on the adhesion of enterotoxigenic *Escherichia coli* to human epithelial cells *in vitro* (Kawasaki et al., 2000). In an *in vivo* mouse study, the counts of adherent bacteria in various locations of the intestinal tract were lower in the LFB treated group than in the control group. While LF could be used to lower the presence of pathogenic bacteria in the gut lining, LF could also act as a growth promoter of *Bifidobacterium* spp. that could be commonly found in the intestinal tracts of breast-fed infants (Miller-Catchpole et al., 1997; Petschow et al., 1999). *In vivo* studies also showed that when administered orally, LFB helped to balance the gut flora of experimental mice (Hentges et al., 1992) and human full-term infants (Roberts et al., 1992). The levels of *Enterobacteriaceae*, *Streptococcus*, *Staphylococcus*, and *Clostridium* in the fecal flora of the infants were decreased by almost 20% after feeding LFB-enriched formula for two weeks. Meanwhile, the percentages of *Bifidobacterium* in the fecal flora increased by almost 50%. Results from these studies indicated that lactoferrin supplemented formula assisted in the establishment of a *Bifidobacterium*-predominant intestinal flora in infants.

Other studies showed that LF exhibited chemopreventative effects in the development and progression of bladder carcinogenesis (Masuda et al., 2000) and esophagus and lung carcinogenesis (Ushida et al., 1999; Iigo et al., 1999).

1.1.3.4. Other Functions of Lactoferrin

Due to its iron-binding capacity, lactoferrin also exhibits strong antioxidative ability by chelating excess metal ions in food systems. Huang et al. (1999) examined the effects of lactoferrin on the oxidation of a corn oil emulsion and a liposome model system. Results showed that the antioxidant activity against iron-catalyzed autoxidation increased with LF concentration. A mixture of 1 μM LF and 0.5 μM ferrous ions exhibited better antioxidative ability than 1 μM LF alone. However, LF became a prooxidant at concentrations higher than 15 μM and was unable to inhibit copper-catalyzed autoxidation. Results showed that the antioxidant or prooxidant activity of LF depended on the lipid system, buffer, LF concentration, the concentration of metal ions, and oxidation time.

The antioxidant activity of LF was studied in a commercially modified infant formula supplemented with iron at a level of 12 mg per liter (Satué-Gracia et al., 2000). Results demonstrated that in the presence of increasing concentrations of lactoferrin, the induction periods for oxidation of the infant formulas increased and the rates of oxidation decreased. Lactoferrin inhibited oxidation in a concentration-dependent manner even at concentrations beyond its capacity to bind iron at its two high affinity binding sites.

It is postulated that lactoferrin can be used as a multi-purpose additive in infant formulae for its ability to improve intestinal flora of infants, antioxidant property, and antimicrobial abilities (Farnaud and Evans, 2003).

1.2. Lactoferricin & Its Derivatives

Lactoferricin (Lfcin) was first described as a "potent antimicrobial peptide" that could be generated from bovine lactoferrin by heat treatment at acidic pH (Saito et al., 1991) and by pepsin digestion (Tomita et al., 1991). LF hydrolysates produced using these two methods exhibited higher antimicrobial ability than untreated lactoferrin. Since then, extensive studies have been conducted for the production and purification of Lfcin as well as the understanding of its structure-function relationships.

1.2.1. Production and Purification of Lactoferricin and Related Peptides

1.2.1.1 Discovering Lactoferricin

The presence of the antimicrobial peptide sequence was first noticed when heat-treated lactoferrin displayed increased antibacterial activity (Saito et al., 1991). A peptide fraction with strong activity was identified after fractionation of heat-treated LF by reverse-phase HPLC. It was suggested that at least one bactericidal domain would be released by heating LF at pH 2.0 at 120 °C for 15 minutes.

At almost the same period of time, hydrolysates of LF were generated by digestion with porcine pepsin, cod pepsin, or aspartic protease at a concentration of 3% (w/w of substrate) at 37 °C and pH 2.5 for 30 minutes (Tomita et al., 1991). The antimicrobial activity of the resulting LF hydrolysates against *Escherichia coli* O111 were at least eightfold stronger than undigested LF. The minimal inhibitory concentration (MIC) of LF hydrolysates remained unaffected even when the peptic hydrolysis continued for more than 4 hours, indicating that the active peptides were resistant to further cleavage by pepsin. The antibacterial property of pepsin digested LF hydrolysates was not affected in the presence of 0.1 mM FeSO₄; however, the antimicrobial property of untreated LF was completely abolished, suggesting that the antibacterial domain functions by a mechanism distinct from chelation of iron or other metal ions. LF hydrolysates prepared by cleavage with porcine trypsin, papain, or other neutral proteases were much less active than those produced by peptic digestion.

1.2.1.2. Identifying Lactoferricin

Pepsin hydrolyzed human lactoferrin and bovine lactoferrin were fractionated by reverse-phase HPLC and one antimicrobial peptide (named human lactoferricin, LfcinH; and bovine lactoferricin, LfcinB) was isolated in each hydrolysate (Bellamy et al., 1992b). Results

from amino acid sequence analysis indicated that LfcinH has a molecular weight of 5,558 Da and consists of two sub-fragments, residues 1 to 11 and residues 12 to 47, linked by a disulfide linkage between Cys10 on sub-fragment 1 and Cys46 on sub-fragment 2. Another disulfide linkage was also observed between Cys20 and Cys37 on sub-fragment 2 (Bellamy et al., 1992b). Bovine lactoferricin is a relatively shorter peptide corresponding to residues 17 to 41 near the N-terminus of LFB. A disulfide linkage between Cys19 and Cys 36 was reported and the peptide has a molecular weight of 3,124 Da as calculated from the amino acid sequence (Bellamy et al., 1992b).

1.2.1.3. Production and Purification Strategies

Pepsin digestion of LF has been the most commonly utilized method to produce bovine lactoferricin in most of the studies reported so far. However, the composition and antimicrobial potency of the resulting peptide mixtures vary depending upon the source and composition of the starting material, as well as the digestion conditions (e.g. digestion pH, temperature, and duration). Furthermore, purity of the resulting Lfcin would rely on the chromatographic techniques used. A number of production and purification strategies for lactoferricin have been conducted in attempt to isolate Lfcin in larger quantities. Some of these strategies will be discussed below.

Dionysius and Milne (1997) reported that three LfcinB related peptides could be isolated, from pepsin digests of LFB, by cation exchange chromatography. The LF hydrolysate was prepared as previously described (Bellamy et al., 1992a and b) and fractionated through a cation exchange column equilibrated with 0.05 M phosphate buffer at pH 7.5. Peptides of interest were eluted with the equilibrating buffer containing 1 M NaCl. Using reverse-phase HPLC, mass spectrometry, N-terminal amino acid sequencing, and amino acid analysis, three peptides originating from the N-terminal of the LF were identified; the amino acid sequences and molecular weights of these peptides are shown in **Figure 1.3**.

Peptide I had a mass of 3195 and corresponded to residues 17 to 42 of LFB with a disulfide linkage between Cys19 and Cys36. Peptide II consisted of two peptides, residues 1 to 16 and residues 43 to 48, with a disulfide bond at Cys9 and Cys45. Peptide III had a mass of 5851 Da and corresponded to residues 1 to 48 of LFB with a cleavage between residues 42 and 43; disulfide bonds could be found between Cys9 and 45 and between Cys19 and 36 (Dionysius and Milne, 1997). All three peptides exhibited improved antimicrobial activity over undigested lactoferrin. However, only the activity of peptide I was comparable to the Lfcin previously reported (Bellamy et al., 1992a, b). The activity of peptides II and III were much weaker. In fact, peptide I was almost identical to LfcinB that was previously described (Bellamy et al., 1992b) except for the presence of an additional alanine at the C-terminus.

The isolation of Lfcin and other related peptides has also been reported using a bead-based cation-exchange chromatography on SP-Sepharose Fast Flow resin (Recio and Visser, 1999). Two major peptides of mass 3123 and 3194 were eluted with 7 M ammonia and 2 M NaCl. These peptides corresponded to residues 17-41 and 17-42 of LF. However, other components were also found in the fraction, including the 27-amino acid peptides and the oxidized form of the 26-amino acid peptide. Shimazaki et al. (1998) also reported that a peptide with molecular mass of 3195.5 Da was isolated using affinity chromatography with an immobilized heparin column. The peptide of interest was eluted from the column with 1 M NaCl in various buffer systems.

Hoek et al. (1997) reported the production of LfcinB and other peptides sharing high sequence homology with LfcinB by recombinant chymosin digestion of bovine LF. Specifically, LFB (5 g) was dissolved in 200 mL of water, and the solution was adjusted to pH 3.0 by HCl. To the solution, 200 mg of recombinant chymosin was added. It was then incubated at 60 °C for 1 hour. The resulting solution was pH adjusted, centrifuged and passed through a cation-exchange membrane filtration system. Peptides eluted with 2M NaCl were further fractionated by RP-HPLC and analyzed by mass spectrometry. The molecular weights and amino acid sequences of four highly homologous peptides were determined as shown in **Figure 1.3**.

Peptides 1a, 1b, and 2 were single peptides with amino acid sequences starting at residue 17 of the LF. All three peptides formed a cyclic structure with a disulfide linkage between Cys 19 and Cys 36. Peptide 3 consists of two peptides joined by a disulfide bond; its main peptide shares sequence homology with the other three and is also disulfide linked. All four peptides exhibited antimicrobial activity against *E. coli* L361. Minimum inhibitory concentrations (MIC) reported for peptides 1a, 1b, 2, and 3 were 12.5, 12.5, 13.2, and 23.4 $\mu\text{g} \cdot \text{mL}^{-1}$, respectively. However, when expressed in molar concentration, MIC for all four peptides were 4 μM (Hoek et al., 1997).

A patent for large-scale production of Lfcin from bovine LF claims that a yield of 10.5 g of Lfcin with 99% purity could be obtained from 600 g of LFB (Tomita et al., 1999). LF was first digested with an enzyme and resulting hydrolysate was passed through a hydrophobic or cation exchange chromatography medium. After the column was washed with water and a citric acid-sodium phosphate buffer at pH 7.0, the adsorbed Lfcin was desorbed with the same buffer at pH 5.0.

To date, research on Lfcin production has been limited to the uses of laboratory-grade LFB and chromatographic media. The development of a fractionation strategy for the large

scale production of Lfcin using food-grade materials is much needed for the incorporation of Lfcin in human food system.

1.2.2. Antimicrobial Spectrum of Lactoferricin and Related Peptides

As mentioned before, both purified LfcinH and LfcinB exhibited stronger antimicrobial activity against *Escherichia coli* O111 than their undigested counterparts (Bellamy et al., 1992b). The MIC against *E. coli* O111 was 3000, 500, and 100 $\mu\text{g} \cdot \text{mL}^{-1}$ for LFH, LF hydrolysate, and LfcinH, respectively, and 2000, 100, and 6 $\mu\text{g} \cdot \text{mL}^{-1}$ for LFB, LFB-hydrolysate, and LfcinB, respectively. Furthermore, a diverse range of Gram-positive and Gram-negative bacteria was found to be susceptible to LfcinB at MIC ranging from 6 to 12 $\mu\text{g} \cdot \text{mL}^{-1}$ (in 1% peptone) for most of the Gram-negative bacteria tested and from 0.3 to 12 $\mu\text{g} \cdot \text{mL}^{-1}$ for most of the Gram-positive bacteria tested. *Bifidobacterium bifidum* strains were resistant to LfcinB (Bellamy et al., 1992a). With MIC ranging from 3 to 18 $\mu\text{g} \cdot \text{mL}^{-1}$, various types of yeasts were inactivated by LfcinB, while 3 to 45 $\mu\text{g} \cdot \text{mL}^{-1}$ of LfcinB were needed to inhibit the growth of filamentous fungi. Lfcin could enhance the effectiveness of antifungal agents against *Candida albicans* (Wakabayashi et al., 1998). Skin disease-causing fungi could also be inactivated by the addition of 6 to 30 $\mu\text{g} \cdot \text{mL}^{-1}$ of Lfcin (Bellamy et al., 1993; Bellamy et al., 1994; Tomita et al., 1994).

However, the antimicrobial effectiveness of LfcinB was decreased in the presence of Na^+ , K^+ , Ca^{2+} , Mg^{2+} , Fe^{3+} , and various buffer salts including K_2HPO_4^- , KH_2PO_4^- , Tris-HCl, HEPES-NaOH, and PIPES-NaOH (Bellamy et al., 1992a; Yamauchi et al., 1993). The antimicrobial activity of LfcinB against *Salmonella enteritidis* was inhibited in nutrient rich media such as tryptic soy broth (Facon and Skura, 1996). Studies have shown that the antimicrobial activity of LfcinB in ground beef (Venkitanarayanan et al., 1999) and carrot juice (Chantaysakorn and Richter, 2000) diminished due to the presence of high levels of cations in the systems.

1.2.3. Structure – Function Relationship Analysis of Lactoferricin and Its Derivatives

1.2.3.1. Basic Structural Properties of Bovine Lactoferricin

As described in previous sections, bovine lactoferricin (LfcinB) is a 25-amino acid peptide corresponding to residues 17-41 from the N-terminal loop region of LF with the sequence $^{17}\text{FKCRR WQWRM KKLGA PSITC VRRAF}^{41}$; a disulfide linkage between Cys19 and Cys36 was also reported (Bellamy et al., 1992b). This 25-amino acid peptide includes 8 basic amino acids that contribute to a net charge of +6.85 at pH 7 (Rekdal et al., 1999). Nuclear magnetic resonance (NMR) analysis of Lfcin revealed that Lfcin formed a slight distorted anti-parallel β -sheet structure with a loop formed between residues 27 to 30 (Hwang et al., 1998).

Due to the presence of the disulfide linkage between Cys19 and Cys36 and the orientation of Trp22, two noticeable kinks were observed between Arg20 and Arg21 and between Cys19 and Trp22 (Hwang et al., 1998). Results from circular dichroism analysis (CD) also demonstrated that LfcinB displayed no α -helical conformation, but consisted of 41% β -sheet in an aqueous environment. The presence of trifluoroethanol (TFE, 50% v/v) increased the α -helical content of LfcinB to 6.5%. When the disulfide bond was reduced, less β -sheet was detected in both the aqueous environment and in the presence of TFE (Shimazaki et al., 1998).

Once the LfcinB was folded into a β -sheet structure, side chains of Phe17, Cys19, Trp22, Trp24, Leu29, Ala31, Pro32, Ile24, and Cys36 comprised a prominent hydrophobic surface on one side of the β -sheet structure (**Figure 1.4a**). Outside of this hydrophobic strip, most side chains are hydrophilic, including Ser17, Gln23, Thr35, and Val37, or positively charged, including Lys18, Arg20, Arg21, Arg25, Lys27, Lys28, Arg38, and Arg39 (**Figure 1.4b and c**). The high degree of amphipathic structure was thought to be responsible for the antimicrobial activity of the peptide by interacting with and thus disrupting the cellular membrane. Recent studies using chemically synthesized lactoferricin and analogs with different structural variations have provided new information on the structure – function relationship of this cationic antimicrobial peptide.

1.2.3.2. Roles of Secondary Structure

In an aqueous environment LfcinB forms a β -sheet structure stabilized by a disulfide bond. When the cyclic structure was cleaved with CNBr and when the disulfide bond was reduced in the presence of β -mercaptoethanol, little change in the antimicrobial activity of Lfcin against a number of bacteria was observed (Hoek et al., 1997; Strøm et al., 2000). This suggested that neither a cyclic nor a linear structure of the peptide is particularly critical for its effectiveness as an antimicrobial agent.

Results from several studies showed that shorter peptide fragments composed of LfcinB residues 17-28 (Tomita et al., 1994), residues 20-30 (Kang et al., 1996) and residues 17-31 (Rekdal et al., 1999), or LfcinH residues 20-35 (Odell et al., 1996) and residues 20-30 (Odell et al., 1996; Chapple et al., 1998) demonstrated similar or greater antimicrobial activity against *Escherichia coli* and other microbes than their native counterparts. CD analysis of LfcinB 20-30 (Kang et al., 1996) showed that this short LfcinB derivative adopted an α -helical structure in the presence of TFE and sodium dodecyl sulfate (SDS). When the helical region of LfcinH 20-30 was disrupted by replacing the methionine at position 26 with a proline, the antibacterial activity of the peptide against *E. coli*, *Staphylococcus aureus*, and an *Acinetobacter* sp. was diminished (Chapple et al., 1998).

Furthermore, using NMR spectroscopy, Schibli et al. (1999) observed that the antimicrobial core of Lfcin (RRWQWR, Tomita et al., 1994) adopted an orderly conformation with three Arg residues on one side of the structure and two Trp residues on the other side of the structure. They further illustrated that the aromatic Trp residues were more deeply buried in the SDS micelles with the Arg and Gln exposed to the solvent. Although Lfcin and its derivatives may form either α -helix or β -sheet in different environments, evidence suggests that the orientation of both basic and hydrophobic amino acids in the peptide chain is critical to the antimicrobial properties of shorter LfcinB derivatives.

1.2.3.3. Roles of Basic Amino Acids

In a study investigating the heparin-binding ability of LfcinB analogs, it was reported that the absence of basic amino acids such as arginine and lysine would decrease the heparin binding ability of LfcinB 17-31 (Shimazaki et al., 1998). Since this heparin binding ability was thought to be responsible for the inhibitory effects of lactoferrin on inflammation, the presence of basic amino acids in LfcinB might also play a critical role in its antimicrobial activity.

In order to examine the importance of basic amino acids in the antimicrobial activity of LfcinB, all the basic amino acids in LfcinB 20-30 were replaced with glutamic acids. The modified peptides showed lower antimicrobial activity against *Escherichia coli* O111 and *Bacillus subtilis* than the unmodified peptide (Kang et al., 1996). Furthermore, CD spectra of the modified LfcinB in 30 mM SDS were similar to the ones in aqueous environment, suggesting that the modified LfcinB did not adopt an α -helical conformation. Similar results were reported when alanine replaced arginine or lysine residues; higher MIC against *E. coli* and *S. aureus* were observed (Strøm et al., 2000). In contrast, the antimicrobial activity of the peptide increased when the glutamic acid in position 30 was replaced with an alanine.

Although the net charge seems to be important in the antimicrobial activity of LfcinB, effects of the size and the position of the basic amino acids should also be considered. When Arg were replaced with Lys, it was found that the Lys substituted LfcinB 20-30 exhibited less antimicrobial activity (Kang et al., 1996). The replacement of Lys with Ala had less effect on MIC than the replacement of Arg (Strøm et al., 2000). These results suggested that the larger size and the positive charge of the guanidinium group of the arginine residues were important in the antimicrobial property, with a more severe disruption of the bacterial cell membrane.

The position of the basic amino acids along the β -sheet region also affects the biological activity of LfcinB. For instance, when the Arg in positions 20, 21, and 25 of LfcinB was replaced with an Ala, the MIC against *E. coli* were 35, 61, and 28 μ M, respectively (Strøm et al., 2000). Each Arg may have a specific role in the interaction with the cellular membrane.

As demonstrated by Schiffer-Edmundson helical wheel models, the asymmetry in charge distribution along the β -sheet is important in improving the antimicrobial activity (Rekdal et al., 1999); LfcinB analogs having all of the basic amino acids located along one face of the sheet demonstrated stronger antimicrobial activities than analogs with more basic amino acids but distributed at different locations.

1.2.3.4. Roles of Hydrophobic Amino Acids

Hydrophobic residues on the cationic antimicrobial peptides are also essential in the formation of an amphipathic structure. Alanine substitution of all the hydrophobic residues in LfcinB 20-30 resulted in no antimicrobial activity in the concentration range tested (Kang et al., 1996). Similar results were reported by Strøm et al. (2000). When one of the two tryptophan residues in position 22 and 24 was replaced by alanine, no inhibitory effect against *E. coli* or *S. aureus* was observed at concentration less than 100 μ M, while the MIC of the unmodified peptides for these two microorganisms were 24 and 48 μ M, respectively. Replacing Met at position 26 with alanine also increased the MIC to 70 μ M.

The importance of tryptophan in the antibacterial activity was investigated by substituting Trp in pentadecapeptides derived from human (LfcinH), caprine (LfcinC), murine (LfcinM), and porcine (LfcinP) origin (Strøm et al., 2000). These Lfcins each have only one Trp residue in the Lfcin segments tested. Upon adding a second Trp residue to LfcinH, LfcinC, or LfcinP, but not to LfcinM, the antimicrobial activity was improved by 1.5 to 6-fold compared to the unmodified peptides. These results indicated that the hydrophobic tryptophan plays a key role in the antimicrobial activity of Lfcin.

The specific role of tryptophan was examined by replacing the Trp residues in LfcinB 17-31 with natural and unnatural aromatic amino acids (Haug and Svendsen, 2001). The replacement of nitrogen in Trp with a sulfur atom in the side chain of (β -(benzothien-3-yl)alanine (Bal) enhanced the antibacterial activity of LfcinB 17-31. These results suggested that hydrogen bonding between the peptide and the cellular membrane was not essential in the antimicrobial properties of the peptide. Similarly, the antibacterial activity of the resulting peptide was also increased when the indole side chain of Trp was replaced with naphthalene. Again, these results suggested that hydrophobic aromatic side chains were more favorable for the interaction between the peptides and the cellular membrane. Antimicrobial activity was also improved when the Trp was replaced with unnatural hydrophobic aromatic amino acids that were larger in size (Haug et al., 2001). Conversely, the antimicrobial effect diminished when the smaller phenylalanine was substituted for Trp. Also, substituting hydrophobic aromatic side chains with a more elongated shape led to increased antimicrobial activities. These improvements were further enhanced when both Trp residues in positions 22 and 24 were

replaced (Haug et al., 2001). These size and shape effects suggested that the hydrophobic side chains of Lfcin were essential for the antimicrobial activity. Larger and elongated side chains may be able to penetrate deeper into the cellular membrane and serve as a stronger anchor, making the overall peptide a more efficient antimicrobial agent.

The combined effect of hydrophobic and basic amino acid side chains was examined using LfcinM (Strøm et al., 2001). As was mentioned above, the addition of one extra Trp in LfcinM was inefficient in providing an effective antimicrobial peptide. However, MIC was considerably improved when the Glu residues were replaced with Arg or Ala, and the Val residue with Tyr. These results showed that the presence of both aromatic and basic amino acids were essential in establishing an amphipathic structure with antimicrobial property.

1.3. Cationic Antimicrobial Peptides

In order to gain a better understanding of the possible antimicrobial mechanism of lactoferricin, it is useful to examine modes of action of other similar peptides. Some general information of other cationic antimicrobial peptides (CAPs) will be briefly discussed. More extensive reviews may be found in Bechinger (1997), Hwang and Vogel (1998), Epand and Vogel (1999), Lohner and Prenner (1999), Shai (1999), and Chan and Li-Chan (2006).

1.3.1. Structures and Modes of Action of Other Cationic Antimicrobial Peptides

More than 140 naturally occurring CAPs have been identified. They are between 11 and 50 amino acids long and have a net positive charge of +2 or more. Most of these CAPs have certain properties in common. They all have affinity for membrane lipids and their specificity for microbial membranes in many cases has been shown to be related to the positive charge on the peptide favoring interaction with the exposed anionic lipids of microorganisms (Epand and Vogel, 1999). In general, these CAPs can fit into four major classes, namely, β -sheet structure stabilized by one to three disulfide bridges, α -helices, extended helices with a predominance of one or more amino acids (including unusual amino acids such as lanthionine derivative, 3-methylanthionine derivative, and dehydroalanine in nisin), and loop structures (Hancock, 1997; Hwang and Vogel, 1998).

The α -helical antimicrobial peptides were the first to be identified and characterized. The antimicrobial mechanisms of these helical peptides are therefore the most well understood. Most CAPs in this class exert their activity by causing membrane permeation and cell lysis via one of two general mechanisms: the 'barrel-stave' mechanism and the 'carpet' mechanism (Shai, 1999). The 'barrel-stave' model describes the formation of transmembrane channels and pores. Bundles of α -helices interact with the outer-membrane followed by the insertion of the hydrophobic face of the helices into the hydrophobic core of the membrane. In the 'carpet'

model, helices are not inserted into the hydrophobic core. Instead, they remain in contact with the phospholipid head group on the membrane and disintegrate or solubilize the membrane by disrupting the bilayer curvature.

As has been discussed in previous sections, lactoferricin forms a hairpin β -sheet structure, and thus belongs to the β -sheet class of CAPs. However, little is known about the mechanism by which this class of antimicrobial peptides produces membrane damage. It appears that different β -sheet CAPs have different antimicrobial mechanisms. No unique mode of action is identified for this group of CAPs (Wu et al., 1999).

In addition to the peptide structure, the chemical composition of the phospholipids of the microbial membrane is also a major determinant of the effectiveness of antimicrobial peptide. Charge-charge interactions, membrane curvature strain, and hydrophobic mismatch between peptides and lipids are all important parameters. For instance, a threshold peptide to lipid ratio is needed for the pore formation on the microbial membrane and the threshold level is specific for different microorganisms depending on their phospholipid composition (Lohner and Prenner, 1999; Huang, 2000).

1.3.2. Proposed Antimicrobial Mechanisms of Lactoferricin

A mechanism for the antimicrobial activity of lactoferricin derivatives has been postulated (Strøm et al., 2001). Like other CAPs, Lfcin must first penetrate through the cell wall of the bacteria. Haukland et al. (2001) reported similar MIC values of Lfcin for *E. coli*, Gram negative bacteria, and *S. aureus*, Gram positive bacteria, suggesting that the presence of the cell wall had no effect of the antimicrobial activity of Lfcin. Once Lfcin penetrated through the cell wall, Lfcin was able to establish interaction with its target microorganism via the positively charged amino acid residues on the peptide and the negatively charged outer membrane of the bacteria. LfcinB would interact with the lipopolysaccharides on the outer membrane of *E. coli*, and with teichoic acid on *S. aureus* (Volland et al., 1999). Once the Lfcin was attached to the membrane, electrostatic attraction might bring the hydrophobic residues such as tryptophan and tyrosine close to the lipophilic portions of the bacterial membrane. The hydrophobic amino acids on the Lfcin might migrate into the phospholipid layer, causing a depolarization of the bacterial inner membrane, and therefore interrupting the regular membrane function of the target bacteria (Ulvatne et al., 2001). Electron micrograph images showed that Lfcin induced the formation of blebs on the surface of *E. coli* (Ulvatne et al., 2001). However, unlike most other CAPs, Lfcin did not cause increases in membrane permeability of intact bacteria. A complete model for the bactericidal mechanisms of LfcinB has not been elucidated yet.

It was reported that Lfcin induced fusion of liposomes, and the fusion process may represent a means of transport of the antimicrobial peptide to cross the lipid barrier and eventually interact with cytoplasmic targets (Ulvatne et al., 2001). Tryptophan-containing antibacterial peptides have been shown to have the ability to inhibit DNA synthesis and protein synthesis (Subbalakshmi et al., 1996; Subbalakshmi and Sitaram, 1998). Lactoferrin from human milk has the ability to bind DNA and it was demonstrated that the DNA-binding site is in fact the antimicrobial domain of the protein (Kanyshkova et al., 1999). It was suggested that Lfcin could exert its antimicrobial activity by interacting with nucleic acids and preventing either replication or transcription of protein.

1.4. Phospholipid Bilayer

Since it is widely accepted that the antimicrobial mechanism of lactoferricin is dependent on its initial contact with the external side of the bacterial membrane, it is important to gain more insight into the structure of the phospholipid bilayer of the bacterial membrane.

The cell membrane is composed of a phospholipid bilayer that is interspersed by other lipid molecules such as cholesterol. This phospholipid bilayer functions to separate the aqueous environment inside and outside of the cell, whereas there is no water in the space between the phospholipid layers. The outside parts of the bilayer are described as being hydrophilic and the inside parts are described as being hydrophobic. Water soluble molecules entering the cell must find ways to pass through this phospholipid hydrophobic barrier (Dowhan, 1997).

The head-group composition of the phospholipids of *E. coli* is relatively invariant under a broad spectrum of growth conditions. On average, *E. coli* is composed of 70-80% of phosphatidylethanolamine (PE), 20-25% of phosphatidylglycerol (PG), and less than 5% of cardiolipin (CL) (Table 1.1). On contrary, PG is the most abundant phospholipids in *Micrococcus* sp. (Dowhan, 1997), responsible for 60 to 70% of the membrane. PE, PG, and CL are three major phospholipids found in the membrane of *Bacillus* sp. (Dowhand, 1997). Although less than 1% of the phospholipids in *Micrococcus* and *Bacillus* sp. are composed of PC, PC makes up 35% of *Bacillus megaterium* (Huijbregts et al., 2000).

The lipid composition of membranes is not constant (Opekarová and Tanner, 2003). The composition is tightly regulated to perform its physiological functions. For instance, the regulation of the acyl chain composition in wild-type cells of *E. coli* is necessary for the organism to be able to grow in a 'window' between a lamellar gel phase and reversed non-lamellar phase (Morein et al., 1996). The cells respond to a higher growth temperature by synthesizing lipids with shorter and more saturated acyl chains to maintain a semi-lamellar

phase. Under normal physiological conditions, position 1 of the phospholipid backbone is occupied predominantly by palmitic acid, and position 2 by the dominant monounsaturated fatty acids palmitoleic and *cis*-vaccenic acids. In cells grown at 37°C, the ratio of saturated to unsaturated fatty acids is about 1:1 (Dowhan, 1997).

1.5. Raman Spectroscopy

The phenomenon of Raman scattering was first described by Sir C. V. Raman in 1928. He observed that the wavelength of a small fraction of the visible radiation scattered by certain molecules differed from that of the incident beam and the shifts in wavelength depended upon the chemical structure of the molecules responsible for the scattering.

In Raman spectroscopy, the sample is first excited by a radiation source having a wavelength that is away from any absorption peaks of the analyte. The molecules will then interact with a photon from the energy source and be excited to a "virtual state" between the ground state and the first electronic excited state. Most of the excited molecules will return to their original energy level before excitation, producing a phenomenon known as Rayleigh scattering. However, approximately one in each million of photons will return to the first excited vibrational state and emit an energy lower than that of the original excitation laser. The lower emitted energy known as a Stokes-Raman shift would provide information on molecular vibrations that, in turn, yield data on structural conformation and the surrounding environment (Carey, 1999).

The vibrational states probed by Raman spectroscopy and infrared spectroscopy are very similar. In fact, these two vibrational spectroscopy techniques are complementary. Vibrations that involve strong dipole moments such as hydroxyl- or amine-stretching, and carbonyl groups are strong in an infrared spectrum and weak in a Raman spectrum. On the contrary, stretching vibrations of carbon double or triple bonds and symmetric vibrations of aromatic groups (non-polar) give very strong Raman bands but usually result in weak infrared signals.

1.5.1. Raman Spectroscopy: Structure – Function Relationship of Proteins

One of the major advantages of Raman spectroscopy is that both normal water (H₂O) and heavy water (D₂O) generate very weak Raman spectra. Thus, this analytical technique could be used to examine virtually any sample morphology. For proteins, this includes solutions, suspensions, precipitates, gels, films, fibers, single crystals, and polycrystalline and amorphous solids. The presence of water, which is almost unavoidable in food protein samples, would therefore create little interference in the Raman spectrum. Consequently, Raman spectroscopy is of particular interest as a tool to monitor *in situ* changes of proteins in

food systems during processing or storage, or accompanying phase transitions from solutions to emulsions, gels or precipitates (Pelton and McLean, 2000).

Raman spectroscopy is a valuable technique for the understanding of protein structures and conformations. The vibrational spectra of various amino acid side chains and the -CO-NH-peptide bond are sensitive to chemical changes and the surrounding microenvironments. For instance, the amide I and III bands (near 1660 cm^{-1} and 1240 cm^{-1} , respectively) are most commonly used for secondary structure characterization of the protein molecule including the levels of α -helix, antiparallel β -sheet, and disordered structure (Li-Chan, 1996). The intensity and location of Raman bands assigned to various stretching or bending vibrational modes of functional groups in the side chains of amino acid residues can be used to provide information on the chemistry and microenvironment of those residues. In particular, valuable information obtained for Raman bands near 530 , 650 , 725 , & 2550 cm^{-1} provide conformational information about the SS, SH, and SC groups of cystine, cysteine, and methionine residues, respectively. Microenvironment around CH structures such as those on aliphatic residues could be determined by Raman bands near 1450 and $2800\text{-}3000\text{ cm}^{-1}$. Side chain structure of tyrosine, tryptophan, phenylalanine, and histidine could also be analyzed (Li-Chan et al., 1994).

1.5.2. Raman Spectroscopy: Structure – Function Relationship of Peptides and Phospholipid Bilayers

Since the presence of water creates little interference in the Raman spectrum, Raman spectroscopy is being recognized as a valuable analytical tool for the understanding of protein and peptide structures in the biological system. For instance, model systems of poly(L-lysine) on phospholipid membranes were examined by Laroche et al. (1988 and 1990). Several studies have also been conducted to examine the conformational changes of tryptophan residues in gramicidin, a cationic antimicrobial pentadecapeptide, in phospholipid micelles and other membrane mimicking environments (Bouchard and Auger, 1993; Maruyama and Takeuchi, 1997 & 1998). The mechanisms of membrane pore formation induced by a 23-residue peptide, magainin, was also examined by Jackson et al. (1992) and Ludtke et al. (1996).

In addition to antimicrobial peptides, Raman spectroscopy has been used to examine conformational behaviours of other bioactive peptides, such as the secondary structure of a neuropeptide bound to liposomes (Williams and Weaver, 1990), the effects of synthetic human pulmonary surfactants on phospholipid bilayer (Vincent et al., 1993), and interactions between DNA and the telomere binding protein subunit (Laporte et al., 1999).

Raman spectroscopy can also be used to study the structural arrangement of phospholipids. Phospholipids commonly exist in three states (**Figure 1.5**). Classical

representations of phospholipid organization in membranes focus on lamellar or bilayer structures such as the ordered gel state (L_{β}) or fluid liquid crystalline state (L_{α}). *In vitro*, some natural phospholipids can assume nonbilayer structures such as the reversed hexagonal (H_{II}) phase. The temperature at the mid-point of transition (transition temperature, T_m) for the L_{β} -to- L_{α} transition, is a measure of a distinct collective property of the phospholipids making up a particular bilayer (Dowhan, 1997).

Two distinct Raman features observed in the C-H stretching mode region (2750 to 3050 cm^{-1}) of the hydrocarbon chains are used to elucidate the structural behaviour of the phospholipid bilayer. The 2850 and 2880 cm^{-1} Raman bands are assigned, respectively, to the symmetric and the asymmetric C-H stretching modes for the coupled methylene moieties of the hydrocarbon chains in the bilayer interior (Gaber and Peticolas, 1977). As temperature increases and upon melting, the intensity of the 2850 cm^{-1} band (I_{2850}) increases in intensity relative to the 2880 cm^{-1} band (I_{2880}) (**Figure 1.6a**). A greater relative peak-height intensity ratio I_{2850}/I_{2880} reflects weaker lateral interchain interactions in the bilayer (**Figure 1.6bA**). This intensity ratio is thus a sensitive probe for the intermolecular coupling and for the lateral packing of the acyl chains. As temperature increases and as the bilayer structure is transitioning from the ordered gel state (L_{β}) to fluid liquid crystalline state (L_{α}), the I_{2850}/I_{2880} ratio will experience a sudden change. Changes in the I_{2850}/I_{2880} ratio indicate the transition temperature, T_m (Snyder et al., 1978, 1980, and 1982).

The band around 2935 cm^{-1} mainly arises from the symmetric C-H stretching mode of terminal methyl groups in the hydrophobic center of the bilayer. As the temperature increases, the intensity of the 2935 cm^{-1} (I_{2935}) Raman band increases (**Figure 1.6bB**). The relative peak-height intensity ratio is therefore indicative of both the lattice packing order and the intrachain conformational order. This is an index of the overall disorder of the lipid acyl chain matrix (Gaber and Peticolas, 1977; Snyder et al., 1980; Vincent et al., 1993):

1.6. Multivariate Data Analysis Techniques

Multivariate data analysis techniques are needed for simultaneous consideration of several variables in complex systems and identification of patterns of interest. Multivariate data analysis techniques have gained much importance in medicinal chemistry and have been used in the understanding of protein signaling in apoptosis (Janes et al., 2003), tumor classification (Nguyen and Rocke, 2002), and the early detection of cancer (Chen et al., 2004; Skates and Iliopoulos, 2004) and heart diseases (Mateos-Caceres et al., 2004).

Among the various statistical methods, principal component analysis (PCA) and partial least squares (PLS) regression are the most commonly used techniques for the analysis of

structure–function relationships of peptides. Edman et al. (1999) used PCA and PLS to characterize sequence patterns and properties in signal peptides from mycoplasmas, Gram-positive bacteria, and *E. coli*. Structure-function relationships of anti-hypertensive peptides isolated from milk proteins were also studied using PCA (Pripp et al., 2004).

1.6.1. Principal Component Analysis

Principal component analysis (PCA) is one of the most popular unsupervised multivariate methods that decrease the complexity of a data set with no prior knowledge of the systems. It uses all the measured variables to examine the inter-relationship of the data by combining a large number of original variables to produce uncorrelated indices known as "principal components" (PC); minimal loss of information could be achieved. In addition, since the calculated PCs are uncorrelated, the overall data set could be adequately represented by a small number of PCs (Aishima and Nakai, 1991).

It is a common practice to visualize and interpret PCA results by plotting the first few major PCs. Sample classification could then be achieved by observing the grouping arrangement of the data points on the PC plots. Although it is possible to include up to three PCs in a 3-dimensional plot, visualization of 3-D plots could be difficult and might lead to poor or even incorrect interpretation of the PCA data. Hence, PC plots usually only depict two PCs at a time (e.g. PC1 versus PC2, PC1 versus PC3, PC2 versus PC3, etc.) Since only two PCs could be interpreted at a time, only limited total numbers of PCs would be analyzed. Furthermore, depending on which two PCs were plotted, different observations and interpretations could be made on the same set of data.

1.6.2. Partial Least Square Regression

Partial least squares (PLS) regression analysis is a type of supervised multivariate technique that can be used for pattern recognition and prediction (Aishima and Nakai, 1991). The emphasis of PLS is on predicting the responses based on many dependent variables and not on trying to understand the underlying relationship between the variables (Geladi and Kowalski, 1986). PLS is based on double principal component analysis. The analysis of one data set is guided by the structure of a second data set (the dependent variables), which is in turn used for modeling both the first and second sets of data. In a comparative study reported by Garthwaite (1994), when there were a large number of variables and random error variance, PLS was shown to be more powerful in predicting equations than principal component analysis.

1.6.3. Principal Component Similarity Analysis

A relatively new unsupervised multivariate analysis technique, principal component similarity (PCS) analysis, combines principal component analysis (PCA) and pattern similarity

computation (Aishima et al., 1987). The procedure for PCS analysis described by Horimoto et al. (1997) is adapted below:

Step 1. Apply PCA to the original set of samples for k parameters and n samples to derive k PCs and k eigenvalues E and then steps 2 to 5 are followed for each sample.

Step 2. Compute independent variable variance V as follows:

$$P_i = E_i / \sum E_k \quad \text{Equation 1}$$

$$V_i = 100 (1 - \sum P_i) \quad \text{Equation 2}$$

where i is the principal component number. In general, only PCs with E_i higher than 1.0 would be included in the computation.

Step 3. Compute dependent variables Y as follows:

$$Y_i = V_i + M (PC_i - PC_q) \quad \text{Equation 3}$$

where q is the reference and M is percentage of variance of each principal component factor.

Step 4. Carry out linear regression analysis for Y versus V for each sample at each time to compute correlation coefficient (r^2) and slope (S).

Step 5. Plot S (slope) versus r^2 .

Step 6. The resultant plot could be used for classification of the original set of samples.

PCS can effectively reduce the number of original variables needed for analysis to just a few selected principal components as PCA is applied (Step 1). The most important advantage of PCS over the traditional PCA technique is that results of several PCs could be considered and interpreted at the same time (Steps 2 & 3). Thus, PCS could be used to explain maximum variability observed in the available data.

Since PCS is a relatively new multivariate statistical method, some of its applications in food samples will be described. PCS was reported for the first time to analyze gas chromatographic data to distinguish mangoes of different cultivars (Vodovotz et al., 1993). It was later applied to analyze HPLC data of cheddar cheese to identify quality defects (Furtula et al., 1994a and 1994b). PCS analysis was also capable of distinguishing milk samples inoculated with *Pseudomonas fragi*, *P. fluorescens*, *Lactococcus lactis*, *Enterobacter aerogenes*, and their mixed culture from uninoculated samples (Horimoto et al., 1997) and identifying an unexpected new type of beany flavor in soymilk that was not detected by a sensory panel (Wang et al., 1997). Detection of *Escherichia coli* and *Staphylococcus aureus* contaminated salmon patties and hamburger patties was also possible using PCS to analyze gas chromatography data of volatile compounds in the samples (Nakai et al., 1999).

1.6.4. Multivariate Data Analysis: Structure – Function Relationship of Lactoferricin and Its Derivatives

Principal component analysis (PCA) was used to analyze the structure – function relationship of eight Lfcin analogs using 10 structural property descriptors, namely, number of amino acids, mean hydrophobicity, Kyte-Doolittle hydrophobicity, mean hydrophobic moment, hydrophobic moment, mean charge moment, charge moment, Garnier α , Chou-Fasman α , and Emini surface probability (Rekdal et al., 1999). Results showed that helicity, charge moments, and peptide length were important factors in the antibacterial activity of Lfcin derivatives.

Nevertheless, PCA alone was unable to link the structural properties with the biological activities of the peptides. Hence, partial least squares regression (PLS) was applied in addition to PCA to correlate peptide structure to antimicrobial ability of 19 synthetic 15-residue derivatives of murine lactoferricin (Strøm et al., 2001). A total of 12 structural property descriptors including 6 helical properties, 4 hydrophobicity data, and two charge parameters were utilized to define the entire peptide sequence. The MIC against *E. coli* and *S. aureus* were used as the dependent variables. PCA results showed that the descriptors used explained 82% of the variation in antimicrobial activity; net charge and micelle affinity were the most important structural parameters. When the structural parameters were used to predict the antimicrobial activity of these derivatives using PLS, a good correlation was obtained between the observed and predicted activity against *E. coli*.

In order to determine if theoretical descriptors of each amino acid in a peptide could be used to represent the entire peptide sequence, a matrix of 29 physicochemical variables for 20 coded amino acids were analyzed using PCA (Hellberg et al., 1987). Three principal components, z_1 , z_2 , and z_3 , were obtained and used in PLS analysis to relate chemical properties to the biological activities. This approach successfully predicted the biological activity of oxytocin, pepstatin, and bradykinin (Hellberg et al., 1987). The z_1 , z_2 , and z_3 descriptors and the PLS approach were adapted to predict the antimicrobial activity of Lfcin analogs (Lejon et al., 2001a). Results showed that in addition to charge and micelle affinity as reported in Strøm et al. (2000), lipophilicity of the peptide was equally important. It was concluded that the activity of peptides predicted by using PCA derived descriptors, z_1 , z_2 , and z_3 , of each amino acid in a peptide provided better antimicrobial activity predictions than using the structural properties of the entire peptides (Lejon et al., 2001a).

However, the above approach would only consider the amino acid composition of the entire peptide; sequential locations and arrangements were not considered. Based on the results of previous studies, it was noted that the effects of substituting an amino acid with another amino acid on the antimicrobial properties could be significantly affected by the specific

location of substitution along the peptides. Hence, it is crucial to consider the sequence of the amino acids while assessing the structure –function relationship of peptides. It was suggested that the position of a specific amino acid in a peptide is of importance to the physico-chemical behaviour of the peptide and information that distinguishes between positions within the peptide is needed to improve results from PCA and PLS analysis (Lejon et al., 2001b).

To consider the position and sequential information of specific amino acids in a peptide, a new statistical program, Homology Similarity Analysis (HSA) was developed. Using HSA, specific structural properties (hydrophobicity, helicity, strand propensity, turn propensity, bulkiness, charge, and hydrogen bonding propensity) of each amino acid in a designated sequence of a sample peptide are compared the corresponding amino acid in the corresponding location in the sequence of a reference peptide (Nakai et al., 2003). Property indices of the amino acids in the sample peptide are plotted against the amino acids in the reference peptide. Linear regression is carried out and the resulting regression coefficient (r^2) is computed as the Homology Similarity Coefficient. HSA is therefore focused on the similarity within segments around conserved sites in the sequences, which could be playing important roles in functions, such as active site and binding site. Hence, information that distinguishes between positions of a specific amino acid with a peptide could be more accurately evaluated and the bioactivity of a peptide can be more clearly explained using HSA (Nakai et al., 2003).

1.7. Hypotheses

1. Lactoferricin and other cationic peptides can be produced by enzymatic digestion of food-grade lactoferrin.
2. The production of lactoferricin and its related peptides are affected by the level of iron saturation of lactoferrin.
3. Structure-function relationships of lactoferricin and its derivatives can be elucidated using multivariate data analysis techniques.
4. Lactoferricin can induce changes in model phospholipid bilayers.
5. Presence and absence of particular amino acids, namely arginine and tryptophan, in lactoferricin can affect the behaviour of lactoferricin on model phospholipid bilayers.

1.8. Objectives

The specific objectives are to:

1. Produce lactoferricin by peptic digestion of food-grade bovine lactoferrin,
2. Evaluate the effects of iron saturation on the profile of cationic peptides produced by peptic digestion of lactoferrin,
3. Elucidate the structure-function relationship of lactoferricin and its derivatives using homology similarity analysis and multivariate data analysis techniques including principal component similarity and artificial neural network,
4. Examine the changes in phospholipid bilayers at different temperatures in the presence or absence of lactoferricin by vibrational spectroscopic techniques, and
5. Observe the effects of arginine and tryptophan moieties in Lfcin on the structures of phospholipid liposomes.

```

1          11          21          31          41          51
APRKNVRWCT ISQPEWFKCR RWQWRMKKLG APSITCVRRR FALECIIRAIA EKKADAVTLD
          **** *
61
GGMVFEAGRD PYKLRPVAEE IYGTKESPQT HYYAVAVVKK GSNFQLDQLQ GRKSCHTGLG
          +
121
RSAGWIIPMG ILRPYLSWTE SLEPLQGAVA KFFSASCVPC IDRQAYPNLC QLCKGEGENQ

181
CACSSREPYF GYSGAFKCLQ DGAGDVAFVK ETTVFENLPE KADRQYELL CLNNSRAPVD
          +
241
AFKECHLAQV PSHAVVARSV DGKEDLIWKL LSQAQEKFGK NKSRSFQLFG SPPGQRDLLF
          +
301
KDSALGFLRI PSKVDSALYL GSRYLTTLKN LRETAEVKA RYTRVVWCAV GPPEQKKCQQ

361
WSQQSQGNVT CATASTTDDC IVLVLKGEAD ALNLDGGYIY TAGKCGLVPV LAENRKSSKH
          ^
421
SSLDCVLRPT EGYLAVAVVK KANEGLTWNS LKDKKSCHTA VDRTAGWNIP MGLIVNQTGS
          ^
481
CAFDEFFSQS CAPGADPKSR LCALCAGDDQ GLDKCVPNSK EKYYGYTGAF RCLAEDVGDV
          ^
541
AFVKNDTVWE NTNGESTADW AKNLNREDFR LLCLDGTRKP VTEAQSCHLA VAPNHAVVSR
          ^
601
SDRAAHVKQV LLHQQALFGK NGKNCPDKFC LFKSETKNLL FNDNTECLAK LGGRPTYEEY

661
LGTEYVTAIA NLKKCSTSPL LEACAFLTR

```

Figure 1.1. Primary amino acid sequence (single letter code) of bovine lactoferrin. * denotes residues 17 to 42, representing the antimicrobial peptide, lactoferricin. + denotes the major contributors to one of the two iron-binding sites, and ^ denotes the major contributors to the second iron-binding site (adapted from Pierce et al., 1991).

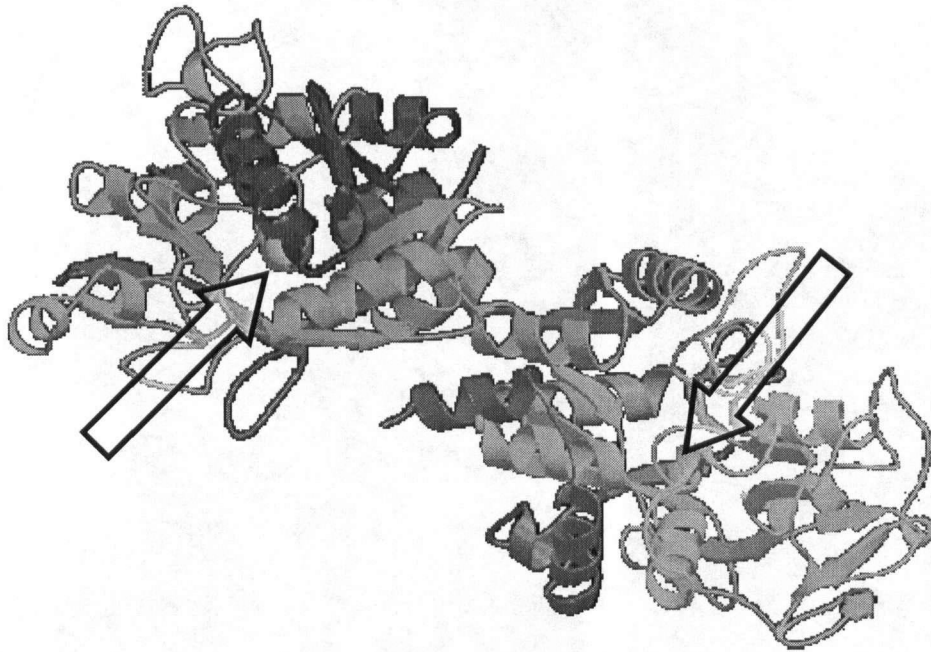


Figure 1.2. Three-dimensional structure of diferric bovine lactoferrin at 2.8 Å resolution where the arrows indicate the location of bound iron (Reprinted from Moore et al., 1997, Copyright 1997, with permission from Elsevier).

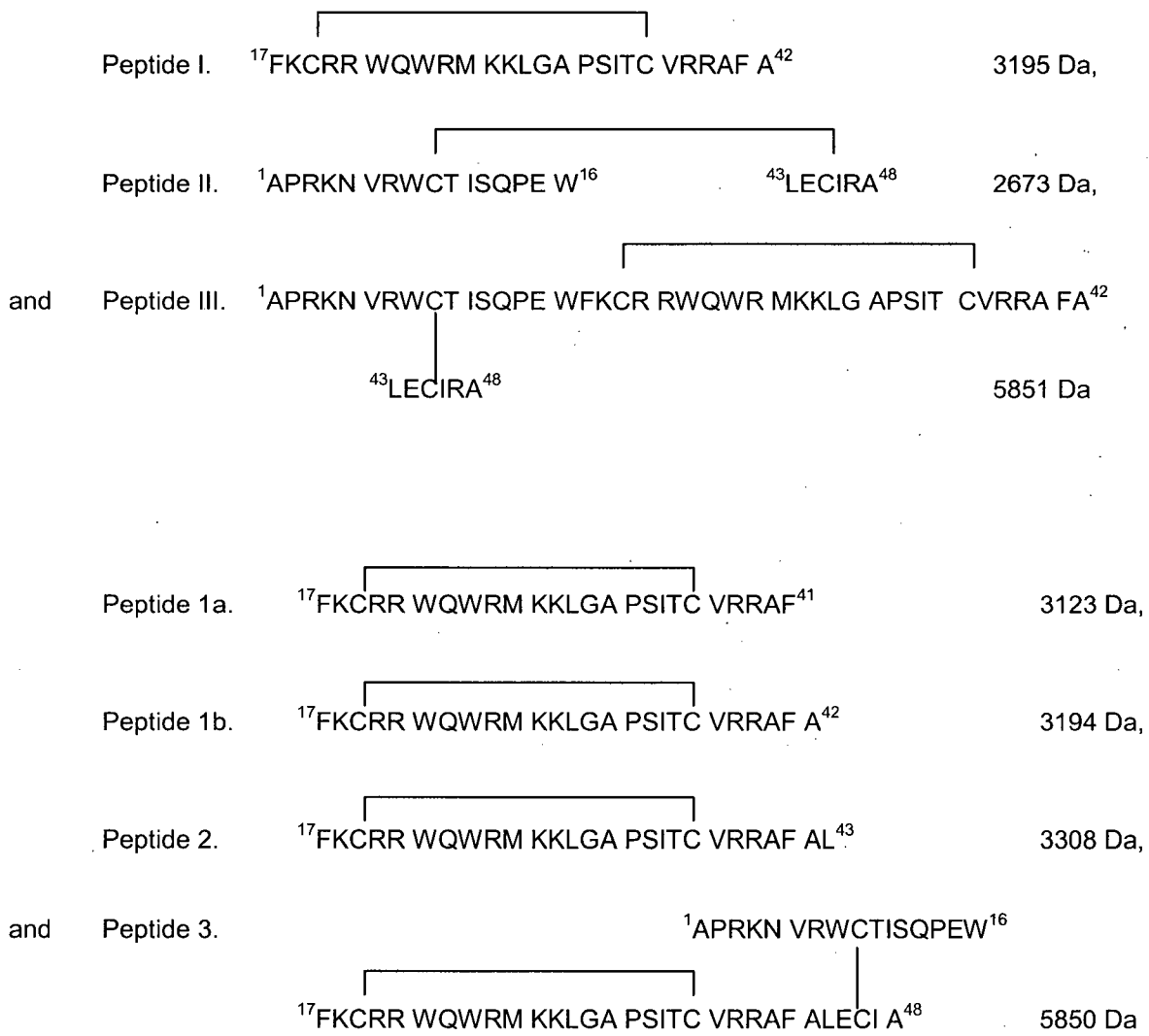


Figure 1.3. Antimicrobial peptide fragments isolated from bovine lactoferrin as reported in the literature; Peptides I, II, III are from Dionysius and Milne (1997) and Peptides, 1a, 1b, 2, and 3 are from Hoek et al. (1997).

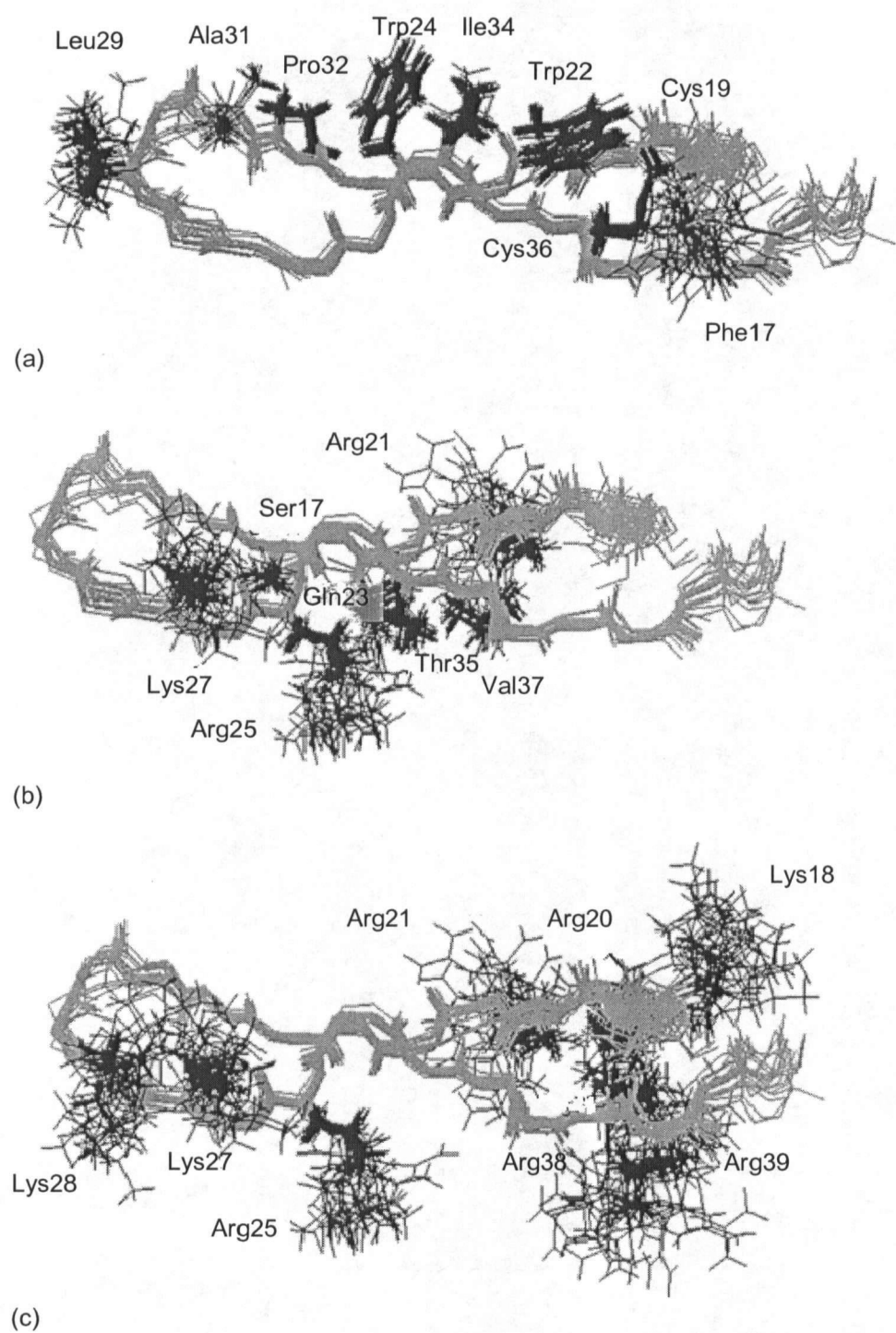


Figure 1.4. Hydrophobic (a), hydrophilic (b), and positive (c) side chains along the β -strands of bovine lactoferricin. The backbone of all residues is shown in gray, while the highlighted side chains are in black (Reprinted from Hwang et al., 1998, Copyright 1998, with permission from American Chemical Society).

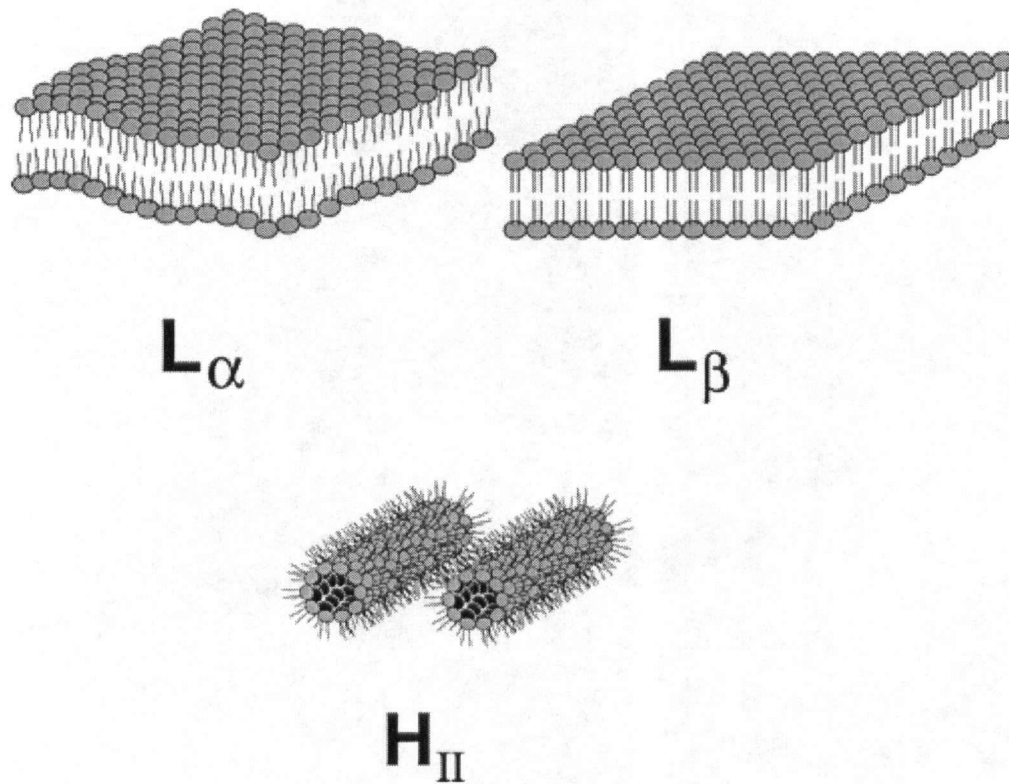


Figure 1.5. Structural representation of the arrangement of phospholipids. Arrangement of the head group and fatty acid domains of phospholipids in the fluid liquid crystalline state (L_{α}), the ordered gel state (L_{β}), and the reversed hexagonal state (H_{II}) (Reprinted from Dowhan, 1997, Copyright 1997, with permission from the Annual Reviews www.annualreviews.org).

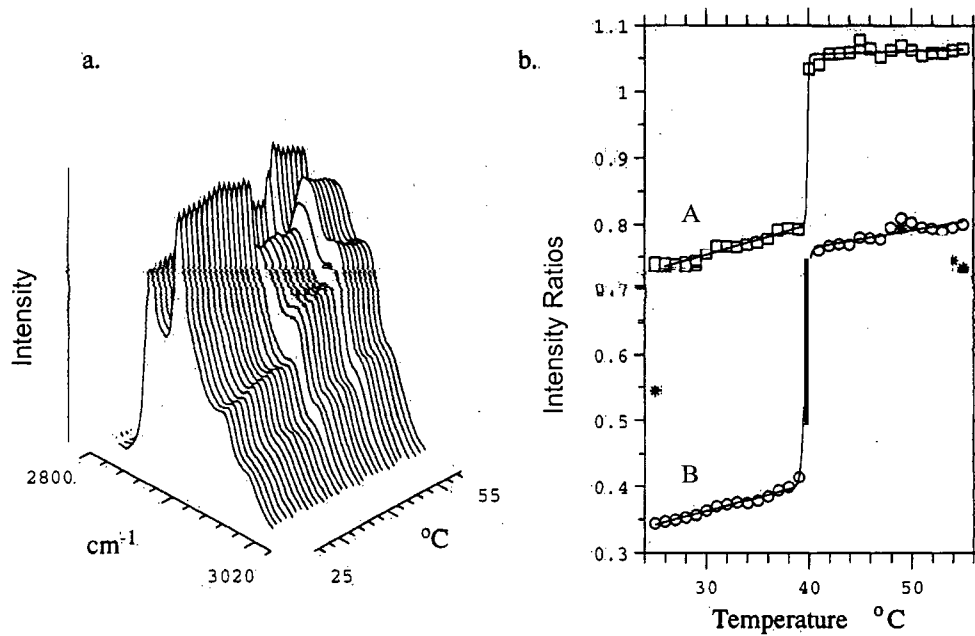


Figure 1.6. Raman spectra of dipalmitoylphosphatidylglycerol (DPPG) in the C-H stretching mode region (2800-3000 cm⁻¹) between 25 and 55 °C (a). Peak height intensity ratios (b): I_{2850}/I_{2880} (A) and I_{2935}/I_{2880} (B) (Reprinted from Vincent et al., 1993, Copyright 1993, with permission from American Chemical Society).

Table 1.1. Percentage of phosphatidylcholine (PC), phosphatidylethanolamine (PE), phosphatidylglycerol (PG), and 1,3-bis(sn-3-phosphatidyl)-sn-glycerol (cardiolipin, CL) in bacterial membranes.

Organism	Percentages of Total Phospholipids				References
	PC	PE	PG	CL	
Gram-positive					
<i>Micrococcus</i> sp.	< 1	< 1	60-70	4-20	Dowhan, 1997
<i>Bacillus</i> sp.	< 1	20-45	25-45	10-50	Dowhan, 1997
<i>Bacillus megaterium</i>	35	48	6	11	Huijbregts et al. 2000
Gram-negative					
<i>Azotobacter</i> sp.	1-2	60-70	25-30	2-5	Dowhan, 1997
<i>Rhodopseudomonas</i> sp.	10-15	45-50	40-50	< 1	Dowhan, 1997
<i>Escherichia coli</i>		70-80	20-25	< 5	Dowhan, 1997
<i>E. coli</i> wild-type strain K12		70-80	15-20	5-20	Morein et al., 1996

1.9. References

- Aishima, T.; Nakai, S. Chemometrics in flavour research. *Food Rev. Int.* **1991**, *7*, 33-101.
- Aishima, T.; Wilson, D. L.; Nakai, S. Application of simple algorithm to flavour optimization based on pattern similarity of GC profile. In *Flavour Science and Technology*. (Eds M. Martens, G. A. Dallen, and H. Russwurm) **1987**. Chichester UK: John Wiley & Sons Ltd., pp. 501-508.
- Andersen, J.; Osbakk, S.; Vorland, L.; Traavik, T.; Gutteberg, T. Lactoferrin and cyclic lactoferricin inhibit the entry of human cytomegalovirus into human fibroblasts. *Antiviral Res.* **2001**, *51*, 141-149.
- Anderson, B. F.; Baker, H. M.; Dodson, E. F.; Norris, G. E.; Rumball, S. V.; Waters, J. M.; Baker, E. N. Structure of human lactoferrin at 3.2Å resolution. *Proc. Natl. Acad. Sci. USA.* **1987**, *84*, 1769-1773.
- Anderson, B. F.; Baker, H. M.; Norris, G. E.; Rice, D. W.; Baker, E. N. Structure of human lactoferrin: crystallographic structure analysis and refinement at 2.8Å resolution. *J. Mol. Biol.* **1989**, *209*, 711-734.
- Antonini, G.; Catania, M. R.; Greco, R.; Longhi, C.; Pisciotto, M. G.; Seganti, L.; Valenti, P. Anti-invasive activity of bovine lactoferrin against *Listeria monocytogenes*. *J. Food Prot.* **1997**, *60*, 267-271.
- Arnold, R. R.; Brewer, M.; Gauthier, J. J. Bactericidal activity of human lactoferrin: sensitivity of a variety of microorganisms. *Infect. Immun.* **1980**, *28*, 893-898.
- Arnold, R. R.; Russell, J. E.; Champion, W. J.; Brewer, M.; Gauthier, J. J. Antibacterial activity of human lactoferrin: differentiation from the stasis of iron deprivation. *Infect. Immun.* **1982**, *35*, 792-799.
- Bechinger, B. Structure and functions of channel-forming peptides: magainins, cecropins, melittin and alamethicin. *J. Membrane Biol.* **1997**, *156*, 197-211.
- Beljaars, L.; Bakker, H.; van der Strate, B.; Smit, C.; Duijvestijn, A.; Meijer, D.; Molema, G. The antiviral protein human lactoferrin is distributed in the body to cytomegalovirus (CMV) infection-prone cells and tissues. *Pharm. Res.* **2002**, *19*, 54-62.
- Bellamy, W.; Takase, M.; Wakabayashi, H.; Kawase, K.; Tomita, M. Antibacterial spectrum of lactoferricin B, a potent bactericidal peptide derived from the N-terminal region of bovine lactoferrin. *J. Appl. Bacteriol.* **1992a**, *73*, 472-479.
- Bellamy, W.; Takase, M.; Yamauchi, K.; Wakabayashi, H.; Kawase, K.; Tomita, M. Identification of the bactericidal domain of lactoferrin. *Biochim. Biophys. Acta* **1992b**, *1121*, 130-136.
- Bellamy, W.; Wakabayashi, H.; Takase, M.; Kawase, K.; Shimamura, S.; Tomita, M. Killing of *Candida albicans* by lactoferricin B, a potent antimicrobial peptide derived from the N-terminal region of bovine lactoferrin. *Med. Microbiol. Immunol.* **1993**, *182*, 97-105.
- Bellamy, W.; Yamauchi, K.; Wakabayashi, H.; Takase, M.; Takakura, N.; Shimamura, S.; Tomita, M. Antifungal properties of lactoferricin B, a peptide derived from the N-terminal region of bovine lactoferrin. *Lett. Appl. Microbiol.* **1994**, *18*, 230-233.

- Bouchard, M.; Auger, M. Solvent history dependence of gramicidin-lipid interactions: a Raman and infrared spectroscopic study. *Biophys. J.* **1993**, *65*, 2484-2492.
- Brock, J. Lactoferrin: a multifunctional immunoregulatory protein? *Immunol. Today* **1995**, *16*, 417-419.
- Bullen, J. J.; Rogers, H. J.; Leigh, L. Iron-binding proteins in milk and resistance to *Escherichia coli* infections in infants. *Br. Med. J.* **1972**, *1*, 69-75.
- Carey, P. R. Raman spectroscopy, the sleeping giant in structural biology, awakes. *J. Biol. Chem.* **1999**, *274*, 26625-26628.
- Chan, J. C. K.; Li-Chan, E. C. Y. Antimicrobial Peptides. In *Nutraceutical Proteins and Peptides in Health and Disease*. (Eds. Y. Mine and F. Shahidi.) **2006**. Boca Raton: CRC/Taylor and Francis, pp. 99-136.
- Chantaysakorn, P.; Richter, R. L. Antimicrobial properties of pepsin-digested lactoferrin added to carrot juice and filtrates of carrot juice. *J Food Prot.* **2000**, *63*, 376-380.
- Chapple, D. S.; Mason, D. J.; Joannou, C. L.; Odell, E. W.; Gant, V.; Evans, R. W. Structure-function relationship of antibacterial synthetic peptides homologous to a helical surface region on human lactoferrin against *Escherichia coli* serotype O111. *Infect. Immun.* **1998**, *66*, 2434-2440.
- Chen, Y.; Shi, G.; Xia, W.; Kong, C.; Zhao, S.; Gaw, A. F.; Chen, E. Y.; Yang, G. P.; Giaccia, A. J.; Le, Q.-T.; Koong, A. C. Identification of hypoxia-regulated proteins in head and neck cancer by proteomic and tissue array profiling. *Cancer Res.* **2004**, *64*, 7302-7310.
- Dionysius, D. A.; Milne, J. M. Antibacterial peptides of bovine lactoferrin: purification and characterization. *J. Dairy Sci.* **1997**, *80*, 667-674.
- Dowhan, W. Molecular basis for membrane phospholipid diversity: why are there so many lipids? *Ann. Rev. Biochem.* **1997**, *66*, 199-232.
- Edman, M.; Jarhede, T.; Sjöström, M.; Wieslander, Å. Different sequence patterns in signal peptides from mycoplasmas, other Gram-positive bacteria, and *Escherichia coli*: a multivariate data analysis. *Proteins.* **1999**, *35*, 195-205.
- Ellison, R. T. I.; Giehl, T. J. Killing of gram-negative bacteria by lactoferrin and lysozyme. *J. Clin. Invest.* **1991**, *88*, 1080-1091.
- Ellison, R. T. I.; Giehl, T. J.; LaForce, F. M. Damage of the outer membrane of enteric gram-negative bacteria by lactoferrin and transferrin. *Infect. Immun.* **1988**, *56*, 2774-2781.
- Epand, R. M.; Vogel, H. J. Diversity of antimicrobial peptides and their mechanisms of action. *Biochim. Biophys. Acta* **1999**, *1462*, 11-28.
- Facon, M. J.; Skura, B. J. Antibacterial activity of lactoferricin, lysozyme and EDTA against *Salmonella enteritidis*. *Int. Dairy J.* **1996**, *6*, 303-313.
- Farnaud, S.; Evans, R. W. Lactoferrin - a multifunctional protein with antimicrobial properties. *Mol. Immunol.* **2003**, *40*, 395-405.
- Furtula, V.; Nakai, S.; Amantea, G. F.; Laleye, L. Reverse-phase HPLC analysis of cheese samples aged by a fast-ripening process. *J. Food Sci.* **1994a**, *59*, 528-532, 567.

- Furtula, V.; Nakai, S.; Amantea, G. F.; Laleye, L. Reverse phase HPLC analysis of reference cheddar cheese samples for assessing accelerated cheese ripening. *J. Food Sci.* **1994b**, *59*, 533-538.
- Gaber, B. P.; Peticolas, W. L. On the quantitative interpretation of biomembrane structure by Raman spectroscopy. *Biochim. Biophys. Acta* **1977**, *465*, 260-274.
- Garthwaite, P. H. An interpretation of partial least squares. *J. Am. Stat. Assoc.* **1994**, *89*, 122-127.
- Geladi, P.; Kowalski, B. Partial least-squares regression: A tutorial. *Anal. Chimica Acta* **1986**, *185*, 1-17.
- Gifford, J. L.; Hunter, H. N.; Vogel, H. J. Lactoferricin: a lactoferrin-derived peptide with antimicrobial, antiviral, antitumor and immunological properties. *Cell Mol. Life Sci.* **2005**, *62*, 2588-2598.
- Groves, M. L. The isolation of a red protein from milk. *J. Am. Chem. Soc.* **1960**, *82*, 3345-3350.
- Hadden, J. M.; Bloemendal, M.; Haris, P. I.; Srari, S. K. S.; Chapman, D. Fourier transform infrared spectroscopy and differential scanning calorimetry of transferrins: human serum transferrin, rabbit serum transferrin and human lactoferrin. *Biochim. Biophys. Acta* **1994**, *1205*, 59-67.
- Hancock, R. E. W. Peptide antibiotics. *Lancet* **1997**, *349*, 418-422.
- Harmsen, M. C.; Swart, P. J.; de Bethune, M. P.; Pauwels, R.; De Clercq, E.; The, T. H.; Meijer, D. K. Antiviral effects of plasma and milk proteins: lactoferrin shows potent activity against both human immunodeficiency virus and human cytomegalovirus replication *in vitro*. *J. Infect. Dis.* **1995**, *172*, 380-388.
- Haug, B. E.; Svendsen, J. S. The role of tryptophan in the antibacterial activity of a 15-residue bovine lactoferricin peptide. *J. Pept. Sci.* **2001**, *7*, 190-196.
- Haug, B. E.; Skar, M. L.; Svendsen, J. S. Bulky aromatic amino acids increase the antibacterial activity of 15-residue bovine lactoferricin derivatives. *J. Pept. Sci.* **2001**, *7*, 425-432.
- Haukland, H. H.; Ulvatne, H.; Sandvik, K.; Vorland, L. H. The antimicrobial peptides lactoferricin B and magainin 2 cross over the bacterial cytoplasmic membrane and reside in the cytoplasm. *FEBS Lett.* **2001**, *508*, 389-393.
- Hellberg, S.; Sjöström, M.; Skagerberg, B.; Wold, S. Peptide quantitative structure-activity relationships, a multivariate approach. *J. Med. Chem.* **1987**, *30*, 1126-1135.
- Hennart, P. F.; Brasseur, D. J.; Delogne-Desnoeck, J. B.; Dramaix, M. M.; Robyn, C. E. Lysozyme, lactoferrin, and secretory immunoglobulin A content in breast milk: influence of duration of lactation, nutrition status, prolactin status and parity of mother. *Am. J. Clin. Nutr.* **1991**, *53*, 32-39.
- Hentges, D. J.; Marsh, W. W.; Petschow, B. W.; Thal, W. R.; Carter, M. K. Influence of infant diets on the ecology of the intestinal tract of human flora-associated mice. *J. Pediatr. Gastroent. Nutr.* **1992**, *14*, 146-152.

- Hoek, K. S.; Milne, J. M.; Grieve, P. A.; Dionysius, D. A.; Smith, R. Antibacterial activity of bovine lactoferrin-derived peptides. *Antimicrob. Agents Chemother.* **1997**, *41*, 54-59.
- Horimoto, Y.; Lee, K.; Nakai, S. Classification of microbial defects in milk using a dynamic headspace gas chromatograph and computer-aided data processing. 1. Principal component similarity analysis. *J. Agric. Food Chem.* **1997**, *45*, 733-742.
- Huang, H. W. Action of antimicrobial peptides: two-state model. *Biochemistry* **2000**, *39*, 8347-8352.
- Huang, S.-W.; Satué-Gracia, T.; Frankel, E. N.; German, J. B. Effect of lactoferrin on oxidative stability of corn oil emulsions and liposomes. *J. Agric. Food Chem.* **1999**, *47*, 1356-1361.
- Huijbregts, R.; Anton, I.; de Kroon, A.; de Kruijff, B. Topology and transport of membrane lipids in bacteria. *Biochim. Biophys. Acta* **2000**, *1469*, 43-61.
- Hutchens, T. W.; Rumball, S. V.; Lonnerdal, B. Lactoferrin: Structure and Function. In *Advances in Experimental Medicine and Biology*. (Eds T. W. Hutchens, S. V. Rumball, B. Lönnerdal) **1994**, 357. New York: Plenum Press, pp. 21-32.
- Hwang, P. M.; Vogel, H. J. Structure-function relationships of antimicrobial peptides. *Biochem. Cell Biol.* **1998**, *76*, 235-246.
- Hwang, P. M.; Zhou, N.; Shan, X.; Arrowsmith, C. H.; Vogel, H. J. Three dimensional solution structure of lactoferricin B, an antimicrobial peptide derived from bovine lactoferrin. *Biochemistry* **1998**, *37*, 4288-4298.
- Iigo, M.; Kuhara, T.; Ushida, Y.; Sekine, K.; Moore, M. A.; Tsuda, H. Inhibitory effects of bovine lactoferrin on coon carcinoma 26 lung metastasis in mice. *Clin. Exp. Metastasis* **1999**, *17*, 35-40.
- Ikeda, M.; Sugiyama, K.; Tanaka, T.; Tanaka, K.; Sekihara, H.; Shimotohno, K.; Kato, N. Lactoferrin markedly inhibits hepatitis C virus infection in cultured human hepatocytes. *Biochem. Biophys. Res. Commun.* **1998**, *245*, 549-553.
- Ikeda, M.; Nozaki, A.; Sugiyama, K.; Tanaka, T.; Naganuma, A.; Tanaka, K.; Sekihara, H.; Shimotohno, K.; Saito, M.; Kato, N. Characterization of antiviral activity of lactoferrin against hepatitis C virus infection in human cultured cells. *Virus Res.* **2000**, *66*, 51-63.
- Jackson, M.; Mantsch, H. H.; Spencer, J. H. Conformation of magainin-2 and related peptides in aqueous solution and membrane environments probed by fourier transform infrared spectroscopy. *Biochemistry* **1992**, *31*, 7289-7293.
- Janes, K. A.; Albeck, J. G.; Peng, L. X.; Sorger, P. K.; Lauffenburger, D. A.; Yaffe, M. B. A high-throughput quantitative multiplex kinase assay for monitoring information flow in signaling networks: Application to sepsis-apoptosis. *Mol. Cell. Proteomics* **2003**, *2*, 463-473.
- Johansson, B. Isolation of an iron containing red protein from human milk. *Acta Chem. Scand.* **1960**, *14*, 510-512.
- Kang, J. H.; Lee, M. K.; Kim, K. L.; Hahm, K.-S. Structure-biological activity relationships of 11-residue highly basic peptide segment of bovein lactoferrin. *Int. J. Pept. Protein Res.* **1996**, *48*, 357-363.

- Kanyshkova, T. G.; Semenov, D. V.; Buneva, V. N.; Nevinsky, G. A. Human milk lactoferrin binds two DNA molecules with different affinities. *FEBS Lett.* **1999**, *451*, 235-237.
- Kappeler, S. R.; Ackermann, M.; Farah, Z.; Puhán, Z. Sequence analysis of camel (*Camelus dromedarius*) lactoferrin. *Int. Dairy J.* **1999**, *9*, 481-486.
- Kawasaki, Y.; Tazume, S.; Shimizu, K.; Matsuzawa, H.; Dosako, S.; Isoda, H.; Tsukiji, M.; Fujimura, R.; Muranaka, Y.; Isihida, H. Inhibitory effects of bovine lactoferrin on the adherence of enterotoxigenic *Escherichia coli* to host cells. *Biosci. Biotechnol. Biochem.* **2000**, *64*, 348-354.
- Laporte, L.; Benevides, J. M.; Thomas, G. J. J. Molecular mechanism of DNA recognition by the a subunit of the *Oxytricha* telomere binding protein. *Biochemistry* **1999**, *38*, 582-588.
- Laroche, G.; Carrier, D.; Pezolet, M. Study of the effect of poly(L-lysine) on phosphatidic acid and phosphatidylcholine/ phosphatidic acid bilayers by Raman spectroscopy. *Biochemistry* **1988**, *27*, 6220-6228.
- Laroche, G.; Dufourc, E. J.; Pezolet, M.; Dufourcq, J. Coupled changes between lipid order and polypeptide conformation at the membrane surface. A 2H NMR and Raman study of polylysine-phosphatidic acid systems. *Biochemistry* **1990**, *29*, 6460-6465.
- Lejon, T.; Strøm, M. B.; Svendsen, J. S. Antibiotic activity of pentadecapeptides modelled from amino acid descriptors. *J. Pept. Sci.* **2001a**, *7*, 74-81.
- Lejon, T.; Strøm, M. B.; Svendsen, J. S. Is information about peptide sequence necessary in multivariate analysis? *Chemometrics Intelligent Lab. Sys.* **2001b**, *57*, 93-95.
- Levay, P. F.; Viljoen, M. Lactoferrin: a general review. *Haematologica* **1995**, *80*, 252-267.
- Lewis, R. N. A. H.; McElhaneý, R. N. Vibrational spectroscopy of lipids. **2002**. John Wiley & Sons Ltd.
- Li-Chan, E. C. Y. The applications of Raman spectroscopy in foods science. *Trends Food Sci. Technol.* **1996**, *7*, 361-370.
- Li-Chan, E. C. Y.; Nakai, S.; Hirotsuka, M. Raman spectroscopy as a probe of protein structure in food systems. In *Protein Structure-Function Relationships in Foods*. (Eds R. Y. Yada, R. L. Jackman, and J. L. Smith) **1994**. New York: Blackie Academic & Professional, pp. 163-197
- Lohner, K.; Prenner, E. J. Differential scanning calorimetry and X-ray diffraction studies of the specificity of the interaction of antimicrobial peptides with membrane-mimetic systems. *Biochim. Biophys. Acta* **1999**, *1462*, 141-156.
- Ludtke, S. J.; He, K.; Heller, W. T.; Harroun, T. A.; Yang, L.; Huang, H. W. Membrane pores induced by magainin. *Biochemistry* **1996**, *35*, 13723-13728.
- Mader, J. S.; Salsman, J.; Conrad, D. M.; Hoskin, D. W. Bovine lactoferricin selectively induces apoptosis in human leukemia and carcinoma cell line. *Mol. Cancer Ther.* **2005**, *4*, 612-624.
- Maruyama, T.; Takeuchi, H. Water accessibility to the tryptophan indole N-H sites of gramicidin A transmembrane channel: Detection of positional shifts of tryptophans 11 and 13 along the channel axis upon cation binding. *Biochemistry* **1997**, *36*, 10993-11001.

- Maruyama, T.; Takeuchi, H. Raman linear intensity difference of membrane-bound peptides: indole ring orientations of tryptophans 11 and 13 in the gramicidin A transmembrane channel. *Biospectroscopy* **1998**, *4*, 171-184.
- Marchetti, M.; Superti, F.; Ammendolia, M.; Rossi, P.; Valenti, P.; Seganti, L. Inhibition of poliovirus type 1 infection by iron-, manganese- and zinc-saturated lactoferrin. *Med. Microbiol. Immunol.* **1999**, *187*, 199-204.
- Masson, P. L.; Heremans, J. F. Lactoferrin in milk from different species. *Comp. Biochem. Physiol.* **1971**, *39B*, 119-129.
- Masuda, C.; Wanibuchi, H.; Sekine, K.; Yano, Y.; Otani, S.; Kishimoto, T.; Tsuda, H.; Fukushima, S. Chemopreventive effects of bovine lactoferrin on N-butyl-N-(4-hydroxybutyl)-nitrosamine-induced rat bladder carcinogenesis. *Jpn. J. Cancer Res.* **2000**, *90*, 262-267.
- Mata, L.; Sánchez, L.; Headon, D. R.; Calvo, M. Thermal denaturation of human lactoferrin and its effect on the ability to bind iron. *J. Agric. Food Chem.* **1998**, *46*, 3964-3970.
- Mateos-Caceres, P. J.; Garcia-Mendez, A.; Lopez Farre, A.; Macaya, C.; Nunez, A.; Gomez, J.; Alonso-Orgaz, S.; Carrasco, C.; Burgos, M. E.; de Andres, R.; Granizo, J. J.; Farre, J.; Rico, L. A. Proteomic analysis of plasma from patients during an acute coronary syndrome. *J. Am. Coll. Cardiol.* **2004**, *44*, 1578-1583.
- Miller-Catchpole, R.; Kot, E.; Haloftis, G.; Furmanov, S.; Bezkorovainy, A. Lactoferrin can supply iron for the growth of *Bifidobacterium breve*. *Nutr. Res.* **1997**, *17*, 205-213.
- Moore, S. A.; Anderson, B. F.; Groom, C. R.; Maridas, M.; Baker, E. N. Three-dimensional structure of diferric bovine lactoferrin at 2.8 Å resolution. *J. Mol. Biol.* **1997**, *274*, 222-236.
- Morein, S.; Andersson, A.-S.; Rilfors, L.; Lindblom, G. Wild-type *Escherichia coli* cells regulate the membrane lipid composition in a 'window' between gel and non-lamellar structures. *J. Biol. Chem.* **1996**, *271*, 6801-6809.
- Nagasako, Y.; Saito, H.; Tamura, Y.; Chimamura, S.; Tomita, M. Iron-binding properties of bovine lactoferrin in iron-rich solution. *J. Dairy Sci.* **1993**, *76*, 1876-1881.
- Nakai, S.; Wang, Z. H.; Dou, J.; Nakamura, S.; Ogawa, M.; Nakai, E.I.; Vanderstoep, J. Gas chromatography / principal component similarity system for detection of *E. coli* and *S. aureus* contaminating salmon and hamburger. *J. Agric. Food Chem.* **1999**, *47*, 576-583.
- Nakai, S.; Chan, J.; Li-Chan, E.; Dou, J.; and Ogawa, M. Homology similarity analysis of sequences of lactoferrin and its derivatives. *J. Agric. Food Chem.* **2003**, *51*, 1215-1223.
- Nguyen, D. V.; Rocke, D. M. Tumor classification by partial least squares using microarray gene expression data. *Bioinformatics* **2002**, *18*, 39-50.
- Nonnecke, B. J.; Smith, K. L. Inhibition of mastitic bacteria by bovine milk apo-lactoferrin evaluated by in vitro microassay of bacterial growth. *J. Dairy Sci.* **1984**, *67*, 606-613.

- Odell, E. W.; Sarra, R.; Foxworthy, M.; Chapple, D. S.; Evans, R. W. Antibacterial activity of peptides homologous to a loop region in human lactoferrin. *FEBS Lett.* **1996**, *382*, 175-178.
- Opekarová, M.; Tanner, W. Specific lipid requirements of membrane proteins—a putative bottleneck in heterologous expression. *Biochim. Biophys. Acta* **2003**, *1610*, 11-22.
- Paulsson, M. A.; Svensson, U.; Kishore, A. R.; Naidu, S. Thermal behaviour of bovine lactoferrin in water and its relation to bacterial interaction and antibacterial activity. *J. Dairy Sci.* **1993**, *76*, 3711-3720.
- Pelton, J. T.; McLean, L. R. Spectroscopic methods for analysis of protein secondary structure. *Anal. Biochem.* **2000**, *277*, 167-176.
- Petschow, B. W.; Talbott, R. D.; Batema, R. P. Ability of lactoferrin to promote the growth of *Bifidobacterium* spp. *in vitro* is independent of receptor binding capacity and iron saturation level. *J. Med. Microbiol.* **1999**, *48*, 541-549.
- Pierce, A.; Colavizza, D.; Benaissa, M.; Maes, P.; Tartar, A.; Montreuil, J.; Spik, G. Molecular cloning and sequence analysis of bovine lactotransferrin. *Eur. J. Biochem.* **1991**, *196*, 177-184.
- Prupp, A. H.; Isaksson, T.; Stepaniak, L.; Sørhaug, T. Quantitative structure-activity relationship modeling of ACE-inhibitory peptides derived from milk proteins. *Eur. Food Res. Technol.* **2004**, *219*, 579-583.
- Puddu, P.; Borghi, P.; Gessani, S.; Valenti, P.; Belardelli, F.; Seganti, L. Antiviral effect of bovine lactoferrin saturated with metal ions on early steps of human immunodeficiency virus type 1 infection. *Int. J. Biochem. Cell Biol.* **1998**, *30*, 1055-1062.
- Recio, I.; Visser, S. Two ion-exchange chromatographic methods for the isolation of antibacterial peptides from lactoferrin *in situ* enzymatic hydrolysis on an ion-exchange membrane. *J. Chromatogr. A.* **1999**, *831*, 191-201.
- Rekdal, Ø.; Andersen, J.; Vorland, L. H.; Svendsen, J. S. Construction and synthesis of lactoferricin derivatives with enhanced antibacterial activity. *J. Pept. Sci.* **1999**, *5*, 32-45.
- Roberts, A. K.; Chierici, R.; Sawatzki, G.; Hill, M. J.; Volpato, S.; Vigi, V. Supplementation of adapted formula with lactoferrin: 1. Effects on the infant faecal flora. *Acta Paediatr.* **1992**, *81*, 119-124.
- Saito, H.; Miyakawa, H.; Tamura, Y.; Shimamura, S.; Tomita, M. Potent bactericidal activity of bovine lactoferrin hydrolysate produced by heat treatment at acidic pH. *J. Dairy Sci.* **1991**, *74*, 3724-3730.
- Sánchez, L., Aranda, P., Pérez, M. D. and Calvo, M. Concentration of lactoferrin and transferrin throughout lactation in cow's colostrum and milk. *Biol. Chem. Hoppe Seyler.* **1988**, *369*, 1005-1008.
- Satué-Gracia, M. T.; Frankel, E. N.; Rangavajhyala, N.; German, J. B. Lactoferrin in infant formulas: effect on oxidation. *J. Agric. Food Chem.* **2000**, *48*, 4984-4990.
- Schibli, D. J.; Hwang, P. M.; Vogel, H. J. The structure of the antimicrobial active center of lactoferricin B bound to sodium dodecyl sulfate micelles. *FEBS Lett.* **1999**, *446*, 213-217.

- Shai, Y. Mechanism of the binding, insertion and destabilization of phospholipid bilayer membranes by α -helical antimicrobial and cell non-selective membrane-lytic peptides. *Biochim. Biophys. Acta* **1999**, *1462*, 55-70.
- Shimazaki, K.; Tazume, T.; Uji, K.; Tanake, M.; Kumura, H.; Mikawa, K.; Shimo-Oka, T. Properties of a heparin-binding peptide derived from bovine lactoferrin. *J. Dairy Sci.* **1998**, *81*, 2841-2849.
- Skates, S.; Iliopoulos, O. Molecular markers for early detection of renal carcinoma: investigative approach. *Clin. Cancer Res.* **2004**, *10*, 6296S-6301S.
- Snyder, R.; Hsu, S.; Krimm, S. Vibrational spectra in the C-H stretching region and the structure of the polymethylene chain. *Spectrochim. Acta* **1978**, *34A*, 395-406
- Snyder, R.; Scherer, J.; Gaber, B. Effects of chain packing and chain mobility on the Raman spectra of biomembranes. *Biochim. Biophys. Acta* **1980**, *601*, 47-53.
- Snyder, R. Strauss, H. and Elliger, C. C-H stretching modes and the structure of n-alkyl chains. I. Long, disordered chains. *J. Chem. Phys.* **1982**, *86*, 5145-5150.
- Sørensen, M.; Sørensen, S. P. L. The proteins in whey. *Compt. Rend. Lab. Carlsberg* **1939**, *23*, 55-99.
- Strøm, M. B.; Rekal, Ø.; Svendsen, J. S. Antibacterial activity of 15-residue lactoferricin derivatives. *J. Pept. Res.* **2000**, *56*, 265-274.
- Strøm, M. B.; Rekdal, Ø.; Stensen, W.; Svendsen, J. S. Increased antibacterial activity of 15-residue murine lactoferricin derivatives. *J. Pept. Res.* **2001**, *57*, 127-139.
- Subbalakshmi, C.; Krishnakumari, N.; Nagaraj, R.; Sitaram, N. Requirements for antibacterial and hemolytic activities in the bovine neutrophil derived 13-residue peptide indolicidin. *FEBS Lett.* **1996**, *395*, 48-52.
- Subbalakshmi, C.; Sitaram, N. Mechanism of antimicrobial action of indolicidin. *FEMS Microbiol. Lett.* **1998**, *160*, 91-96.
- Superti, F.; Ammendolia, M.; Valenti, V.; Seganti, L. Antirotaviral activity of milk proteins: lactoferrin prevents rotavirus infection in the enterocyte-like cell line HT-29. *Med. Microbiol. Immunol.* **1997**, *186*, 83-91.
- Tomita, M.; Bellamy, W.; Takase, M.; Yamauchi, K.; Wakabayashi, H.; Kawase, K. Potent antibacterial peptides generated by pepsin digestion of bovine lactoferrin. *J. Dairy Sci.* **1991**, *74*, 4137-4142.
- Tomita, M.; Takase, M.; Bellamy, W.; Shimamura, S. A review: The active peptide of lactoferrin. *Acta Paediatr. Jpn.* **1994**, *36*, 585-591.
- Tomita, M.; Shimamura, S.; Kawase, K.; Fukuwatari, Y.; Takase, M.; Bellamy, W.; Hagiwara, T.; Matukuma. A process for large-scale production of antimicrobial peptide in high purity. **1999**. Canada: Canadian Intellectual Property Office, CA 2070882.
- Ulvatne, H.; Haukland, H. H.; Olsvik, Ø.; Vorland, L. H. Lactoferricin B causes depolarization of the cytoplasmic membrane of *Escherichia coli* ATCC 26922 and fusion of negatively charged liposomes. *FEBS Lett.* **2001**, *492*, 62-65.

- Ushida, Y.; Sekine, K.; Kuhara, T.; Takasuka, N.; Iigo, M.; Maeda, M.; Tsuda, H. Possible chemopreventative effects of bovine lactoferrin on esophagus and lung carcinogenesis in the rat. *Jpn. J. Cancer Res.* **1999**, *91*, 582-588.
- van der Strate, B.; Beljaars, L.; Molema, G.; Harmsen, M.; Meijer, D. Antiviral activities of lactoferrin. *Antiviral Res.* **2001**, *52*, 225-239.
- Venkitanarayanan, K. S.; Zhao, T.; Doyle, M. P. Antibacterial effect of lactoferrin B on *Escherichia coli* O157:H7 in ground beef. *J. Food Protect.* **1999**, *62*, 747-750.
- Vincent, J. S.; Revak, S. D.; Cochrane, C. D.; Levin, I. W. Interactions of model human pulmonary surfactants with a mixed phospholipid bilayer assembly: Raman spectroscopic studies. *Biochemistry* **1993**, *32*, 8228-8238.
- Vodovotz, Y.; Arteaga, G. E.; Nakai, S. Principal component similarity analysis for classification and its application to GC data of mango. *Food Res. Int.* **1993**, *26*, 355-363.
- Voland, L. H.; Ulvatne, H.; Rekdal, Ø.; Svendsen, J. S. Initial binding sites of antimicrobial peptides in *Staphylococcus aureus* and *Escherichia coli*. *Scand. J. Infect. Dis.* **1999**, *31*, 467-473.
- Wakabayashi, H.; Abe, S.; Okutomi, T.; Tansho, S.; Kawase, K.; Yamaguchi, H. Cooperative anti-Candida effects of lactoferrin or its peptides in combination with azole antifungal agents. *Microbiol. Immunol.* **1996**, *40*, 821-825.
- Wakabayashi, H.; Abe, S.; Teraguchi, S.; Hayasawa, H.; Yamaguchi, H. Inhibition of hyphal growth of azole-resistant strains of *Candida albicans* by triazole antifungal agents in the presence of lactoferrin-related compounds. *Antimicrob. Agents Chemother.* **1998**, *42*, 1587-1591.
- Wakabayashi, H.; Uchida, T.; Yamauchi, K.; Teraguchi, S.; Hayasawa, H.; Yamaguchi, H. Lactoferrin given in food facilitates dermatophytosis cure in guinea pig models. *J. Antimicrob. Chemother.* **2000**, *46*, 595-601.
- Wang, Z. H.; Dou, J.; Macura, D.; Durance, T. D.; Nakai, S. Solid phase extraction for GC analysis of beany flavours in soymilk. *Food Res. Int.* **1997**, *30*, 503-511.
- Wei, Z.; Nisimura, T.; Yoshida, S. Presence of a glycan at a potential N-glycan site, Asn-281, of bovine lactoferrin. *J. Dairy Sci.* **2000**, *83*, 683-689.
- Williams, R. W.; Weaver, J. L. Secondary structure of substance P bound to liposomes in organic solvents and in solution from Raman and CD spectroscopy. *J. Biol. Chem.* **1990**, *265*, 2505-2513.
- Wu, M.; Maier, E.; Benz, R.; Hancock, R. E. W. Mechanism of interaction of different classes of cationic antimicrobial peptides with planar bilayers and with the cytoplasmic membrane of *Escherichia coli*. *Biochemistry* **1999**, *38*, 7235-7242.
- Yamauchi, K.; Tomita, M.; Giehl, T. J.; Ellison, R. T. I. Antibacterial activity of lactoferrin and a pepsin-derived lactoferrin peptide fragment. *Infect. Immun.* **1993**, *61*, 719-728.
- Yamazaki, N.; Yamauchi, K.; Kawase, K.; Hayasawa, H.; Nakao, K.; Moto, I. Antibacterial effects of lactoferrin and a pepsin-generated lactoferrin peptide against *Helicobacter pylori* in vitro. *J. Infect. Chemother.* **1997**, *3*, 85-89.

CHAPTER 2. PRODUCTION OF LACTOFERRICIN AND OTHER CATIONIC PEPTIDES FROM FOOD GRADE BOVINE LACTOFERRIN WITH VARYING IRON SATURATION LEVELS¹

2.1. Introduction

The presence of an antimicrobial peptide sequence in bovine lactoferrin (LF) was first noted when heat treatment of LF increased its antibacterial activity (Saito et al., 1991). It was suggested that at least one bactericidal domain was released by heating LF at pH 2.0 at 120 °C for 15 minutes. Heat-treated LF was later fractionated by reverse-phase HPLC, and a peptide fraction with strong activity, namely lactoferricin (Lfcin), was identified. Peptic digestion of LF at 37 °C also led to similar results (Bellamy et al., 1992). Since then, a number of production and purification strategies have been conducted for the isolation of Lfcin, including the use of a cation exchange column followed by reverse-phase HPLC (Dionysius and Milne, 1997), bead-based cation-exchange chromatography on SP-Sepharose Fast Flow resin (Recio and Visser, 1999), affinity chromatography with an immobilized heparin column (Shimazaki et al., 1998), and chymosin digestion of LF followed by ion-exchange membrane filtration and reverse-phase HPLC (Hoek et al., 1997). All of these studies were conducted on a laboratory scale using laboratory-grade reagents and conditions, producing a small quantity of Lfcin for scientific research purposes. In 1999, Tomita et al. (1999) patented a method using hydrophobic or cation exchange medium to produce Lfcin from peptic digested LF in large scale.

Pepsin is a non-specific protease and could cleave at multiple locations on LF. Since LF is a basic protein with a pI of 8.69, it is very likely that cationic peptides other than Lfcin are concurrently produced during the peptic digestion. Furthermore, LF is an iron-binding protein which is 20-25% saturated with iron under normal and healthy physiological conditions. The binding of iron to lactoferrin is an important factor in the thermal stability of its structure. Hadden et al. (1994) observed that the removal of iron from human LF led to increases in the extent of ¹H-²H exchange and postulated a "loosening" of human LF upon iron removal. Likewise, Paulsson et al. (1993) reported that iron-saturated (holo-) bovine lactoferrin was more resistant to heat-induced changes than was the iron-depleted (apo-) LF. However, the potential effect of varying iron levels on the profile of peptides produced upon peptic digestion has not been previously reported.

¹ A version of this chapter has been presented. Chan, J.C.K., and Li-Chan, E. (March 2004). Production of lactoferricin B and other cationic peptides from lactoferrin. Selected finalist at the Withycombe-Charalambous Graduate Student Symposium, 227th American Chemical Society National Meeting, Anaheim, CA.

A version of this chapter has been submitted for publication. Chan, J. C. K., and Li-Chan, E. C. Y. Production of lactoferricin and other cationic peptides from food grade bovine lactoferrin with varying iron saturation levels. *Journal of Agricultural and Food Chemistry*.

The objectives of this study were to develop an isolation strategy with potential for industrial scale production of Lfcin, to identify other cationic peptides generated during the peptic digestion of LF, and to investigate the effects of initial iron-saturation levels of LF on the composition of the resultant peptide mixture produced by peptic digestion.

2.2. Materials and Methods

2.2.1. Preparation of Lactoferrin with Varying Iron Saturation Levels

Food-grade bovine lactoferrin (LF, a gift from DMV International Nutritional, Fraser, NY) was used to prepare samples with different levels of iron saturation based on previously described methods (Nagasako et al., 1993; Marchetti et al., 1999; and Moore et al., 1997). Apo-lactoferrin (apo-LF, iron-depleted) was prepared by dialyzing LF against 0.1 M citric acid at pH 2.0. Holo-lactoferrin (holo-LF, iron-saturated) was prepared by adding a 10 fold molar excess of FeCl₃ to LF. Excess citric acid or iron was then removed by exhaustive dialysis against ddH₂O. All dialyses were conducted overnight at 4 °C until there was no change in the conductivity of the external ddH₂O.

2.2.2. Digestion of Lactoferrin

Peptic digestion of LF was based on methods previously described (Tomita et al., 1991; Dionysius and Milne, 1997). The LF (5%, w/v) was digested with porcine pepsin (3% of LF, 2,500-3,500 units mg⁻¹ protein, Sigma Product Number P7012, Sigma-Aldrich, Saint Louis, MO) at 37 °C for 4 hours. The digest was maintained at pH 2.0 using 2 M HCl and was terminated by adjusting the pH to 7.0 using 2 M NaOH and heating at 80 °C for 15 minutes. The resultant digest was centrifuged at 15,000 x g for 20 minutes at 4 °C and the supernatant was stored at -25 °C until further analysis

2.2.3. Purification of Lactoferricin and Other Peptides

The supernatant from the peptic digest was thawed at 4 °C and applied at a flow rate of 0.25 mL per minute to a column packed with an industrial grade, carboxylic acid cation exchanger (Purolite C-106 EP, Purolite, Bala Cynwyd, PA). The resin was pre-equilibrated with 50 mM sodium phosphate buffer (PB) at pH 6.5. After washing off unbound peptides with PB at 1.0 mL per minute, bound (cationic) peptides were eluted with PB containing stepwise gradient of 0.2, 0.5, 0.8, 1.0, and 2.0 M NaCl, at 1.0 mL per minute. The fractionation process was monitored by measuring the conductivity and UV absorbance at 280 nm of the eluant. Fractions were lyophilized and stored at -25 °C.

2.2.4. Peptide Mass Analysis

The whole peptic digest as well as fractions separated by cation exchange chromatography were analyzed after desalting (ZipTip_{C18}, Millipore, Bellerica, MA) by matrix assisted laser desorption ionization time of flight mass spectrometry (MALDI-ToF MS) using an Applied Biosystems Voyager System (Voyager-DE™ STR Biospectrometry™, AME Bioscience Ltd., London, UK) under the following conditions: voltage, 20,000 V; laser intensity, 2500; laser rep rate, 20.0 Hz; calibration matrix, α -cyano-4-hydroxycinnamic acid. Post source decay following MALDI-ToF was performed to obtain peptide sequence information. All MALDI-ToF analyses were performed by Ms. Suzanne Perry at the LMB-BL Proteomic Core Facility, University of British Columbia.

2.2.5. Identification of Peptide Sequences

Peptide sequences were identified using the FindPept software tool (<http://ca.expasy.org/tools/findpept.html>) (Gattiker et al., 2002).

2.2.6. Iron Content in Lactoferrins

Iron content of lactoferrin solutions containing different iron saturation levels was determined using inductively coupled plasma-mass spectrometry (ICP-MS) with an ultrasonic nebulization pulse membrane desolvation inlet Elemental Research Inc., North Vancouver, Canada.

2.2.7. Protein Structure by Raman Spectroscopy

Raman spectra of each LF sample (10% w/v, adjusted to pH 2.0) were measured using a laser Raman spectrometer (Model NR-1100, JASCO Inc., Tokyo, Japan) with excitation from the 488 nm line of an argon ion laser (Coherent Innova 70C series, Coherent Laser Group, Santa Clara, CA, cooled with the Coherent Laser Pure heat exchanger system). The Raman scattering of samples placed in a hematocrit capillary tubes in a transverse arrangement (capillary held horizontally and incident laser beam perpendicular to the capillary axis) was measured under the following conditions: laser power, 200 mW; slit height, 4 mm; spectral resolution, 5 cm⁻¹ at 19,000 cm⁻¹; sample speed, 120 cm⁻¹ min⁻¹ with data collected at every cm⁻¹. Spectra from at least 6 scans were averaged for each duplicate sample. Secondary structure composition of LFs was estimated by applying the algorithm of Williams (1983) to analyze the Raman spectra in the amide I region, using the RSAP program (version 2.1) of Przybycien and Bailey (1989).

2.3. Results

2.3.1. Production of Lactoferricin and Other Cationic Peptides from Lactoferrin

Pepsin digestion of food grade LF resulted in a mixture of peptides with a wide range of masses (**Figure 2.1**). A peptide with mass of 968 Da was the most dominant product, followed by peptides with masses of 4430 and 4268 Da. Peptides with masses around 3100 and 1900 Da were also detected as broad peaks by MALDI-ToF analysis.

The cation exchange chromatogram of pepsin-digested LF (**Figure 2.2**) shows that most of the LF digestion products that had pI below neutral pH did not bind to the industrial grade cation exchange resin at pH 6.5, and were recovered in the flow through fraction. The majority of the bound LF digestion products were eluted using buffers containing 0.2 M, 0.5 M, and 0.8 M NaCl. Elutions with 1.0 M and 2.0 M NaCl released more tightly bound peptides with higher pI from the column.

A 965 Da peptide was the most dominant peptide found in the flow through fraction as revealed on a MALDI-ToF mass spectrum (**Figure 2.3a**). Peptides with masses of 4275 and 4433 Da were also detected in the flow through fraction. The MALDI-ToF mass spectrum of the 0.2 M NaCl fraction showed similar components to those of the flow through fraction (**Figure 2.3b**); however, the peptides with masses 4268, and 4430 Da were more dominant constituents in the 0.2 M NaCl fraction, compared to the peptide at 965 Da. Peptides with masses near 2700 Da also became noticeable in this fraction.

The addition of 0.5 M NaCl to phosphate buffer (PB) eluted a peptide mixture with very different mass profile (**Figure 2.3c**). In addition to the 4268 and 4430 Da peptides that were previously detected in other fractions, broad peaks near 1971 and 3196 Da were observed, indicating that many peptides with masses near 1971 and 3196 Da were present in the fraction. The 0.8 M NaCl eluate contained peptides with masses close to 3196 Da. In addition, peptides with lower masses (1971 and 2675 Da) were also noted (**Figure 2.3d**). Peptides with masses of 1052, 1971, 3196, 4275, and 4430 Da were found in the 1.0 M NaCl fraction (**Figure 2.3e**). Peptides with masses of 3124 and 3196 Da dominated the 2.0 M NaCl fraction (**Figure 2.3f**). These masses correspond to the 25- and 26-mer of Lfcin, residues 17-41 or 42 of LF, respectively (Recio and Visser, 1999). The peptides in the 2.0 M NaCl fraction with masses of 3124 and 3196 Da represent 7% of the theoretical amount of Lfcin in the pepsin hydrolysates of food-grade bovine LF.

2.3.2. A Two-Step Process for Lactoferricin Isolation

The aforementioned results indicated that the peptides of interest, Lfcin with a mass of 3124 or 3196 Da, were eluted by PB containing high NaCl levels, suggesting that Lfcin was

highly cationic and bound strongly with the cation exchange resin. Hence, a large amount of LF digest was loaded to exceed the column capacity to allow a competitive displacement of the other peptides by highly cationic Lfcin in the LF digest. LF peptic hydrolysate from 5.0 g of LF was applied to 5.0 mL cation exchange resin and fractionated using conditions described in the previous section, except that only PB containing 1.0 M and 2.0 M NaCl were used to elute Lfcin. **Figure 2.4a** shows the elution profile of the fractionation. A large amount of peptides passed through the column as LF digest was being loaded on to the column. These peptides include those which passed through the column without binding to the cation exchange resin, as well as some which might have formed weak bonds with the resin and were later displaced by other stronger cationic peptides in the digest. Peptides that formed stronger bonding with the cation exchange resin were later eluted off the column by 1.0 M NaCl and 2.0 M NaCl in PB.

Figures 2.4b, c, and d illustrate the MALDI-ToF mass spectra of fractions eluted at various points in time. Towards the end of the sample loading, the flow through fraction contained primarily peptides with masses around 3200 and 4200 Da (**Figure 2.4b**). Subsequent elution using 1.0 M NaCl buffer produced a mixture of peptides with masses of 3196 and 3124 Da, along with lower levels of peptides with masses around 1970 and 1053 Da (**Figure 2.4c**). The MALDI-ToF mass spectrum of the 2.0 M NaCl fraction (**Figure 2.4d**) shows that the fraction was predominantly composed of peptides of masses of 3196 and 3124 Da. The signal intensity observed in **Figure 2.4d** indicates that the purity of Lfcin recovered in the 2.0 M fraction is comparable to the purity (> 99%) of the standard used for the calibration of the MALDI-ToF mass spectrometer (data not shown). Assuming that the peptides with 3196 and 3124 Da corresponded to the 26- and 25-mer of Lfcin, a total of 70 mg (35% of the theoretical yield from 5 g of LF) of highly purified Lfcin was recovered in the 2.0 M NaCl fraction using this purification strategy.

2.3.3. The Identification of Lactoferricin and Other Cationic Peptides

Identification of the fractionated peptides using FindPept software was based on the mass data obtained, cleavage properties of pepsin, digestion conditions, and known sequence information of LF. The results indicated that peptides with masses of 3196 and 3124 Da could represent the 26- and 25-mer peptide segments of residues 17-42 and 17-41, respectively in LF, with the following sequences, ¹⁷FKCRR WQWRM KKLGA PSITC VRRAF⁴¹ A⁴².

These findings were verified by post source decay performed on the 3196 and 3124 Da peptides detected in the 2.0M NaCl fraction, yielding many smaller peptides with masses of 122, 445, 485, 488, 2319, 2372, 3124, and 3196 Da (**Figure 2.5a**). These masses correspond to peptide fragments isolated from FKCRR WQWRM KKLGA PSITC VRRAF A (**Figure 2.5b**).

PeptIden tool was used to identify potential peptide sequences in LF containing cationic amino acids with high pI values and whose calculated mass values were within ± 2 Da of the mass measured by MALDI-ToF MS. Sequence information obtained by PeptIden of other cationic peptides produced during peptic hydrolysis of LF was summarized in **Table 2.1**. Although many of these potentially bioactive peptides are located near the current peptide of interest (lactoferricin), a number of them are at different locations on the lactoferrin sequence.

2.3.4. Effects of Iron Saturation Levels of Lactoferrin

ICP-MS analyses showed the iron saturation level of the LF solution dialyzed against 0.1 M citric acid (apo-LF) was decreased to 16%, compared to 20% in the original untreated LF. When excess Fe^{3+} was added to the LF (holo-LF), iron saturation was increased to 350%. Structural analyses of the LFs determined by Raman spectroscopy show that the Raman amide I band near $1500 - 1800 \text{ cm}^{-1}$ of apo-LF was less intense than the spectra of LF and holo-LF (data not shown). In addition, as determined using the RSAP program, holo-LF contained little α -helical structure accompanied with more β -sheet and overall random content at pH 2.0 (**Table 2.2**). The Raman spectra and estimated secondary structural content of LF and apo-LF appeared to be similar. Removing some of the Fe from LF decreased the α -helix content from 42 to 34%, increased the β -sheet content from 32 to 47%, and lowered the overall random content from 27 to 19% (**Table 2.2**).

Results from the MALDI-ToF analyses show that digests of LF (**Figure 2.1**) and especially of apo-LF (**Figure 2.6a**) contained more peptide fragments with lower masses (less than 1000 Da) than the digest of holo-LF (**Figure 2.6b**). Similarly, peptides eluted by 1.0 M NaCl in PB from the LF (**Figure 2.3e**) and apo-LF digest (**Figure 2.7a**) also contained more peptide fragments with lower masses (less than 1000 Da) than those of holo-LF (**Figure 2.7b**). However, the compositions of the 2.0 M fractions produced from LF's with different levels of iron saturation were similar (**Figure 2.8** and **Figure 2.3f**). The 3196 Da peptide remained the most dominant peptide in all three preparations, whereas the 3124 Da peptide was the second most abundant peptide.

2.4. Discussion

2.4.1. Production of Lactoferricin and Other Cationic Peptides from Lactoferrin

Peptic digestion of food grade bovine lactoferrin (LF) produced a mixture of peptides with various masses (**Figure 2.1**). Pepsin is an enzyme with low substrate specificity (Keil, 1992), and may cleave at the P1 or P1' position of Phe, Tyr, Trp, and Leu, corresponding to over 200 possible cleavage sites on LF. Furthermore, its cleavage specificity is lost at pH greater than or equal to 2.0 (Keil, 1992). Slight changes of the pH during the digestion process

would result in varying peptic cleavage patterns. Hence, the profile of the resulting peptides would vary greatly depending on the digestion conditions used. Under the digestion conditions used in the present study, 5% (w/v) LF solution with 3% (w/w) pepsin at pH 2.0 and 37 °C for 4 hours, an array of peptides with wide ranges of size and charge properties were produced. Due to differences in amino acid composition of these peptides, they carried different charges and were bound to the cation-exchange column with different strengths. The use of buffer containing various levels of salt allowed the fractionation of peptides produced from the pepsin digested LF as shown in **Figure 2.2**. MALDI-ToF analyses showed that fractions eluted with buffers containing different levels of salt were composed of peptides with differing masses (**Figure 2.3**). Peptides with mass of 3196 Da could be fractionated with a buffer containing 0.8 M NaCl PB along with many other peptides with lower molecular masses (**Figure 2.3d**). The use of a 1.0 M NaCl PB allowed the purification of the 3196 Da component together with a few other peptides (**Figure 2.3e**). Subsequently, eluting the cation exchange column with 2.0 M NaCl PB at pH 6.5 led to the production of a peptide mixture containing two predominant peptides with masses of 3196 and 3124 Da from the digest of food-grade LF (**Figure 2.3f**); these peptides were verified to be Lfcin using post source decay analysis (**Figure 2.5**). Lfcin was thus successfully isolated from a peptide mixture using a stepwise salt gradient on an industrial cation exchange resin.

Although the digestion and isolation of Lfcin has been reported in the past, many of these purifications were performed using laboratory-grade reagents resulting in only small quantities of recovered Lfcin. For example, both Dionysius and Milne (1997) and Hoek et al. (1997) reported the isolation of Lfcin from peptic digest of bovine LF followed by cation exchange chromatography on a column of S-Sepharose Fast Flow HPLC using a preparative C18 reverse-phase column, and HPLC with an analytical C18 column. Lfcin was produced at the microgram level following the method described by Recio and Visser (1999). Affinity chromatography (Shimazaki et al., 1998) was also attempted, but again, only microgram levels of Lfcin were produced.

Tomita et al. (1999) described a patented method using 3000 mL of butyl moiety-containing hydrophobic or carboxymethyl moiety-containing cation exchange chromatography medium to purify Lfcin from 600 g of peptic digested LF. Lfcin was desorbed from the hydrophobic medium using 10 mM of HCl along with a mixture of 0.1 M citric acid and 0.2 M Na_2HPO_4 at pH 5.0. When cation exchange chromatography was used, 1 to 4 M salt solutions were used to elute Lfcin off the medium. Following the methods described, 10.5 g of highly pure (>90%) Lfcin was produced from 600 g of LF, corresponding to approximately 40% of the theoretical yield. In the present study, the concept of competitive displacement chromatography (Li-Chan et al., 1990) was applied to isolate the highly positively charged Lfcin

from other cationic peptides in a two-step process. First, 5.0 g of pepsin digested LF was loaded on to 5.0 mL of weak acid cation exchanger, Purolite C-106 EP, at beyond the capacity of the cation exchange column. Because of the high pI of Lfcin, other less positively charged peptides were continuously displaced by Lfcin during the loading of the pepsin digested LF, eventually resulting in a cation exchange column loaded primarily with highly purified Lfcin. It was therefore possible to produce highly purified Lfcin in the subsequent elution step. Results from the present study showed that peptic digestion of food-grade LF followed by cation exchange chromatography on an industrial-grade resin allowed the production of highly pure Lfcin in milligrams quantity with a 35% recovery of its theoretical yield.

2.4.2. Identification of Other Cationic Bioactive Peptides

LF itself is a cationic protein with antimicrobial activity and previous study has shown that the digestion of LF could enhance its antimicrobial functions (Tomita et al., 1991). Although it is commonly believed that the enhanced antimicrobial property is mainly due to the release of Lfcin during the digestion, it is possible that other functional peptides may also be released during peptic treatment. In the present study, MALDI-ToF analyses of the peptic digest of food-grade LF showed that a wide range of cationic peptides were indeed released during the digestion.

Based on the molecular masses detected by MALDI-ToF and knowledge of the sequence of LF, the potential candidate sequences and positions of these cationic LF peptides were identified. For instance, the mass of 4268 Da fragment found in the 0.2M and 0.5M NaCl fractions could be one or more of the following peptides: ¹¹⁰QGRKS CHTGL GRSAG WIIPM GILRP YLSWT ESLEP LQGA¹⁴⁸ with a pI of 9.31, ⁶⁸GRDPY LKRPV AAEIY GTKES PQTHY YAVAV VKKGS NFQ¹⁰⁵ with a pI of 9.52, or ¹⁰⁵QLDQL QGRKS CHTGL GRSAG WIIPM GILRP YLSWT ESL¹⁴² with a pI of 9.31. In fact, all or some of these peptides with similar masses and pI's could have been eluted at the same time, as suggested by the broad bases on the MALDI-ToF mass spectra (**Figures 2.3b** and **2.3c**). The broad 3196 bands appearing in the 0.5M, 0.8M, and 1.0M NaCl fractions (**Figure 2.3c**, **2.3d**, and **2.3e**, respectively) could consist of more than one peptide. As demonstrated using the proteomic tools on www.expasy.com, peptic digestion of LF could result in multiple peptides with similar mass of 3196 Da, but with different pI. Results presented in this chapter indicated that some of the peptides, with a mass of 3196 Da but lower pI than Lfcin, could be eluted by NaCl PB containing lower ionic strengths.

Among the possible cationic peptides that could be produced from the peptic digestion of bovine LF, many of the putative peptides contain either arginine (R) or lysine (K) and have an overall pI above 7.0. The presence of these positively charged amino acids, R and K, is a common feature among many bioactive peptides and is responsible for their bioactive functions

(Lehrer and Ganz, 2002). Future research should be conducted to investigate the biological activities of these cationic peptides produced during peptic hydrolysis of food-grade LF.

2.4.3. Effects of Iron Saturation Levels of Lactoferrin

Under normal physiological conditions, bovine LF contains approximately 20-25% iron (Shimazaki, 2000). The food-grade LF used in this study was consistent with the reported level and had an iron saturation level of 20% as determined by ICP-MS analysis. At this iron saturation level and at pH 2.0, Raman spectroscopic analyses showed that approximately 32% of LF folded into β -sheet structures, 41% of LF had α -helical structures, and the rest of the molecule was present as random coil structures (**Table 2.2**).

After some iron was removed from LF by dialyzing LF against citric acid, apo-LF (16% as determined by ICP-MS) contained less α -helical structure and random coil. Consequently, more β -sheet conformation was found in apo-LF. When LF was saturated with iron, a dramatic drop in the α -helical content with a concurrent increase in the β -sheet structure was detected. The Raman spectroscopic results showed that the presence of iron was important for the overall three dimensional structure of LF.

Previous data from the literature supported results observed in the present study. The differential scanning calorimetry (DSC) thermogram of native LF revealed two denaturation temperatures at 65 °C and 92 °C (Paulsson et al., 1993). Apo-LF and holo-LF showed prominent thermal denaturation peaks at 71 °C and 93 °C, respectively, indicating that the presence or absence of iron affected the thermal stability of LF. The transition at high temperature, near 92 °C, indicated the unfolding of the iron-binding domains of LF (Paulsson et al., 1993). Furthermore, apo-LF that was 30% saturated also denatured faster than holo-LF that was 100% saturated with Fe (Sánchez et al., 1992).

The binding of iron to human LF has been reported to be an important factor in the stabilization of its structure. Iron-depleted human LF demonstrated an increase in the extent of ^1H - ^2H exchange, suggesting a "loosening" of human LF upon iron removal (Hadden et al., 1994). Using differential scanning calorimetry, Mata et al. (1998) showed significant increases in maximum peak temperature, transition enthalpy, and activation energy of human milk LF which was fully saturated with iron (90.6 °C, 3209 kJ \cdot mol $^{-1}$, and 387.6 kJ \cdot mol $^{-1}$, respectively), compared to the corresponding values for LF that was less than 15% saturated with iron (67.0 °C, 2276 kJ \cdot mol $^{-1}$, and 275.5 kJ \cdot mol $^{-1}$, respectively). Crystallographic analysis of human LF also showed that the binding of iron to LF caused conformational changes and the molecule became more compact. Iron entered into the open interdomain cleft in each lobe and then the domains closed over the iron atoms (Anderson et al., 1989). This change in lactoferrin

structure explained why iron-saturated LF was more resistant to denaturation and proteolysis than the apo form (Anderson, 1990).

Based on results reported in this chapter, it can be speculated that removal of iron from LF decreased its overall stability and increased accessibility of pepsin to potential cleavage sites on LF. Hence, more cleavages led to the production of a larger amount of low-mass peptide fragments in the digest of apo-LF. In contrast, the addition of iron increased the β -sheet content in holo-LF, making it more resistant to structural changes under the thermal and acidic conditions for peptic digestion. Decreased accessibility of peptic cleavage sites on holo-LF thus may have led to more larger-sized peptide fragments in the digest of holo-LF. These effects of iron saturation levels are deemed important when specific peptides are needed. For instance, when peptides of higher masses (e.g. 4065, 4275 Da) are desired, the addition of Fe^{3+} to the LF solution would allow a higher yield of larger peptides than untreated LF or iron-depleted solutions (**Figure 2.7**).

Nevertheless, the level of iron saturation of LF did not affect the production and purity of Lfcin. This is probably due to the fact that the Lfcin sequence, residues 17-41 or residues 17-42, is located far away from the iron-binding domains of LF (D60-Y92-Y192-H254 and D395-Y433-Y526-H595). Hence, changes in the micro-environment of these two iron-binding sites exert little effect on the structure and stability around residues 17-42. The disulfide bond between C19 and C36 on Lfcin further enhances the stability of this peptide fragment, making it resistant to further peptic digestion regardless of the iron status in the environment.

Furthermore, the 2.0M NaCl fractions recovered by cation exchange chromatography from the peptic digests of all three LF preparations (untreated-LF, apo-LF, and holo-LF) demonstrated similar peptide mass profiles. All other peptides produced during the digestion processes, regardless of the initial iron saturation levels, were eluted by buffers with lower ionic strengths, leaving only the highly cationic Lfcin on the cation exchange resin. When eluted with the 2.0 M NaCl buffer, the 26-mer and 25-mer peptides corresponding to Lfcin were the most dominant peptides, resulting in a highly pure Lfcin fraction.

In summary, the production of Lfcin was not affected by the iron-status of LF. However, the removal of iron from LF increased the production of small-size peptides from LF and the addition of iron to LF increased the production of large-size peptides. An economically feasible isolation and purification strategy for the production of Lfcin from food-grade LF using an industrial-grade cation exchange resin was presented. At the time of the present study, it costs approximately US\$450 for each kilogram of LF (quote obtained from DMV International Nutritional, Fraser, NY, 1999) and US\$2000 for each gram of Lfcin (quote obtained from the Centre for Food Technology, Hamilton, Australia, 2001). Using the purification strategy

described in the present study, 14 grams of Lfcin can be produced from each kilogram of LF.

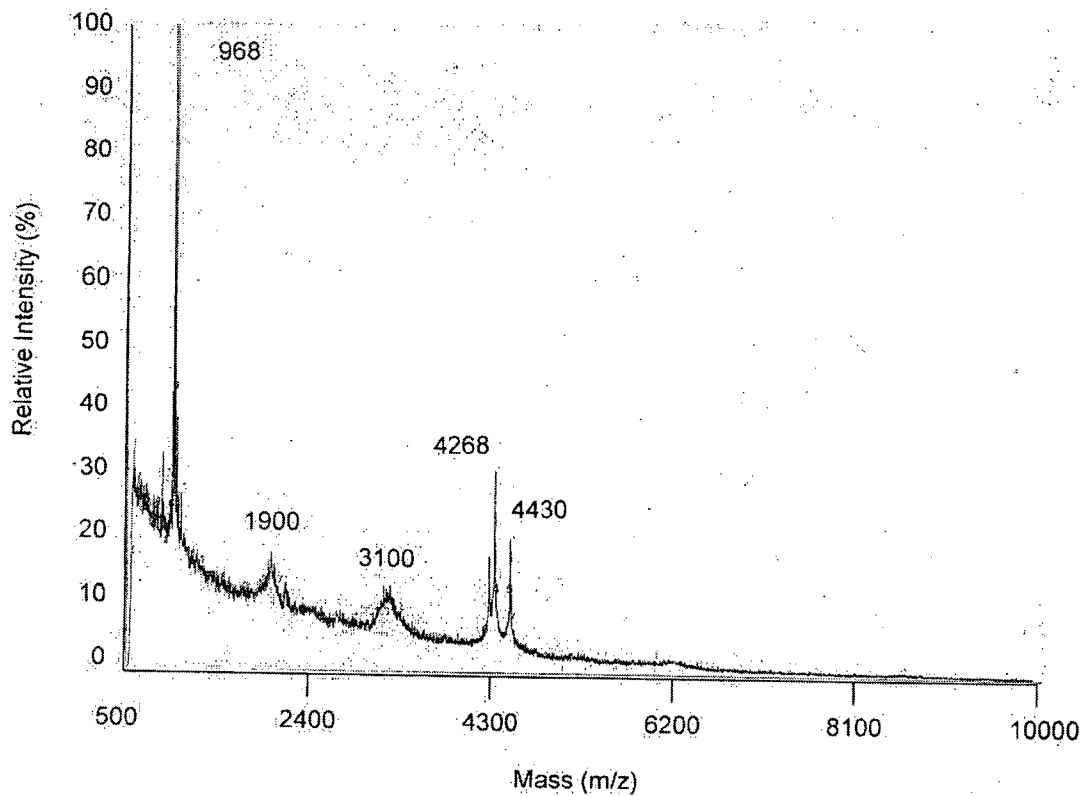


Figure 2.1. MALDI-ToF mass spectrum of lactoferrin digest produced by peptic digestion for 4 hours at 37 °C at pH 2.0.

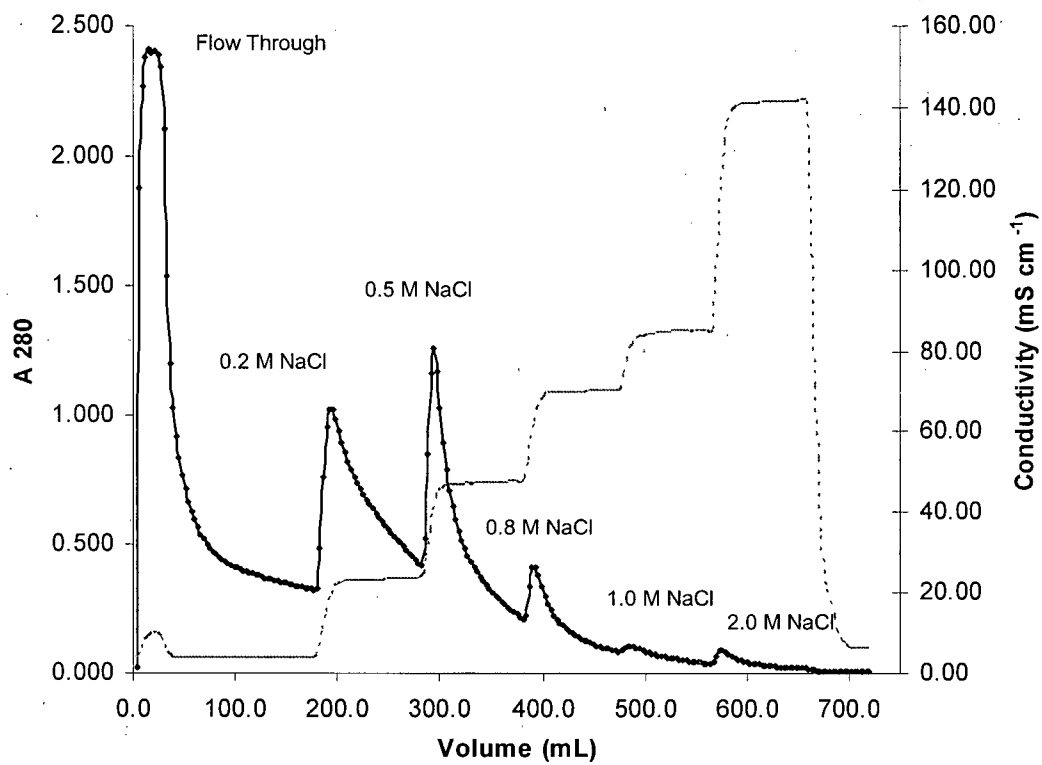


Figure 2.2. Purolite C-106 cation exchange chromatography of peptic LF digest (Solid line, Absorbance at 280nm; dotted line, conductivity). The supernatant of a 0.5 g of peptic LF digest was loaded onto a 10 mL column and eluted with 50 mM sodium phosphate buffer (pH 6.5) containing 0, 0.2, 0.5, 0.8, 1.0, and 2.0 M of NaCl at a flow rate of 1.0 mL per minute. Fraction peaks were collected and further analyzed.

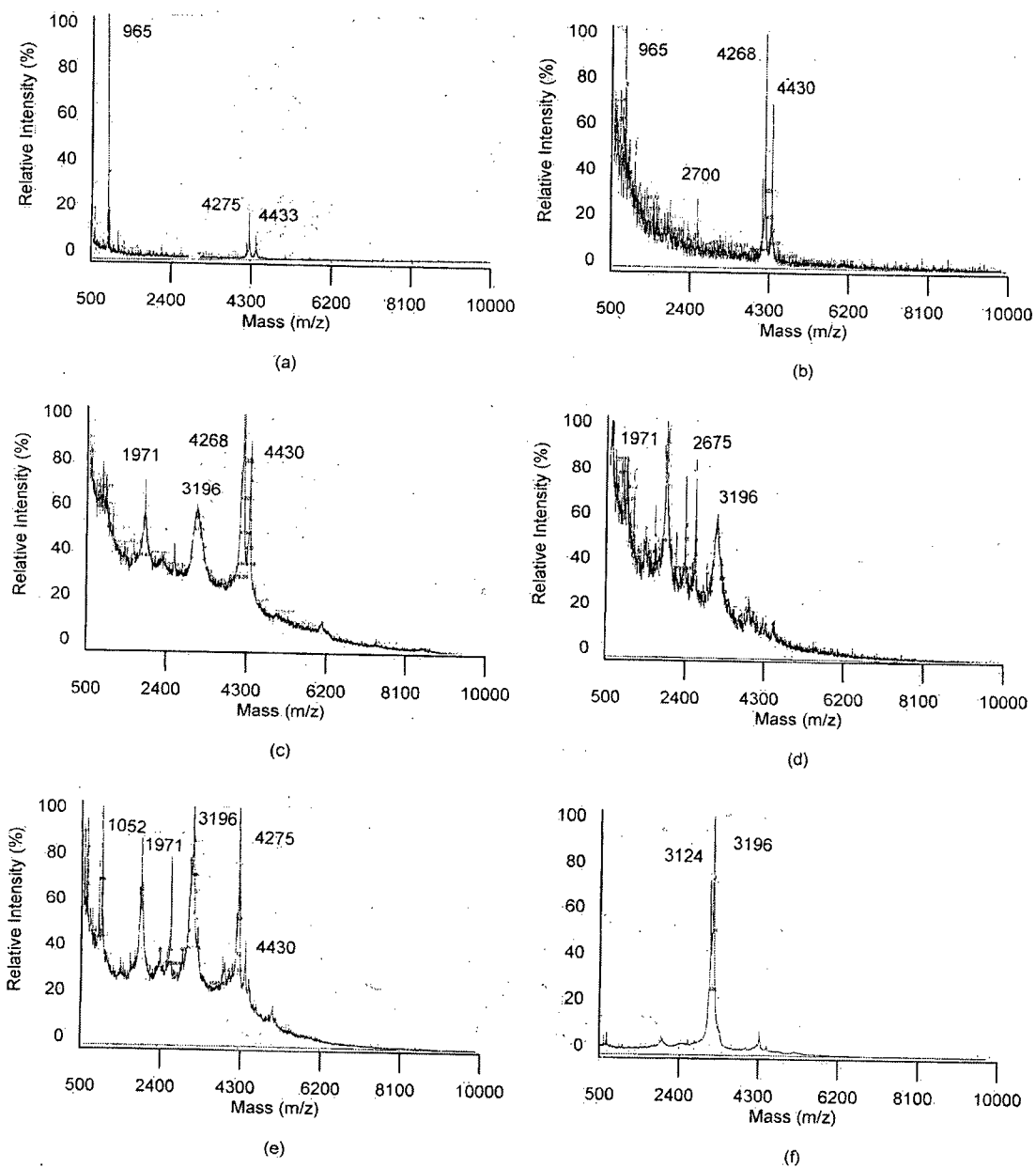


Figure 2.3. MALDI-ToF mass spectra of LF digest fractions eluted from a 10 mL cation exchange column with Purolite C-106 resin using 50 mL phosphate buffer at pH 6.5 containing no NaCl (a), 0.2 M NaCl (b), 0.5 M NaCl (c), 0.8 M NaCl (d), 1.0 M NaCl (e), and 2.0 M NaCl (f).

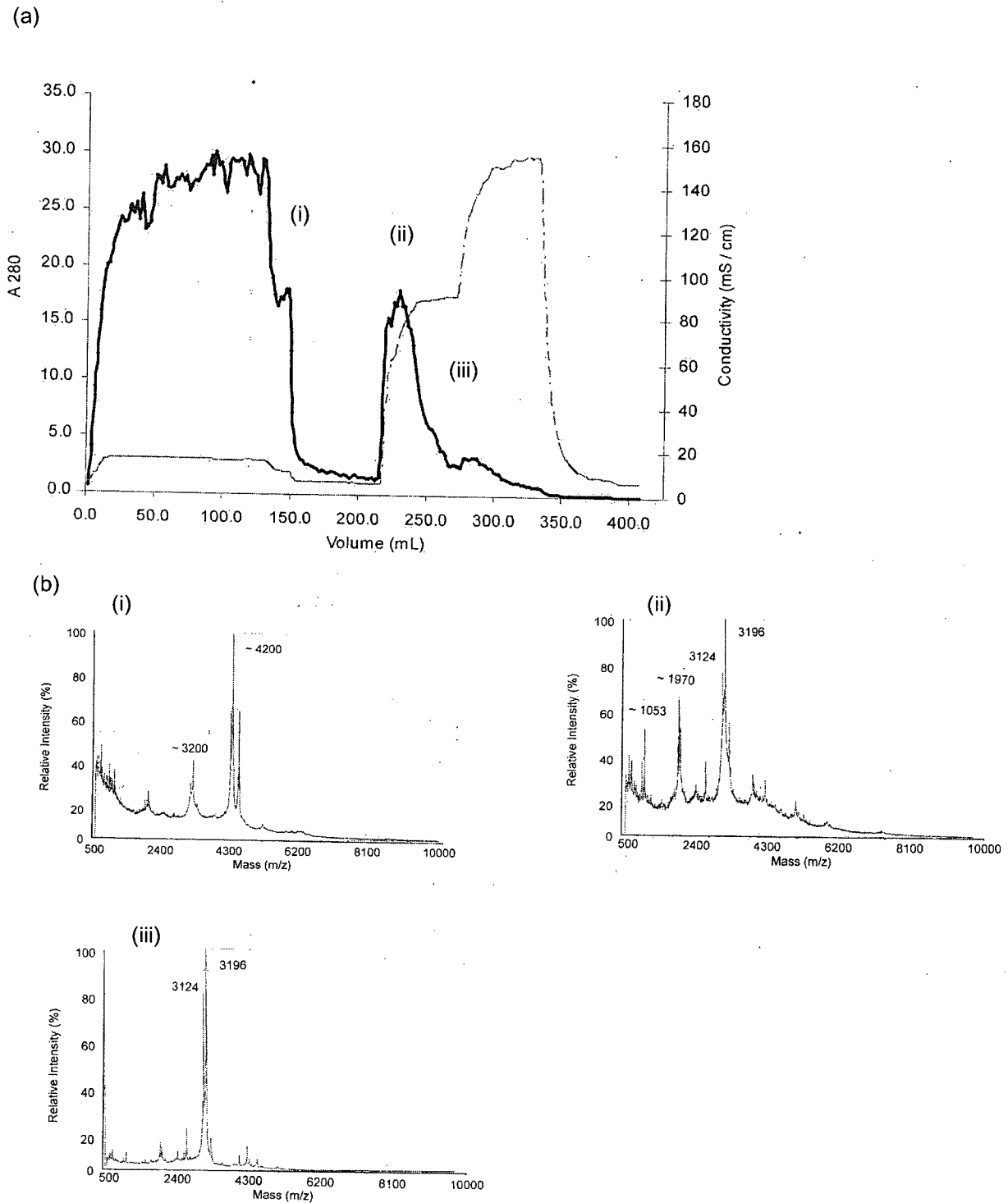
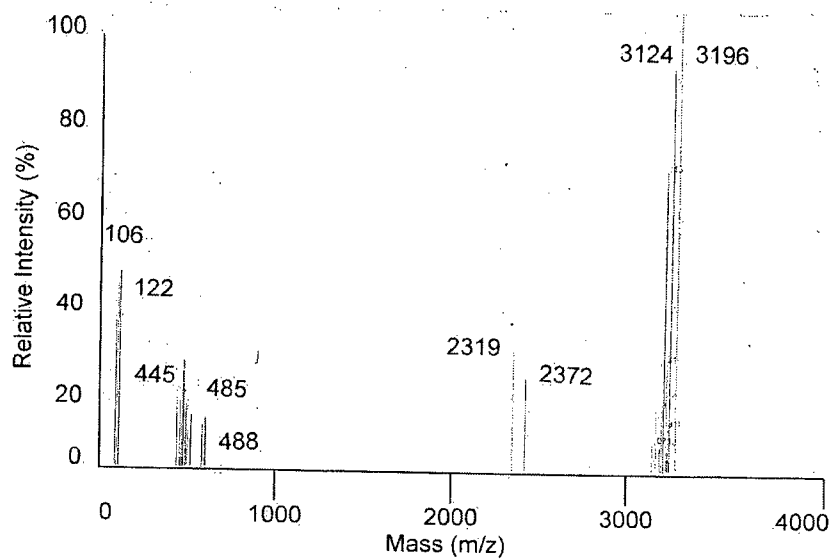


Figure 2.4. Purolite C-106 cation exchange chromatography in competitive displacement mode of peptic LF digest (a: Solid line, Absorbance at 280nm; dotted line, conductivity). The supernatant of a 5.0 g of peptic LF digest was loaded onto a 5.0 mL column and eluted with 50 mM sodium phosphate buffer (pH 6.5) containing 0, 1.0, and 2.0 M NaCl (a). Fraction peaks were collected and further analyzed by MALDI-ToF (b, i: fraction collected after sample loading was completed; ii: 1.0 M NaCl fraction; iii: 2.0 M NaCl fraction.)

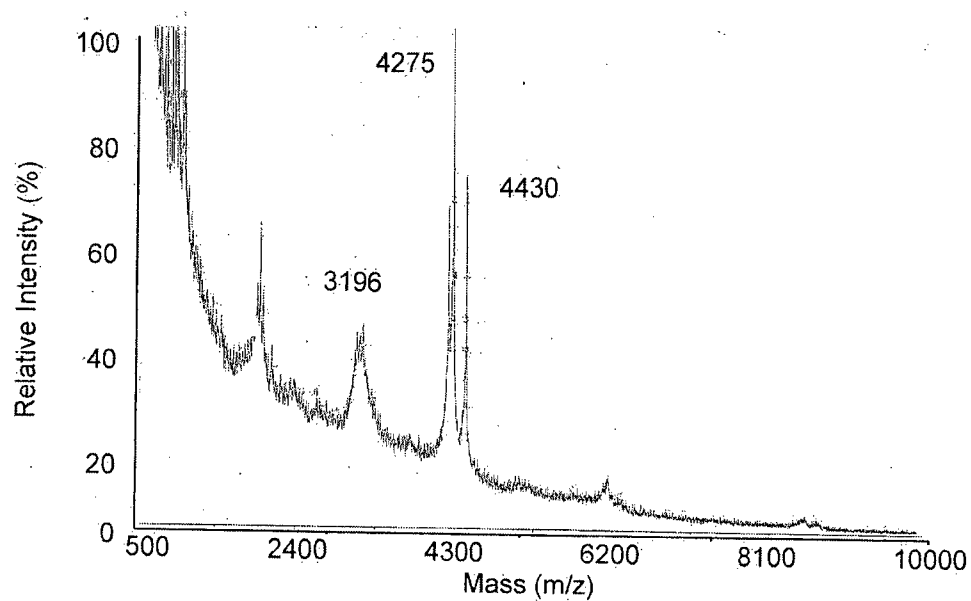


(a)

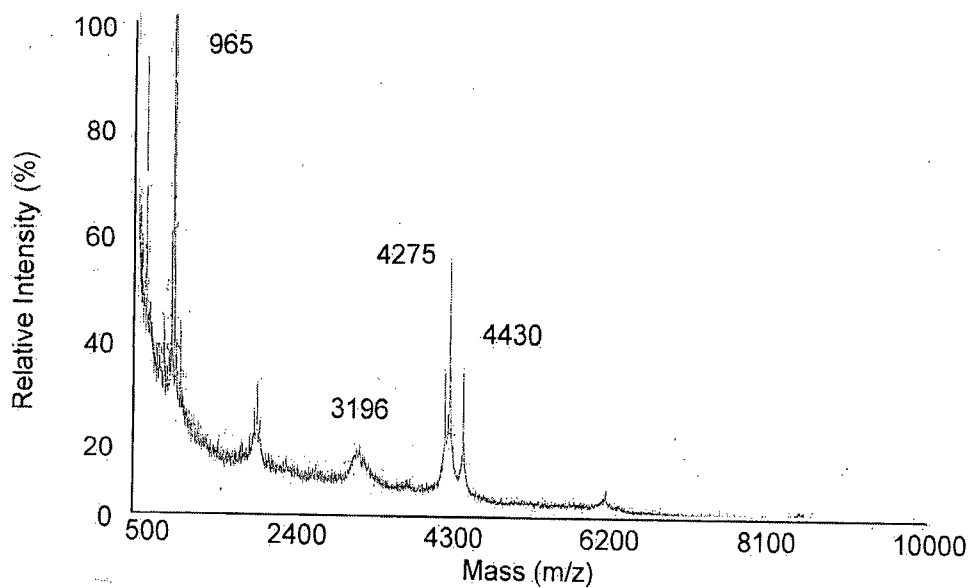
Mass (Da)	Sequences and Locations
3196	17 - FKCRW WQWRM KKLGA PSITC VRRAF A - 42
106.05	S
122.03	C
122.03	C
444.25	GA PSI
444.25	LGA PS
445.41	KKLG
485.31	KLGA P
488.27	A PSIT
2319.22	CRR WQWRM KKLGA PSITC V
2319.22	QWRM KKLGA PSITC VRRAF A
2372.31	RR WQWRM KKLGA PSITC VR
2372.31	R WQWRM KKLGA PSITC VRR
3124.69	FKCRW WQWRM KKLGA PSITC VRRAF

(b)

Figure 2.5. MALDI-ToF post source decay mass spectrum of peak with mass of 3196 Da (a) and possible peptides that were resulted from the post source decay (b).

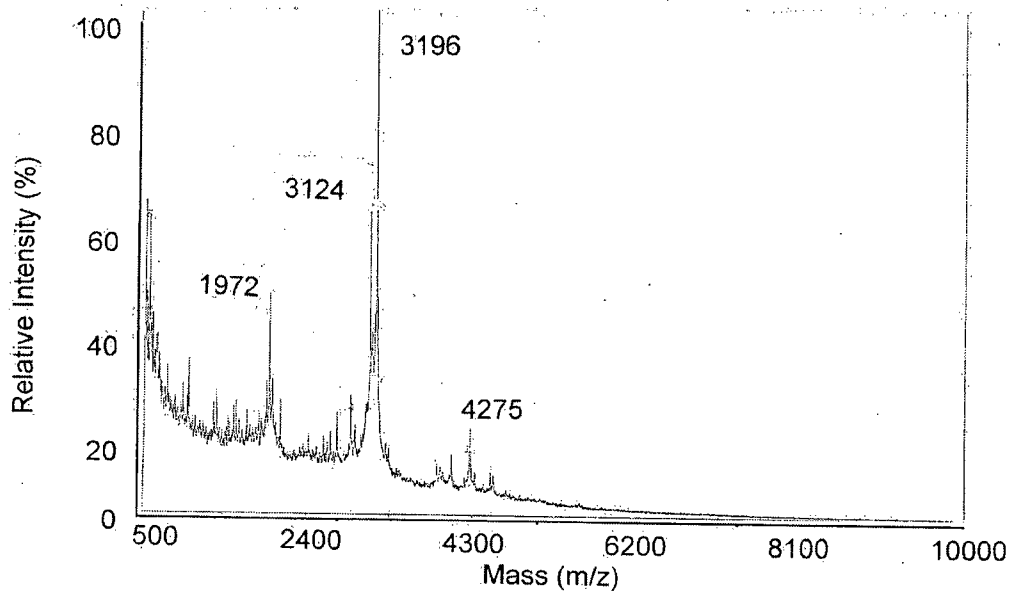


(a)

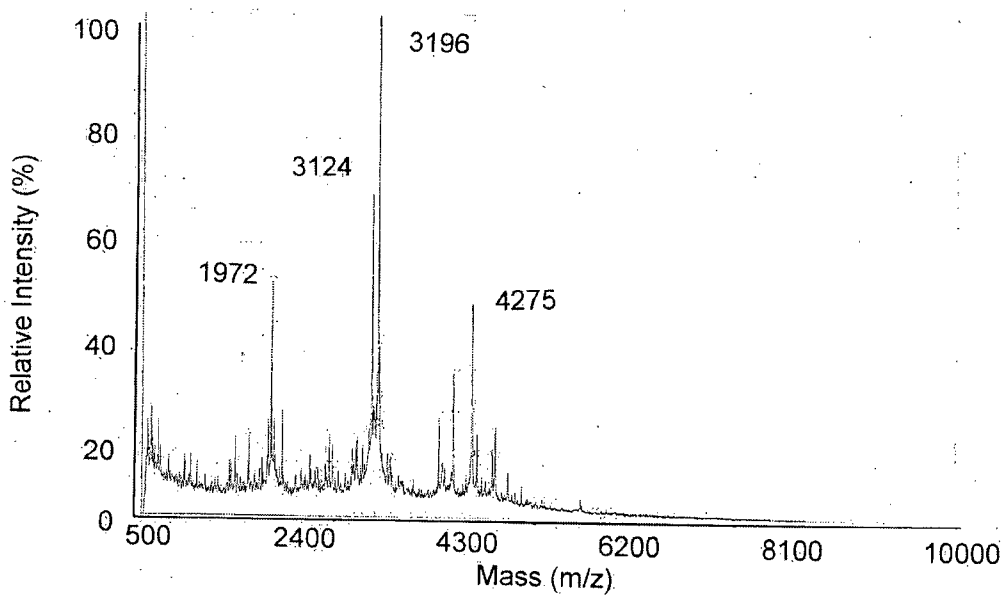


(b)

Figure 2.6. MALDI-ToF mass spectra of lactoferrin digest resulting from peptic digestion of apo-LF (a) and holo-LF (b).



(a)



(b)

Figure 2.7. MALDI-ToF mass spectra of 1.0 M NaCl fractions resulting from peptic digestion of apo-LF (a) and holo-LF (b).

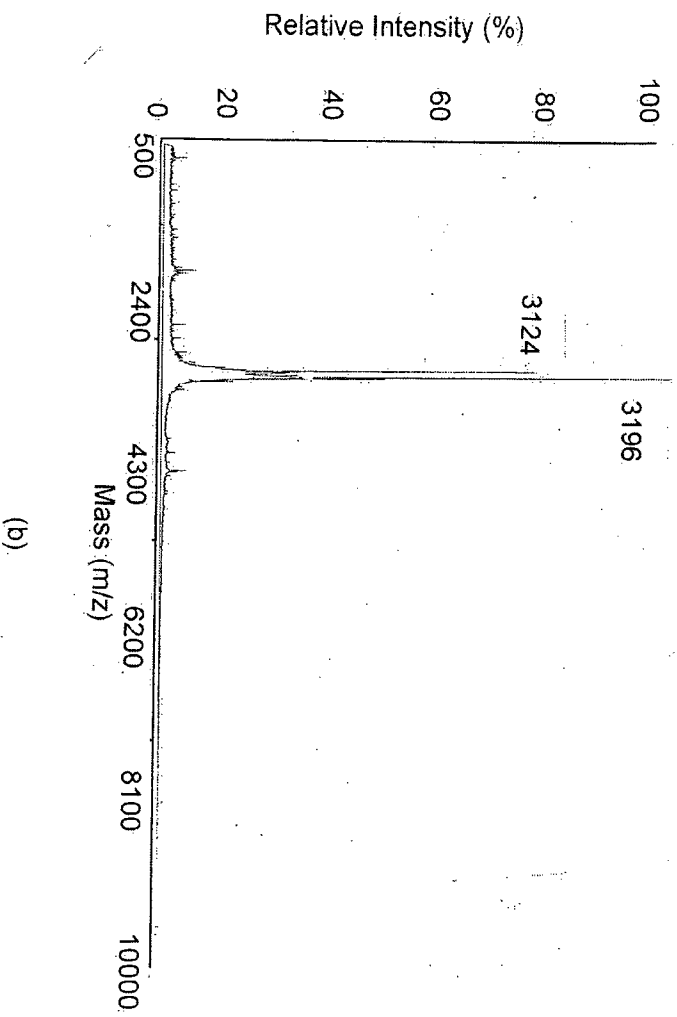
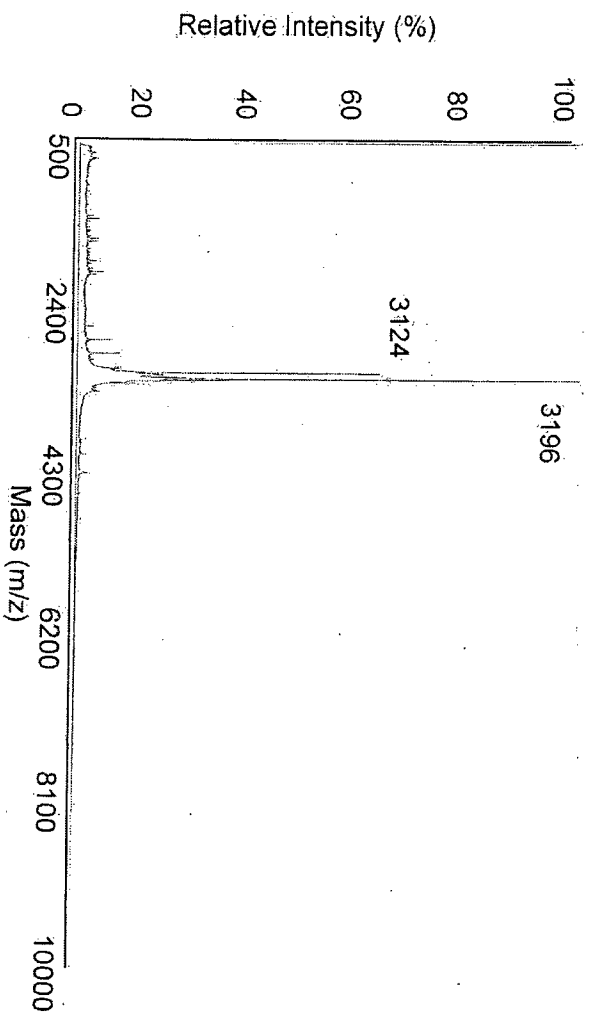


Figure 2.8. MALDI-ToF mass spectra of 2.0 M NaCl fractions resulting from peptic digestion of apo-LF (a) and holo-LF (b).

Table 2.1. Possible cationic peptides produced from the peptic digestion of bovine lactoferrin at 37 °C for 4 hours at pH 2.0. Cationic amino acids are indicated in bold.

Buffer NaCl Concentration ¹	Observed Mass (Da)	Calculated Mass (Da)	Putative Peptide Sequence ²	Peptide Position	pI ³
0.2 M NaCl & 0.5 M NaCl	4268	4267.94	QGRKS CHTGL GRSAG WIIPM GILRP YLSWT ESLEP LQGA	110-148	9.31
	4268	4269.83	GRDPY KLRPV AAELY GTKES POTHY YAVAV VKKGS NFQ	68-105	9.52
	4268	4269.95	QLDQL QGRKS CHTGL GRSAG WIIPM GILRP YLSWT ESL	105-142	9.31
	4430	4427.95	EEVKA RYTRV VWCAV GPPEEQ KKCQQ WSQQS GQNVY CATA	336-374	8.02
	4430	4427.95	TAEVY KARYT RVVWC AVGPY EQKKC QQWSQ QSGQN VTCA	334-372	7.62
0.8 M NaCl	1971	1971.27	APRKN VRWCT ISQPE W	1-16	9.51
	1971	1973.43	WRM KK LGAPS ITCVR RA	24-40	11.72
	2675	2675.21	GAPSI TCVRR AFALE CIRAI A EKKA	30-54	9.50
	3162	3162.69	APRKN VRWCT ISQPE WFKCR RWQW	1-24	10.86
	3162	3162.88	KCRRW QWRM K KLGAP SITCV RRAFA L	18-33	11.84
	3162	3163.64	AVAPN HAVVS RSDRA AHVKQ VLLHQ QALF	590-618	10.84
1.0 M NaCl	1053	1051.17	GKNKS RSFQ	279-287	11.17
	1973	1973.43	WRM KK LGAPS ITCVR RA	24-40	11.72
	2675	2675.21	GAPSI TCVRR AFALE CIRAI A EKKA	30-54	9.50
	3196	3196.90	FKCRR WQWRM KKLGA PSITC VRRAF A	17-42	11.84
	3196	3197.68	NSLKD KKSCH TAVDR TAGWN IPMGL IVNQ	447-477	9.20
	3196	3198.63	GKNKS RSFQL FGSPP GQRDL LFKDS ALGF	279-307	10.28
	4275	4276.80	SPQTH YYAVA VV KKG SNFQL DQLQG RKSCH TGLGR SAGW	97-125	9.86
	2.0 M NaCl	3124	3125.82	FKCRR WQWRM KKLGA PSITC VRRAF	17-41
3196		3196.90	FKCRR WQWRM KKLGA PSITC VRRAF A	17-42	11.84
3196		3197.68	NSLKD KKSCH TAVDR TAGWN IPMGL IVNQ	447-477	9.20
3196		3198.63	GKNKS RSFQL FGSPP GQRDL LFKDS ALGF	279-307	10.28

¹ In 50 mM phosphate buffer at pH 6.5

² As determined using PeptideCutter tool available at <http://ca.expasy.org/tools/peptidecutter/> (Gasteiger et al., 2005)

³ As determined using Compute pI/Mw tool available at http://ca.expasy.org/tools/pi_tool.html (Bjellqvist et al., 1993)

Table 2. 2. Secondary structure of bovine lactoferrin preparations (LF) at pH 2.0 as determined using Raman spectroscopy in this study and human lactoferrin (LFH) as reported in the literature.

	Raman			X-ray ¹		FTIR ²		
	α -helix	β -sheet	coil	α -helix	β -sheet	α -helix	β -sheet	coil
Untreated LF	42	32	27					
Apo-LF	34	47	19					
Holo-LF	8	57	35					
Apo-LFH						43	27	22
Holo-LFH				41	24	44	28	21

¹ X-ray data from Anderson et al. (1989).

² FTIR data from Hadden et al. (1994).

2.5. References

- Anderson, B. F. Apolactoferrin structure demonstrates ligand-induced conformational change in transferrins. *Nature* **1990**, *344*, 784-787.
- Anderson, B. F.; Baker, H. M.; Norris, G.E.; Rice, D. W.; Baker, E. N. Structure of human lactoferrin: crystallographic structure analysis and refinement at 2.8 Å resolution. *J. Mol. Biol.* **1989**, *209*, 711-734.
- Bellamy, W.; Takase, M.; Wakabayashi, H.; Kawase, K.; Tomita, M. Antibacterial spectrum of lactoferricin B, a potent bactericidal peptide derived from the N-terminal region of bovine lactoferrin. *J. Appl. Bacteriol.* **1992**, *73*, 472-479.
- Bjellqvist, B.; Hughes, G. J.; Pasquali, Ch.; Paquet, N.; Ravier, F.; Sanchez, J.-Ch.; Frutiger, S.; Hochstrasser, D.F. The focusing positions of polypeptides in immobilized pH gradients can be predicted from their amino acid sequences. *Electrophoresis* **1993**, *14*, 1023-1031.
- Dionysius, D. A.; Milne, J. M. Antibacterial peptides of bovine lactoferrin: purification and characterization. *J. Dairy Sci.* **1997**, *80*, 667-674.
- Gasteiger, E.; Hoogland, C.; Gattiker, A.; Duvaud, S.; Wilkins, M.R.; Appel, R.D.; Bairoch, A. Protein identification and analysis tools on the ExPASy server. In *The Proteomics Protocols Handbook* (Ed. J. M. Walker). **2005**. New Jersey, Humana Press. pp. 571-607
- Gattiker, A.; Bienvenut, W.V.; Bairoch, A.; Gasteiger E. FindPept, a tool to identify unmatched masses in peptide mass fingerprinting protein identification. *Proteomics* **2002**, *2*, 1435-1444.
- Hadden, J. M.; Bloemendal, M.; Haris, P. I.; Srari, S. K. S.; Chapman, D. Fourier transform infrared spectroscopy and differential scanning calorimetry of transferrin: human serum transferrin, rabbit serum transferrin and human lactoferrin. *Biochim. Biophys. Acta* **1994**, *1205*, 59-67.
- Hoek, K. S.; Milne, J. M.; Grieve, P. A.; Dionysius, D. A.; Smith, R. Antibacterial activity of bovine lactoferrin-derived peptides. *Antimicrob. Agents Chemother.* **1997**, *41*, 54-59.
- Keil, B. *Specificity of Proteolysis*. **1992**. Berlin, Springer-Verlag.
- Lehrer, R. I.; Ganz, T. Cathelicidins: a family of endogenous antimicrobial peptides. *Curr. Opin. Hematol.* **2002**, *9*, 18-22.
- Li-Chan, E.; Kwan, L.; Nakai, S. Isolation of immunoglobulins by competitive displacement of cheese whey proteins during metal chelate interaction chromatography. *J. Dairy Sci.* **1990**, *73*, 2075-2086.
- Marchetti, M.; Superti, F.; Ammendolia, M.; Rossi, P.; Valenti, P.; Seganti, L. Inhibition of poliovirus type 1 infection by iron-, manganese- and zinc-saturated lactoferrin. *Med. Microbiol. Immunol.* **1999**, *187*, 199-204.
- Mata, L.; Sánchez, D.; Headon, D. R.; Clavo, M. Thermal denaturation of human lactoferrin and its effect on the ability to bind iron. *J. Agric. Food Chem.* **1998**, *46*, 3964-3970.
- Moore, S. A.; Anderson, B. F.; Groom, C. R.; Maridas, M.; Baker, E. N. Three-dimensional structure of diferric bovine lactoferrin at 2.8 Å resolution. *J. Mol. Biol.* **1997**, *274*, 222-236.

- Nagasako, Y.; Saito, H.; Tamura, Y.; Chimamura, S.; Tomita, M. (1993). Iron-binding properties of bovine lactoferrin in iron-rich solution. *J. Dairy Sci.* **1993**, *76*, 1876-1881.
- Paulsson, M.A.; Svensson, U.; Kishore, A.R.; Naidu, S. Thermal behaviour of bovine lactoferrin in water and its relation to bacterial interaction and antibacterial activity. *J. Dairy Sci.* **1993**, *76*, 3711-3720.
- Przybycien, T.M.; Bailey, J.C. Structure-function relations in the inorganic salt-induced precipitation of α -chymotrypsin. *Biochim. Biophys. Acta* **1989**, *995*, 231-245.
- Recio, I.; Visser, S. Two ion-exchange chromatographic methods for the isolation of antibacterial peptides from lactoferrin in situ enzymatic hydrolysis on an ion-exchange membrane. *J. Chromatogr. A.* **1999**, *831*, 191-201.
- Saito, H.; Miyakawa, H.; Tamura, Y.; Shimamura, S.; Tomita, M. Potent bactericidal activity of bovine lactoferrin hydrolysate produced by heat treatment at acidic pH. *J. Dairy Sci.* **1991**, *74*, 3724-3730.
- Sánchez, L.; Peiró, J. M.; Castillo, H.; Pérez, M. D.; Ena, J. M.; Calvo, M. Kinetic parameters for denaturation of bovine milk lactoferrin. *J. Food Sci.* **1992**, *57*, 873-879.
- Shimazaki, K.-I. Lactoferrin: a marvelous protein in milk? *Anim. Sci. J.* **2000**, *71*, 329-347.
- Shimazaki, K.; Tazume, T.; Uji, K.; Tanake, M.; Kumura, H.; Mikawa, K.; Shimo-Oka, T. Properties of a heparin-binding peptide derived from bovine lactoferrin. *J. Dairy Sci.* **1998**, *81*, 2841-2849.
- Tomita, M.; Bellamy, W.; Takase, M.; Yamauchi, K.; Wakabayashi, H.; Kawase, K. Potent antibacterial peptides generated by pepsin digestion of bovine lactoferrin. *J. Dairy Sci.* **1991**, *74*, 4137-4142.
- Tomita, M.; Shimamura, S.; Kawase, K.; Fukuwatari, Y.; Takase, M.; Bellamy, W.; Hagiwara, T.; Matukuma, H. A process for large-scale production of antimicrobial peptide in high purity. **1999**. Canada: Canadian Intellectual Property Office, CA 2070882.
- Williams, R.W. Estimation of protein secondary structure from the laser amide I spectrum. *J. Mol. Biol.* **1983**, *152*, 783-813.

CHAPTER 3. HOMOLOGY SIMILARITY ANALYSIS OF SEQUENCES OF LACTOFERRICIN AND ITS DERIVATIVES²

3.1. Introduction

To understand the roles of individual amino acids on the antimicrobial activity of lactoferricin, Lfcin from different sources and synthetic Lfcin derivatives have been examined in various studies (Kang et al., 1996; Odell et al., 1996; Chapple et al., 1998; Rekdal et al., 1999; Strøm et al., 2000 and 2001; Haug et al., 2001a and b). Amino acid composition of different Lfcin derivatives was compared to their antimicrobial activity. Specific amino acids of Lfcin were replaced, deleted, or modified to understand their roles in Lfcin. For instance, Strøm et al. (2000) replaced positively charged amino acids such as arginine and lysine in Lfcin with alanine; and Haug et al. (2001a) replaced tryptophan residues with alanine and unusual amino acids. Although these studies were effective in examining the roles of individual amino acids in the antimicrobial activity of Lfcin, they did not account for the importance of the overall amino acid composition and their sequential order along Lfcin.

Quantitative structure-activity relationships (QSAR) are important in the study of functionality of bioactive peptides. The structure-function relationship of 15-residue murine Lfcin derivatives were examined using principal component analysis (PCA) and partial least squares (PLS) regression analysis (Strøm et al., 2001). However, the importance of the position of specific amino acid residues in a peptide sequence was not fully taken into consideration in their QSAR computation (Lejon et al., 2001). In an exhaustive QSAR study of protein sequences, Klein et al. (1986) stressed the importance of using attributes relating to hydrophobicity, charge and their distributions as represented by frequency of occurrence, periodicity of appearance, in addition to propensity of secondary structure, for the accurate classification of protein functionality. To date, however, there has been no established method to determine the distribution of amino acid attributes along protein sequences (Hellberg et al., 1987; Siebert, 2001).

In order to recognize the importance of the position of amino acid residues within a peptide sequence, a computer program, Homology Pattern Similarity (HSA), was developed to compare structural properties of amino acid sequences; such as helix propensity, bulkiness, hydrophobicity, and overall charge (Nakai et al., 2002). HSA data could then be further analyzed using Principal Component Similarity (PCS) analysis, which allows the simultaneous analysis of multiple PCs (Vodovotz et al., 1993). PCS analysis has been successfully used to classify several cationic antimicrobial peptides into different groups according to charge and helical propensity parameters of

² A version of this chapter has been published. Nakai, S., Chan, J. C. K., Li-Chan, E. C. Y., Dou, J., and Ogawa, M. 2003. Homology similarity analysis of sequences of lactoferricin and its derivatives. *Journal of Agricultural and Food Chemistry* 51: 1215-1223. Reproduced in part with permission from the *Journal of Agricultural and Food Chemistry*, Copyright 2003, American Chemical Society.

amino acids in their sequences. LfcinB and indolicidin were classified to have low charge but high helical content, while protamine was classified as being high charge (Nakai et al., 2003).

The objectives of this study were to apply Homology Similarity Analysis (HSA) and Principal Component Similarity (PCS) to elucidate the structural mechanisms for the antimicrobial activity of lactoferricin and its derivatives.

3.2. Materials and Methods

3.2.1. Lactoferricin Sequences

The sequences of lactoferricin and 70 Lfcin derivatives, as well as their antimicrobial activity expressed as minimal inhibitory concentration (MIC) against *E. coli*, were compiled from the literature and are listed in **Tables 3.1 to 3.5**. Peptide #2 is the 25-residue bovine lactoferricin peptide, while peptide #13 (**Table 3.1**) is the corresponding 15-residue lactoferricin derivative that was used as a reference in the HSA and PCS computation in this study.

3.2.2. Peptide Property Scales

The properties of amino acid side chains used in HSA are listed in **Table 3.6** and included helix propensities, charge, hydrophobicity, and bulkiness, as previously reported for optimization of site-directed mutagenesis (Nakai et al., 1998). Helix propensity was described as the free energy required to fix the different amino acids in the α -helical region (Muñoz et al., 1994); helix propensity values ranged from 0.617 for alanine to 1.780 for proline. The isoelectric points of the amino acids were used to represent charge of side chains (Gromiha, 1993). The amino acid hydrophobicity scale was statistically derived from a large set of experimental chromatographic retention data, with values ranging from -2.24 for histidine to 3.50 for leucine (Data Set 1 in Wilce et al., 1995). Lastly, bulkiness values of amino acids ranged from 3.40 of glycine (the least bulky) to 21.61 of tryptophan (the most bulky) (Gromiha, 1993).

3.2.3. Homology Similarity Analysis (HSA)

The software packages for HSA used in this study can be downloaded from <ftp://ftp.landfood.ubc.ca/foodsci/>. Since it was reported that a 15-mer Lfcin derivative exhibited similar antimicrobial activity to the 25-residue native peptide (Strøm et al., 2000), and the hexamer corresponding to residues 4 to 9 was reported to be the antimicrobial core of Lfcin (Tomita et al., 1994), HSA was conducted on three selected segments of the peptide sequences, corresponding to residues 1 to 15 of bovine lactoferricin, namely residues 1 to 3 (Segment I), residues 4 to 9 (Segment II), and residues 10 to 15 (Segment III) of bovine lactoferricin.

In HSA, specific structural properties of designated amino acids along the sample peptide and the reference peptide (peptide #13) were plotted against each other and the procedure was

repeated for each amino acid pair along the peptide fragment. Linear regression on the reference was carried out and the resulting coefficient of determination (r^2) was referred to as the homology similarity coefficient. Average property indices within the segments were also calculated.

3.2.4. Principal Component Similarity (PCS) Analysis

The software packages for PCS used in this study can be downloaded from <ftp://ftp.landfood.ubc.ca/foodsci/>. The principle of the PCS program has been previously described (Vodovotz et al., 1993). HSA data obtained for various structural properties of different segments from all 70 peptides were analyzed.

3.2.5. Artificial Neural Networks (ANN)

After PCA computation, major PC scores with eigen values above 1.0 were selected for the subsequent ANN computation using STATISTICA Neural Networks (Statsoft, 1999). Two output variables, log MIC and $1000 \cdot \text{MIC}^{-1}$, were tested to reflect how MIC was measured (2-fold decrease in each sequential dilution series) and to increase the sensitivity in detecting low MIC.

3.3. Results

3.3.1. Homology Similarity Analysis of Lactoferricin Sequences

Results of HSA analysis of lactoferricin and its derivatives were classified into five groups (**Tables 3.1 to 3.5**).

Lactoferricin derivatives with high antimicrobial activity (low MIC) and having similarity coefficients for helical propensity in segment II (residues 4 to 9) that were close to 1.0 (representing high similarity to the reference sample) were classified into group I (**Table 3.1**). Lfcin derivatives with high antimicrobial activity, but which were highly cationic (average values of charge over 8) in segment I (residues 1 to 3), were classified into group II (**Table 3.2**). Group III (**Table 3.3**) was the group exceptional to the general rules herein adopted, consisting of peptides with unexpectedly high and low antimicrobial activities that could not be easily correlated to structural attributes. Group IV (**Table 3.4**) consisted of Lfcin derivatives with low antimicrobial activity and low similarity coefficients for charge in segment II. Lastly, Lfcin derivatives in group V (**Table 3.5**) were also low in antimicrobial activity, and showed low or negative similarity coefficients for helical propensity in segment II.

Segment II in the sequences appears to play an important role in the antimicrobial activity of Lfcin derivatives against *E. coli*. Lfcin derivatives with higher similarity coefficient values for helical propensity in segment II demonstrated greater antimicrobial activity. When the helical pattern similarity was low in segment II (Group V), Lfcin derivatives exhibited lower inhibitory effect against *E. coli*. Conversely, lactoferricin derivatives with high similarity in helical propensity in segment II (Group

I) exhibited higher antimicrobial effect. However, it is important to note that high similarity in helical propensity of derivatives compared to the reference peptide is not necessarily correlated with high average helical propensity values per se.

In addition to the helical pattern, the pattern of charge distribution in segment II is of significance in the antimicrobial ability of Lfcin derivatives. Although peptides in group IV (**Table 3.4**) exhibited similar helical pattern in segment II to the reference, they exhibited lower antimicrobial activity. The low pattern similarity in charge distribution and lower average cationic values in segment II of these peptides might have been responsible for their higher MIC against *E. coli*. Nevertheless, when the cationic values in segment I were high (Group I), the low cationic values in segment II could be compensated and led to improved antimicrobial activity.

With some exceptions, homology similarities of the charge, hydrophobicity and bulkiness patterns in segments III did not appear to be important structural parameters that would affect the antimicrobial ability of Lfcin and its derivatives.

Loadings of PC scores 1-5 are shown in **Table 3.7**. The importance of helix structure is explicitly shown in the higher loading of similarity constants of helix values. Charge distribution at segment I (positions 1-3) is another major determinant in PC1 and PC2 (**Table 3.7**). Similar results are found when the average values were used in PCA. Average helix propensity of the amino acids in segment II were the major determinants of all PCs. Average charge values in segment I were also important in the calculation of PC2. Loadings of PC scores demonstrate the importance of helix propensity properties of the peptide sequence in segment II and the charge of the peptide sequence in segment I.

3.3.2. Principal Component Similarity Analysis

Based on the information obtained by HSA, the major structural factors that influenced the MIC values of Lfcin derivatives were similarity coefficients and average values for helical propensity in segment II, charge in segment II, and charge in segment I. Thus, these six variables were used for PCA followed by PCS analysis. The sensitivity ranks of the five input variables (PC scores 1 to 5) were 1:4:2:5:3 and 1:4:5:3:2 for log MIC and reciprocal MIC, respectively. This implies that the importance of variables in correlation is in this order.

As shown in **Figures 3.1 to 3.5**, using PCS, peptides in groups I, II, IV and V were successfully classified. Peptides in group III were distributed into group I (peptides 33, 34 and 35) and group IV (peptides 31 and 32). These results confirm the importance of helicity and charge in the antimicrobial activity of lactoferricin.

3.3.3. Regression Analysis Using Artificial Neural Networks

When the reciprocal of MIC ($1000 \cdot \text{MIC}^{-1}$) was used to train the ANN, correlation coefficients between the predicted MICs and observed MICs ranged from 0.88 to 0.90. Log MICs were also used to train the ANN, yielding correlation coefficients between predicted and observed MICs ranging from 0.95 to 0.97. The predicted values vs. observed values illustrated in **Figure 3.2** show correlation coefficients of 0.900 and 0.950, for log MIC and $1000 \cdot \text{MIC}^{-1}$, respectively.

3.4. Discussion

In the pioneering work on peptide QSAR (Hellberg et al., 1987), 29 variables were employed to characterize amino acid side chains, the dimension of which was reduced using PCA into three PCs: z1, z2, and z3. However, potentially important conformational effects of peptides were ignored. To overcome these shortcomings, Strøm et al. (2001) employed two parameters of α -helices representing micelle affinity, three parameters describing α -helical propensities, two parameters related to charge, four hydrophobicity parameters, and one parameter relating to the surface property. However, the use of several similar parameters created a problem of collinearity in subsequent regression analysis. Although PCA can extract important information to be used for regression analysis for QSAR, it is difficult to identify and isolate the true influencing factors in the antimicrobial activity of lactoferricin and its derivatives.

Unlike the three-z method of Hellberg et al. (1987), the present study used only one scale for each side chain property. Selection of only one index for each structural property was made by choosing the most reliable values with respect to analytical principles. Furthermore, by comparing segments rather than entire sequences, more detail in the underlying mechanisms of functions may be disclosed since the distribution of property patterns within sequences are taken into consideration. The new approach employed in this study, namely HSA, can incorporate potential distribution effects of side chain properties within the peptide sequences. It may be useful in addressing the question posed by Lejon et al. (2001) that the position of a specific amino acid in a peptide is of importance to the structure-function behaviours of peptides. HSA is a way to improve multivariate data analysis by distinguishing positioning information between sample and reference peptides.

Uniformity in group I as seen in **Table 3.1** is demonstrated by the pattern similarities values all being near 1.0. The lesser importance of segment III (positions 10 to 15) appears as a departure of the similarity values from 1.0 in some derivatives in this segment, as well as weaker contributions to PC scores 1 to 5 as represented in the loadings (**Table 3.7**). This does not necessarily imply a less important role played by segment III in MIC. Examples of the importance of segment III in particular derivatives are the smaller charge value of peptide #33 (classified into group III), the lower similarity in hydrophobicity of peptides #36 and #39 (classified into group IV), and the lower bulkiness

similarity in peptides #34 and #44 (in groups III and IV, respectively). Peptide #31 (in group III) with multiple lower similarities is also another example of similar deviations.

When the reciprocal MIC was assigned as the output variable in ANN computation in contrast to log MIC, better comparison of higher antimicrobial activities (low MIC) was allowed. This could be useful for searching for cationic antimicrobial peptides with greater antimicrobial activity. For instance, the low antimicrobial activity of peptide #35 (Group III) may be attributed to the simultaneous replacement of two W at positions 6 and 8 in segment II. In contrast, the corresponding single replacements made separately in peptide #23 and #24 in group I did not appreciably affect the activity. The specific function of tryptophan residues can be seen in indolicidin (Hwang and Vogel, 1998). Indolicidin activity was elucidated based on overall charge and amphipathic character of the extended-helix (Falla and Hancock, 1997); unlike lactoferricin, charge plays a more important role in indolicidin (Nakai et al., 2003).

To avoid the most crucial problem of ANN, namely over-learning, the number of input variables should be restrained to the minimum. The SD ratio (prediction error SD / data SD) may be considered as an index to demonstrate the effectiveness of ANN (Statsoft). Results from the present study show no appreciable difference between the SD ratio between the training and verification sets obtained (0.26-0.33 vs. 0.38-0.46 and 0.46-0.55 vs. 0.26-0.4, for logMIC and rcpMIC, respectively). This indicates the absence of over-learning in our ANN regression computation in the present study.

The most popular technique used for dimension reduction has been PCA, as shown by Strøm et al. (2000). However, as discussed by Lejon et al. (2001), there is a further problem in that the selected major PC scores may not be always related to the objective function (MIC in this case). The same is true in the case of the result of PCS analysis shown in **Figure 3.1**, which yields classification without considering the actual relation with MIC. The use of HSA and PCS provides a rapid method to predict the structure-activity relationship of Lfcin derivatives; nevertheless, it does not illustrate how the structural properties and antimicrobial activity are related. More research using complementary analytical tools are needed to fully understand how Lfcin works as an antimicrobial agent.

It is likely that unknown factors are still influential in the MIC data. Furthermore, potential errors may have arisen from using the output data of MIC values reported from different sources. At any rate, the accuracy in prediction of output variables could be evaluated. To enhance the validity of the conclusions, additional data should be included for the reciprocal MIC computation using ANN in the future.

Since the literature values of MIC reported by different researchers in different laboratories were used in this study, the reliability of the observed trends is dependent on consistency of these reported MIC values. However, this problem may be common as long as large scale databases are

the source data for data mining. Hence, the regression results shown in this study should be regarded, as an approximation of a trend, and more detailed interpretation may have to await collection of an adequate number of reliable data through collaborative study among researchers in the future. By using both HSA and PCA in the above data mining system, the present approach could be more effective in elucidating the function mechanism as it provides more detailed contributions of major PC scores to functions as found in this study than when using PCA alone.

In conclusion, the new data mining system using pattern similarity data based on properties of amino acid residues of segments in homology profiles can enhance reliability in predictability of QSAR compared to using the properties of the whole sequences.

Table 3.1. Homology similarity coefficient and average property values for helix (Hx), charge (Ch), hydrophobicity (Hp) and bulkiness (Bk) calculated for three segments in the sequences of Group I lactoferricin derivatives, with minimum inhibitory concentrations (MIC) against *E. coli* as reported in the literature. Segment I = position 1-3, Segment II = position 4-9, and Segment III = position 10-15 in the reference (Peptide 13) with 15-amino acid sequence identical to bovine lactoferricin. Shaded zones in the sequences represent regions with high similarity to the reference peptide, while the shading of Hx II indicates the high similarity coefficient for helix propensity in Segment II for Group I derivatives. Peptide #13 was used as the reference peptide and its values were shaded for easy comparison.

Peptide #	1	2	3	4	5	6	7	8	9	10	11	12	13
									P E W				
Segment I		F K C	F K S					F K C	F K C	F K C	K C		F K C
Segment II	R W W R	R Q W R	R Q W R	R Q W R	K W W K	R W W R	K W W R	R W W R	R W W R	R Q W R	R Q W R	R Q W R	R Q W R
Segment III		M K K L G A	M K K L G A	M K K L G	M K K L G	M K K L G	M K K L G	M K K L G	M K K L G	M K K L G	M K K L G	M K K L G	M K K L G
		P S I T C V R R A F	P S I T S V R R A F					P S I T C V R R A F					
MIC ($\mu\text{g} \cdot \text{mL}^{-1}$)	50	23	30	23	30	11	30	30	70	40	80	100	50
Literature ¹	A	B	B	B	B	B	B	E	E	E	E	E	F
Hx II													
Coefficient	1.000	1.000	1.000	1.000	0.987	1.000	0.982	1.000	1.000	1.000	1.000	1.000	1.000
Average	0.808	0.808	0.808	0.808	0.824	0.808	0.819	0.808	0.808	0.808	0.808	0.808	0.808
Ch II													
Coefficient	1.000	1.000	1.000	1.000	1.000	1.000	0.984	1.000	1.000	1.000	1.000	1.000	1.000
Average	8.400	8.400	8.400	8.400	7.850	8.400	8.033	8.400	8.400	8.400	8.400	8.400	8.400
Ch I													
Coefficient	0.000	1.000	0.982	0.000	0.000	0.000	0.000	1.000	1.000	1.000	0.994	0.000	1.000
Average	6.000	6.767	7.067	6.000	6.000	6.000	6.000	6.767	6.767	6.767	6.933	6.000	6.767
Ch III													
Coefficient	0.000	1.000	1.000	1.000	1.000	1.000	1.000	1.000	1.000	1.000	1.000	1.000	1.000
Average	6.000	7.233	7.233	7.233	7.233	7.600	7.233	7.233	7.233	7.233	7.233	7.233	7.233
Hp III													
Coefficient	0.000	1.000	1.000	0.425	0.425	0.361	0.425	1.000	1.000	1.000	1.000	1.000	1.000
Average	-10.000	0.113	0.113	-1.563	-1.563	-1.307	-1.563	0.113	0.113	0.113	0.113	0.113	-0.113
Bk III													
Coefficient	0.000	1.000	1.000	0.832	0.832	0.834	0.832	1.000	1.000	1.000	1.000	1.000	1.000
Average	0.000	13.925	13.925	12.008	12.008	11.535	12.008	13.925	13.925	13.925	13.925	13.925	13.925

¹ Literature Sources: A, Tomita et al., 1994; B, Kang et al., 1996; E, Rekdal et al., 1999; and F, Strøm et al., 2000.

Table 3.1. (cont'd).

Peptide #	14	15	16	17	18	19	20	21	22	23	24	25
Segment I	A	F	F	F	F	F	F	F	A	F	F	F
	K	A	K	K	K	K	K	K	K	K	K	K
	C	G	A	C	C	C	C	C	C	C	C	C
Segment II	R	R	R	R	R	R	R	R	R	R	R	R
	R	R	R	R	R	R	R	R	R	R	R	R
	W	W	W	W	W	W	W	W	W	F	W	W
	Q	Q	Q	A	Q	Q	Q	Q	Q	Q	Q	Q
	W	R	W	W	W	W	W	W	W	W	F	W
Segment III	M	M	M	M	M	M	M	M	M	M	M	M
	K	K	K	K	A	K	K	K	R	K	K	K
	K	K	K	K	K	A	K	K	K	K	K	K
	L	L	L	L	L	A	L	L	Y	L	L	L
	G	G	G	G	G	G	G	A	G	G	G	G
A	A	A	A	A	A	A	A	A	G	A	A	

MIC (ug · mL ⁻¹) Literature ¹	70	80	25	30	70	50	50	25	50	50	25	15
	F	F	F	F	F	F	F	F	G	H	H	I
Hx II												
Coefficient	1.000	1.000	1.000	0.840	1.000	1.000	1.000	1.000	0.998	0.981	0.981	1.000
Average	0.808	0.808	0.808	0.783	0.808	0.808	0.808	0.808	0.806	0.818	0.818	0.808
Ch II												
Coefficient	1.000	1.000	1.000	1.000	1.000	1.000	1.000	1.000	0.707	0.998	0.998	1.000
Average	8.400	8.400	8.400	8.400	8.400	8.400	8.400	8.400	7.600	8.317	8.317	8.400
Ch I												
Coefficient	0.994	0.928	0.982	1.000	1.000	1.000	1.000	1.000	0.994	1.000	1.000	0.997
Average	6.933	5.533	7.067	6.767	6.767	6.767	6.767	6.767	6.933	6.767	6.767	6.900
Ch III												
Coefficient	1.000	1.000	1.000	1.000	0.632	0.632	1.000	1.000	0.988	1.000	1.000	1.000
Average	7.233	7.233	7.233	7.233	6.617	6.617	7.233	7.233	7.417	7.233	7.233	7.233
Hp III												
Coefficient	1.000	1.000	1.000	1.000	0.931	0.931	0.694	1.000	0.966	1.000	1.000	1.000
Average	0.113	0.113	0.113	0.113	0.393	0.393	-0.460	0.098	-0.012	0.113	0.113	0.113
Bk III												
Coefficient	1.000	1.000	1.000	1.000	0.959	0.959	0.763	0.882	0.879	1.000	1.000	1.000
Average	13.925	13.925	13.925	13.925	13.225	13.225	12.342	15.275	11.843	13.925	13.925	13.925

¹ Literature Sources: F, Strøm et al., 2000; G, Strøm et al., 2001; H, Hang et al., 2001a; and I, Haug et al., 2001b.

Table 3.2. Homology similarity coefficient and average property values for helix (Hx), charge (Ch), hydrophobicity (Hp) and bulkiness (Bk) calculated for three segments in the sequences of Group II lactoferricin derivatives, with minimum inhibitory concentrations (MIC) against *E. coli* as reported in the literature. Segment I = position 1-3, Segment II = position 4-9, and Segment III = position 10-15 in the reference (Peptide 13) with 15-amino acid sequence identical to bovine lactoferricin. Shaded zones in the sequences represent regions with high similarity to the reference peptide, while the shading of Ch I indicates the high average values for charge in Segment I characteristic of Group II derivatives.

Peptide #	26	27	28	29	30
	K	R	R	R	R
Segment I	K	K	K	K	K
	C	C	C	C	C
	R	L	L	L	L
Segment II	R	R	R	R	R
	W	W	W	W	W
	Q	Q	Q	Q	Q
	W	W	W	W	W
	R	R	E	A	R
	M	M	M	M	M
Segment III	K	R	R	R	R
	K	K	K	K	K
	L	V	Y	Y	Y
	G	G	G	G	G
	A	G	G	G	G
MIC ($\mu\text{g} \cdot \text{mL}^{-1}$)	60	20	40	25	20
Literature ¹	E	G	G	G	G
Hx II					
Coefficient	1.000	0.998	0.955	0.892	0.998
Average	0.808	0.806	0.793	0.783	0.806
Ch II					
Coefficient	1.000	0.707	0.149	0.447	0.707
Average	8.400	7.600	6.333	6.800	7.600
Ch I					
Coefficient	0.566	0.407	0.407	0.407	0.407
Average	8.167	8.533	8.533	8.533	8.533
Ch III					
Coefficient	1.000	0.988	0.988	0.988	0.988
Average	7.233	7.417	7.417	7.417	7.417
Hp III					
Coefficient	1.000	0.950	0.966	0.966	0.966
Average	0.113	-0.062	-0.012	-0.012	-0.012
Bk III					
Coefficient	1.000	0.900	0.879	0.879	0.879
Average	13.925	12.422	11.843	11.843	11.843

¹ Literature Sources: E, Rekdal et al., 1999; and G, Strøm et al., 2001.

Table 3.3. Homology similarity coefficient and average property values for helix (Hx), charge (Ch), hydrophobicity (Hp) and bulkiness (Bk) calculated for three segments in the sequences of Group III lactoferricin derivatives, with minimum inhibitory concentrations (MIC) against *E. coli* as reported in the literature. Segment I = position 1-3, Segment II = position 4-9, and Segment III = position 10-15 in the reference (Peptide 13) with 15-amino acid sequence identical to bovine lactoferricin. Shaded zones in the sequences represent regions with high similarity to the reference peptide. Group III derivatives included exceptional cases with unexplained high or low MIC values.

Peptide #	31	32	33	34	35
Segment I		F K C		F K C	F K C
Segment II	R R W Q R W	F R W Q W R	R R W Q W R	R R W Q W R	R R F Q F R
Segment III	M K K L G	M K K L G	M K K L G	A K K L G	M K K L G
MIC ($\mu\text{g} \cdot \text{mL}^{-1}$) Literature ¹	23 B	20 E	200 E	140 F	300 H
Hx II					
Coefficient	0.213	0.512	1.000	1.000	1.000
Average	0.808	0.844	0.808	0.808	0.828
Ch II					
Coefficient	0.333	0.651	1.000	1.000	0.998
Average	8.400	7.517	8.400	8.400	8.233
Ch I					
Coefficient	0.000	1.000	0.566	1.000	1.000
Average	6.000	6.767	5.700	6.767	6.767
Ch III					
Coefficient	1.000	1.000	1.000	1.000	1.000
Average	7.233	7.233	7.233	7.233	7.233
Hp III					
Coefficient	0.425	1.000	1.000	0.999	1.000
Average	-1.563	0.113	0.113	0.088	0.113
Bk III					
Coefficient	0.832	1.000	1.000	0.947	1.000
Average	12.008	13.925	13.925	13.133	13.925

¹ Literature Sources: E, Rekdal et al., 1999; F, Strøm et al., 2000; and H, Haug et al., 2001a.

Table 3.4. Homology similarity coefficient and average propensity values for helix (Hx), charge (Ch), hydrophobicity (Hp) and bulkiness (Bk) calculated for three segments in the sequences of Group IV lactoferricin derivatives, with minimum inhibitory concentrations (MIC) against *E. coli* as reported in the literature. Segment I = position 1-3, Segment II = position 4-9, and Segment III = position 10-15 in the reference (Peptide 13) with 15-amino acid sequence identical to bovine lactoferricin. Shaded zones in the sequences represent regions with high similarity to the reference peptide, while the shading of Ch II indicates low similarity coefficient and average values of charge in Segment II of Group IV derivatives.

Peptide #	36	37	38	39	40	41	42	43	44	45	46
Segment I	E	E	S	F	F	F	E	S	E	A	
	K	K	K	K	K	K	K	K	K	K	K
	C	C	C	C	C	C	C	C	C	C	C
Segment II	E	L	L	R	A	R	R	L	R	L	L
	R	R	Q	R	A	R	R	Q	R	R	R
	W	W	W	W	W	W	W	W	W	W	W
	Q	Q	Q	Q	Q	Q	Q	Q	Q	Q	Q
	W	N	N	S	W	W	W	W	W	W	W
Segment III	E	E	E	K	R	R	A	E	K	E	E
	M	M	M	I	M	M	M	M	I	M	M
	E	R	R	R	K	K	K	R	R	R	R
	E	K	K	R	K	K	K	K	R	K	K
	L	V	V	T	L	L	L	V	T	V	V
	G	G	G	N	G	G	G	G	N	G	G
	G	G	P	A	A	A	G	P	G	G	
	P	P	L	S	C	V	K	K	S	S	
MIC (ug · mL ⁻¹) Literature ¹	120 B	200 E	1000 F	1000 F	70 F	120 F	55 F	1000 F	440 F	1000 G	800 G
Hx II											
Coefficient	0.971	0.910	0.910	0.963	0.883	0.883	0.883	0.955	0.988	0.955	0.955
Average	0.769	0.823	0.823	0.828	0.786	0.786	0.786	0.793	0.816	0.793	0.793
Ch II											
Coefficient	-1.000	0.191	0.191	0.698	0.707	0.707	0.707	0.149	0.698	0.149	0.149
Average	4.600	6.233	6.233	7.417	7.600	7.600	7.600	6.333	7.417	6.333	6.333
Ch I											
Coefficient	0.000	0.933	0.933	0.994	1.000	1.000	1.000	0.933	0.994	0.933	0.994
Average	6.000	6.000	6.000	6.933	6.767	6.767	6.767	6.000	6.933	6.000	6.933
Ch III											
Coefficient	-1.000	0.988	0.988	0.996	1.000	1.000	1.000	0.988	0.996	0.988	0.988
Average	5.067	7.417	7.417	7.500	7.233	7.233	7.233	7.417	7.500	7.417	7.417
Hp III											
Coefficient	0.297	0.950	0.950	0.409	1.000	1.000	1.000	0.950	0.409	0.950	0.950
Average	-1.057	-0.062	-0.062	0.485	0.113	0.113	0.113	-0.062	0.485	-0.062	-0.062
Bk III											
Coefficient	0.833	0.900	0.900	0.381	1.000	1.000	1.000	0.900	0.381	0.900	0.900
Average	11.298	12.422	12.422	16.002	13.925	13.925	13.925	12.422	16.002	12.422	12.422

¹ Literature Sources: B, Kang et al., 1996; E, Rekdal et al., 1999; F, Strøm et al., 2000; and G, Strøm et al., 2001.

Table 3.4. (cont'd).

Peptide #	47	48	49	50	51	52	53	54	55	56
Segment I	E	A	R	E	A	R	A	E	A	E
	K	K	K	K	K	K	K	K	K	K
	C	C	C	C	C	C	C	C	C	C
Segment II	L	L	L	L	L	L	L	L	L	L
	R	R	R	R	R	R	R	R	R	R
	W	W	W	W	W	W	W	W	W	W
	Q	Q	Q	Q	Q	Q	Q	Q	Q	Q
	W	W	W	W	W	W	W	W	W	W
Segment III	A	A	E	R	R	A	E	A	A	R
	M	M	M	M	M	M	M	M	M	M
	R	R	R	R	R	R	R	R	R	R
	K	K	K	K	K	K	K	K	K	K
	V	V	V	V	V	V	Y	Y	Y	Y
	G	G	G	G	G	G	G	G	G	G
	G	G	G	G	G	G	G	G	G	G
MIC ($\mu\text{g} \cdot \text{mL}^{-1}$) Literature ¹	1000	270	75	200	62	62	300	1000	175	125
	H	H	H	H	H	H	H	H	H	H
Hx II										
Coefficient	0.892	0.892	0.955	0.998	0.998	0.892	0.955	0.892	0.892	0.998
Average	0.783	0.783	0.793	0.806	0.806	0.783	0.793	0.783	0.783	0.806
Ch II										
Coefficient	0.447	0.447	0.149	0.707	0.707	0.447	0.149	0.447	0.447	0.707
Average	6.800	6.800	6.333	7.600	7.600	6.800	6.333	6.800	6.800	7.600
Ch I										
Coefficient	0.933	0.994	0.407	0.933	0.994	0.407	0.994	0.933	0.994	0.933
Average	6.000	6.933	8.533	6.000	6.933	8.533	6.933	6.000	6.933	6.000
Ch III										
Coefficient	0.988	0.988	0.988	0.988	0.988	0.988	0.988	0.988	0.988	0.988
Average	7.417	7.417	7.417	7.417	7.417	7.417	7.417	7.417	7.417	7.417
Hp III										
Coefficient	0.950	0.950	0.950	0.950	0.950	0.950	0.966	0.966	0.966	0.966
Average	-0.062	-0.062	-0.062	-0.062	-0.062	-0.062	-0.012	-0.012	-0.012	-0.012
Bk III										
Coefficient	0.900	0.900	0.900	0.900	0.900	0.900	0.879	0.879	0.879	0.879
Average	12.422	12.422	12.422	12.422	12.422	12.422	11.843	11.843	11.843	11.843

¹ Literature Source: H, Haug et al., 2001a.

Table 3.5. Homology similarity coefficient and average property values for helix (Hx), charge (Ch), hydrophobicity (Hp) and bulkiness (Bk) calculated for three segments in the sequences of Group V lactoferricin derivatives, with minimum inhibitory concentrations (MIC) against *E. coli* as reported in the literature. Segment I = position 1-3, Segment II = position 4-9, and Segment III = position 10-15 in the reference (Peptide 13) with 15-amino acid sequence identical to bovine lactoferricin. Shaded zones in the sequences represent regions with high similarity to the reference peptide, while the shading of HxII indicates low similarity coefficient values for helix propensity in Segment II of Group V derivatives.

Peptide #	57	58	59	60	61	62	63
	S	K	S	F	F	T	S
Segment I	K	K	K	K	K	K	K
	C	C	C	C	C	C	C
	Y	F	Y	R	R	F	Y
Segment II	Q	R	Q	R	R	Q	Q
	W	W	W	A	W	W	W
	Q	Q	Q	Q	Q	Q	Q
	R	W	R	W	A	W	W
	R	R	R	R	R	N	R
	M	M	M	M	M	M	M
Segment III	R	K	R	K	K	R	R
	K	K	K	K	K	K	K
	L	L	L	L	L	V	L
	G	G	G	G	G	R	G
	A	A	A	A	A	G	A
	P						
	S						
	I						
	T						
	C						
	V						
	R						
	R						
	T						
	S						
MIC (ug · mL ⁻¹)	750	200	500	200	200	150	350
Literature ¹	E	E	F	F	F	F	F
Hx II							
Coefficient	0.007	0.512	0.007	0.040	0.041	0.000	0.393
Average	0.828	0.844	0.828	0.759	0.759	0.903	0.854
Ch II							
Coefficient	0.000	0.651	0.000	1.000	1.000	-0.703	0.447
Average	7.600	7.517	7.600	8.400	8.400	5.817	6.800
Ch I							
Coefficient	0.994	0.566	0.994	1.000	1.000	0.994	0.994
Average	6.933	8.167	6.933	6.767	6.767	6.933	6.933
Ch III							
Coefficient	0.988	1.000	0.988	1.000	1.000	0.640	0.988
Average	7.417	7.233	7.417	7.233	7.233	8.217	7.417
Hp III							
Coefficient	0.987	1.000	0.987	1.000	1.000	0.915	0.987
Average	0.242	0.113	0.242	0.113	0.113	-0.228	0.242
Bk III							
Coefficient	0.995	1.000	0.995	1.000	1.000	0.477	0.995
Average	13.688	13.925	13.688	13.925	13.925	14.235	13.688

¹ Literature Sources: E, Rekdal et al., 1999; and F, Strøm et al., 2000.

Table 3.5. (cont'd).

Peptide #	64	65	66	67	68	69	70	71
Segment I							T K C	T K C
Segment II	R R A A R R A K K A G	F Q W Q R N M R K V R G P P V S						
MIC (ug · mL ⁻¹) Literature ¹	120 B	1000 C	1000 C	1000 D	580 D	2000 D	200 E	1000 F
Hx II	Coefficient -0.764 -0.297 -0.297 -0.297 -0.297 -0.297 -0.297 -0.297							
Ch II	Average 0.685 0.877 0.877 0.877 0.877 0.877 0.877 0.877							
Ch I	Coefficient 1.000 -0.521 -0.521 -0.521 -0.521 -0.521 -0.521 -0.521							
Ch III	Average 8.400 6.617 6.617 6.617 6.617 6.617 6.617 6.617							
Hp III	Coefficient 0.000 0.000 0.000 0.000 0.000 0.000 0.994 0.994							
Bk III	Average 6.000 6.000 6.000 6.000 6.000 6.000 6.933 6.933							
	Coefficient 1.000 0.640 0.640 0.640 0.640 0.640 0.640 0.640							
	Average 7.233 8.217 8.217 8.217 8.217 8.217 8.217 8.217							
	Coefficient 0.173 0.915 0.265 0.915 0.265 0.263 0.915 0.915							
	Average -2.162 -0.228 -1.920 -0.228 -1.920 -1.837 -0.228 -0.228							
	Coefficient 0.658 0.477 0.431 0.477 0.431 0.438 0.477 0.477							
	Average 9.633 14.235 13.668 14.235 13.668 13.865 14.235 14.235							

¹ Literature Sources: B, Kang et al., 1996; C, Odell et al., 1996; D, Chapple et al., 1998; E, Rekdal et al., 1999; and F, Strøm et al., 2000.

Table 3.6. Amino acid structural propensity values used for Homology Similarity Analysis (HSA).

	Helix	Charge	Hydrophobicity	Bulkiness
Ala	0.617	6.0	0.06	11.50
Arg	0.753	10.8	-0.85	14.28
Asn	1.089	5.4	0.25	12.82
Asp	0.932	2.8	-0.20	11.68
Cys	1.107	5.1	0.49	13.46
Gln	0.770	6.0	0.31	14.45
Glu	0.675	3.2	-0.10	13.57
Gly	1.361	6.0	0.15	3.40
His	1.034	7.6	-2.24	13.67
Ile	0.876	6.0	3.00	21.40
Leu	0.740	6.0	3.50	21.00
Lys	0.784	9.7	-1.62	15.70
Met	0.730	6.0	0.21	16.25
Phe	0.968	5.5	4.80	19.80
Pro	1.780	6.0	0.71	17.43
Ser	0.980	6.0	-0.62	9.47
Thr	1.053	6.0	0.65	15.80
Trp	0.910	6.0	2.29	21.61
Tyr	1.009	6.0	1.89	18.03
Val	0.940	6.0	1.59	21.50
Literature ¹	A	B	C	D

¹ Literature Sources: A, Muñoz et al., 1994; B, Isoelectric Point; C, Wilce et al., 1995; and D, Gromiha and Ponnuswamy, 1993.

Table 3.7. Loadings of input variables, homology similarity constant (SimCnst, determined using homology similarity analysis, HSA) and Average (Ave) of Helical Propensity in position 4 to 9, charge in position 4 to 9, charge in position 1 to 3, and charge in position 10 to 15, determined by Principal Component Analysis (PCA).

	Helix 4-9		Charge 4-9		Charge 1-3		Charge 10-15	
	SimCnst	Ave	SimCnst	Ave	SimCnst	Ave	SimCnst	Ave
PC1	-0.55	0.51	-0.24	-0.01	0.35	0.15	0.47	0.09
PC2	0.42	-0.62	0.19	0.06	0.47	0.34	0.06	-0.21
PC3	-0.66	0.60	0.42	-0.02	0.04	0.10	-0.01	0.05
PC4	-0.49	0.44	0.64	0.06	0.03	0.25	-0.26	-0.08
PC5	-0.67	-0.20	-0.14	0.36	0.39	-0.27	-0.27	0.24

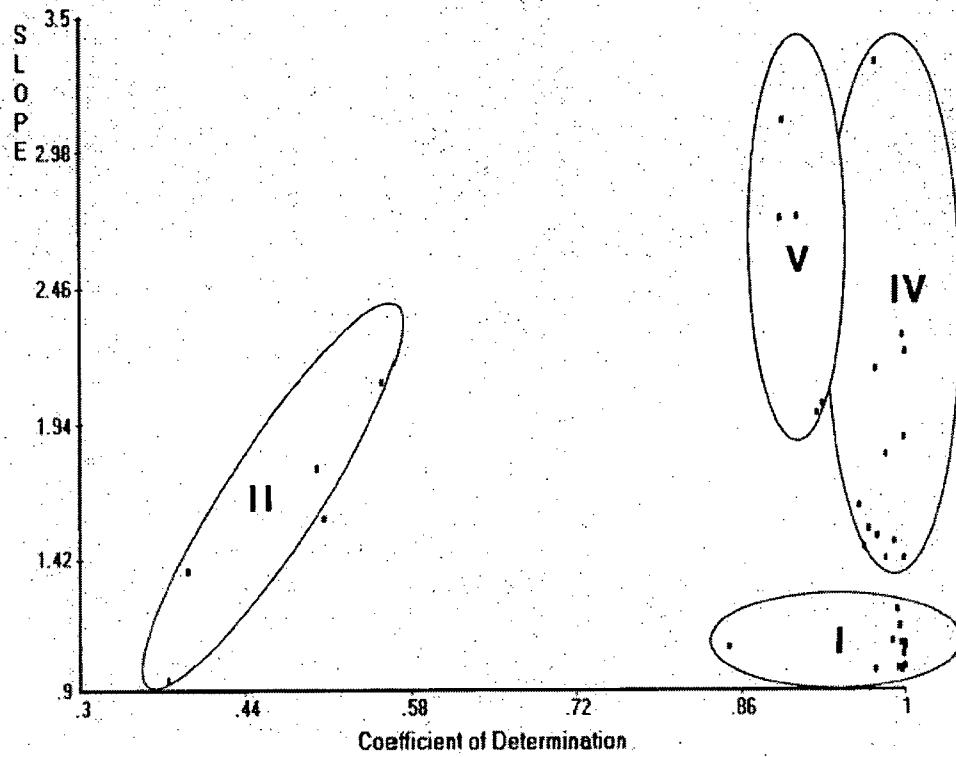


Figure 3.1. Principal component similarity (PCS) scattergram of lactoferricin derivatives using data obtained from homology similarity analysis (HSA). Group I-V are listed in Tables 3.1 – 3.5.

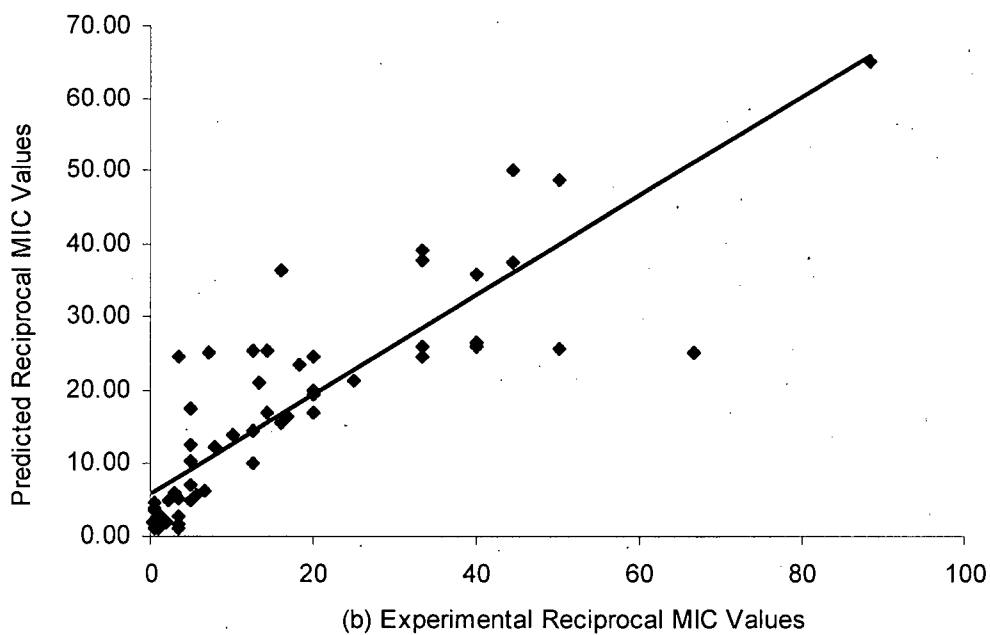
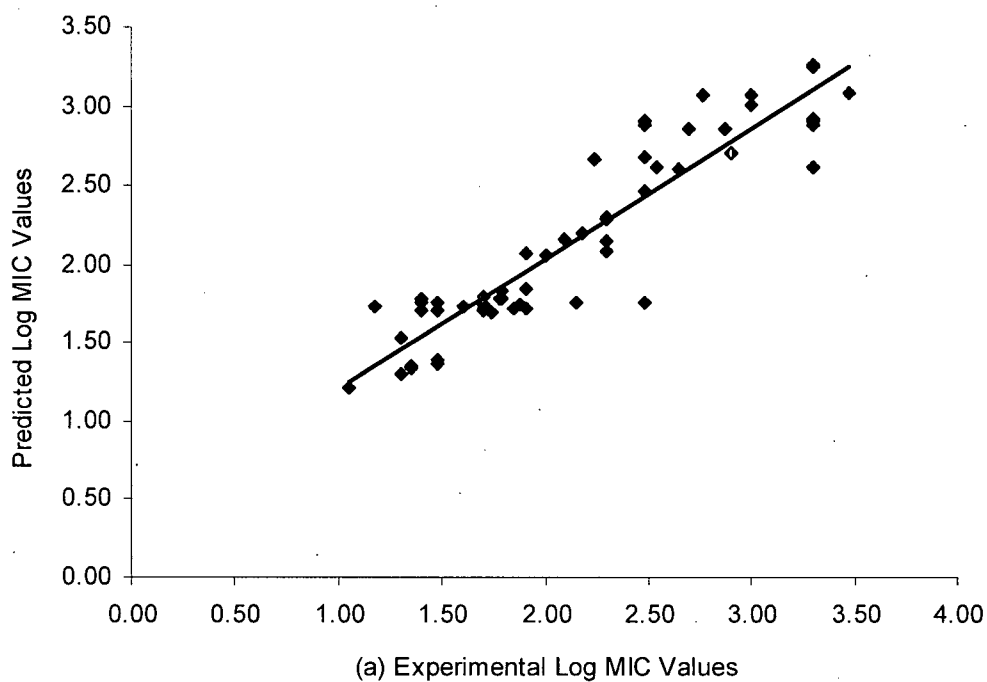


Figure 3.2. Plots of predicted values vs. observed values by artificial neural network: (a) Log MIC and (b) Reciprocal MIC.

3.5. References

- Chapple, D. S.; Mason, D. J.; Joannou, C. L.; Odell, E. W.; Gant, V.; Evans, R. W. Structure-function relationship of antibacterial synthetic peptides homologous to a helical surface region on human lactoferrin against *Escherichia coli* serotype O111. *Infect. Immun.* **1998**, *66*, 2434-2440.
- Falla, R. J.; Hancock, R. E. W. Improved activity of a synthetic indolicidin analog. *Antimicrob. Agents Chemother.* **1997**, *41*, 771-775.
- Gromiha, M. M.; Ponnuswamy, P. K. Relationship between amino acid properties and protein compressibility. *J. Theor. Biol.* **1993**, *165*, 87-100.
- Haug, B. E.; Svendsen, J. S. The role of tryptophan in the antibacterial activity of a 15-residue bovine lactoferricin peptide. *J. Pept. Sci.* **2001a**, *7*, 190-196.
- Haug, B. E.; Skar, M. L.; Svendsen, J. S. Bulky aromatic amino acids increase the antibacterial activity of 15-residue bovine lactoferricin derivatives. *J. Pept. Sci.* **2001b**, *7*, 425-432.
- Hellberg, S.; Sjöström, M.; Skagerberg, B.; Wold, S. Peptide quantitative structure-activity relationships, a multivariate approach. *J. Med. Chem.* **1987**, *30*, 1126-1135.
- Hwang, P. M.; Vogel, H. J. Structure-function relationships of antimicrobial peptides. *Biochem. Cell Biol.* **1998**, *76*, 235-246.
- Kang, J. H.; Lee, M. K.; Kim, K. L.; Hahm, K.-S. Structure-biological activity relationships of 11-residue highly basic peptide segment of bovine lactoferrin. *Int. J. Pept. Protein Res.* **1996**, *48*, 357-363.
- Klein P.; Jacquez, I. A.; Delis, C. Prediction of protein function by discriminant analysis. *Math. Biosci.* **1986**, *81*, 177-189.
- Lejon, T.; Strøm, M. B.; Svendsen, J. S. Is information about peptide sequence necessary in multivariate analysis? *Chemometr. Intel. Lab. Syst.* **2001**, *57*, 93-95.
- Muñoz, V.; Serrano, L. Intrinsic secondary structure propensities of the amino acids, using statistical ϕ - ϕ matrices: Comparison with experimental scales. *Proteins* **1994**, *20*, 301-311.
- Nakai, S.; Nakamura, S.; Scaman, C. H. Optimization of site-directed mutagenesis. 2. Application of random-centroid optimization to one-site mutation of *B. stearothermophilus* neutral protease for improving thermostability. *J. Agric. Food Chem.* **1998**, *46*, 1655-1661.
- Nakai, S.; Amantea, G.; Nakai, H.; Ogawa, M.; Knanagawa, S. Definition of outliers using unsupervised principal component similarity analysis for sensory evaluation of foods. *Int. J. Food Prop.* **2002**, *5*, 289-306.
- Nakai, S.; Ogawa, M.; Nakamura, S.; Dou, J.; Funane, K. A computer-aided strategy for structure-function relation study of food proteins using unsupervised data mining. *Int. J. Food Prop.* **2003**, *6*, 25-47.
- Odell, E. W.; Sarra, R.; Foxworthy, M.; Chapple, D. S.; Evans, R. W. Antibacterial activity of peptides homologous to a loop region in human lactoferrin. *FEBS Lett.* **1996**, *382*, 175-178.

- Rekdal, Ø.; Andersen, J.; Vorland, L. H.; Svendsen, J. S. Construction and synthesis of lactoferricin derivatives with enhanced antibacterial activity. *J. Pept. Sci.* **1999**, *5*, 32-45.
- Siebert, K. Quantitative structure-activity relationship modeling of peptide and protein behaviour as a function of amino acid composition. *J. Agric. Food Chem.* **2001**, *49*, 851-858.
- Statsoft, Addendum for Version 4, In *Statistica Neural Networks*, **1999**. Tulsa, Statsoft.
www.statsoft.com.
- Strøm, M. B.; Rekdal, Ø.; Svendsen, J. S. Antibacterial activity of 15-residue lactoferricin derivatives. *J. Pept. Res.* **2000**, *56*, 265-274.
- Strøm, M. B.; Rekdal, Ø.; Stensen, W.; Svendsen, J. S. Increased antibacterial activity of 15-residue murine lactoferricin derivatives. *J. Peptide Res.* **2001**, *57*, 127-139.
- Tomita, M.; Takase, M.; Bellamy, W.; Shimamura, S. A review: The active peptide of lactoferrin. *Acta Paediatr. Jpn.* **1994**, *36*, 585-591.
- Vodovotz, Y.; Arteaga, G. E.; Nakai, S. Principal component similarity analysis for classification and its application to GC data of mango. *Food Res.Int.* **1993**, *26*, 355-363.
- Wilce, M. C. J.; Aguilar, M.-I.; Heam, M. T. Physicochemical basis of amino acid hydrophobicity scales: Evaluation of four new scales of amino acid hydrophobicity coefficients derived from RP-HPLC of peptides. *Anal. Chem.* **1995**, *67*, 1210-1219.

CHAPTER 4. RAMAN SPECTROSCOPIC STUDY OF THE EFFECTS OF LACTOFERRICIN ON THERMAL TRANSITIONS OF PHOSPHOLIPIDS IN LIPOSOMES³

4.1. Introduction

Cationic antimicrobial peptides (CAPs) play a critical role in the host defense system of many higher organisms such as plants, insects, and mammals, and are being considered as a potential source of new antibiotics on the basis of their fast killing action, selective toxicity and low potential for resistance. Studies on CAPs have shown that the presence of cationic and hydrophobic amino acids was responsible for their interactions with the bacterial membrane (Erand and Vogel, 1999), leading to the disruption of the bacterial membrane and possible action on intracellular targets, such as DNA and RNA (Kanyshkova et al., 1999).

There is evidence that CAPs show specificity for particular membrane lipid components. Herbig et al. (2005) detected strong interactions of the peptide with negatively charged phospholipids. The peptide cinnamycin caused an increase in permeability and aggregation of liposomes containing phosphatidylethanolamine (PE), but liposomes containing phosphatidylserine (PS), phosphatidylinositol (PI) or cardiolipin (CL) were not appreciably reactive with cinnamycin (Choung et al., 1988). Magainins also demonstrated preferential interaction with negatively charged phospholipids, effectively permeabilizing phosphatidylglycerol (PG)-rich membranes and killing bacteria whose inner membranes contain higher amounts of PG (Matsuzaki et al., 1997). Similar results were also demonstrated when LL-37, an antimicrobial peptide found in humans, was readily incorporated into 1,2-dipalmitoyl-*sn*-glycerol-3-[phospho-*rac*-(1-glycerol)] (DPPG) monolayers (Neville et al., 2006).

Phospholipid liposomes are widely used as a model system for biomembranes. Studies on 1,2-dipalmitoyl-*sn*-glycerol-3-[phospho-*rac*-(1-choline)] (DPPC) liposomes are commonly found in the literature because phosphatidyl choline (PC) or lecithins are the major component of most mammalian biomembranes (Opekarová and Tanner, 2003.) Phospholipid compositions of individual genera and species of Gram-negative and Gram-positive bacteria are very different from those of mammals (Yeagle, 1993). For instance, PC is often absent from Gram-positive bacteria. In contrast, PG and its derivatives are the only phospholipids found in the membrane of *Staphylococcus aureus* and PE is the dominant component of the membrane of *Escherichia coli*, a Gram-negative species (Opekarová and Tanner, 2003).

Studies of the interaction of antimicrobial peptides with model membranes can provide some important insights into the antimicrobial mechanisms and how the peptides may affect the structure of

³ A version of this chapter will be submitted for publication. Chan, J. C. K., and Li-Chan, E. C. Y. Raman spectroscopic study of the effects of lactoferricin on thermal transitions of phospholipids in liposomes. *Biochimica et Biophysica Acta (BBA) – Biomembranes*.

the membranes. Even if the site of action of an antimicrobial peptide is intracellular, the peptide first has to pass through the bacterial membrane, and this process is not understood at the molecular level at present.

To date, there is a paucity of literature on the interaction of Lfcin with different phospholipids. An understanding of the molecular interactions between Lfcin and different phospholipids would shed light on the antimicrobial mechanisms of Lfcin. It could also facilitate the design of Lfcin derivatives or other CAPs that exhibit effective antimicrobial action without the undesirable interactions with mammalian membranes that can lead to hemolysis (Kang et al., 1996).

Raman spectroscopy can be useful to study the structural arrangement of phospholipids. The Raman spectra of phospholipids are strongly modified by environmental factors such as temperature and interactions with other substances in the bilayer structure. Sharp changes are observed in correspondence to endothermic gel and liquid crystal transition. Remarkable agreement between observations made using the Raman technique and those obtained by calorimetric measurements or theoretical calculations has been reported (Gaber and Peticolas, 1977). Raman spectroscopy has been used to study the interactions of model phospholipid membrane and bioactive peptides (Susi et al., 1979; Lafleur et al., 1989; Bouchard and Auger, 1993). In a series of studies on pulmonary surfactants, Vincent et al. (1991 and 1993) used Raman spectroscopy to measure the carbon-hydrogen stretching mode region (2800 to 3100 cm^{-1}) of DPPC and DPPG liposomes. Peak heights of Raman peaks near 2850, 2880, and 2935 cm^{-1} at various temperatures were evaluated to assess the effects of human surfactant peptides on the thermotropic behaviour on these liposomes.

In this study, we use Raman spectroscopy in the C-H stretching region over the temperature range from -10 °C to 70 °C to investigate the effects of Lfcin on liposomes composed of PG, PC, and PE as a model bacterial cell membrane system.

4.2. Materials and Methods

4.2.1. Materials

Sodium salts of 1,2-dipalmitoyl-*sn*-glycerol-3-phosphocholine (DPPC), 1-palmitoyl-2-oleoyl-*sn*-glycerol-3-phosphocholine (POPC) 1,2-dipalmitoyl-*sn*-glycerol-3-[phospho-*rac*-(1-glycerol)] (DPPG), 1-palmitoyl-2-oleoyl-*sn*-glycerol-3-[phospho-*rac*-(1-glycerol)] (POPG), 1,2-dipalmitoyl-*sn*-glycerol-3-phosphoethanolamine (DPPE), and 1-palmitoyl-2-oleoyl-*sn*-glycerol-3-phosphoethanolamine (POPE) were purchased from Avanti Polar Lipids (Alabaster, AL) in lyophilized powder forms. Purified bovine lactoferricin (Lfcin) was purchased from the Centre for Food Technology (Hamilton, Australia). MALDI-ToF mass spectrometry confirmed that the Lfcin preparation had a mass of 3124 Daltons with purity over 90%.

4.2.2. Preparation of Liposomes

The method for preparation of multilamellar liposomes was adapted from methods previously reported in the literature examining interactions between peptides and different phospholipid systems (Laroche et al., 1988; Devlin and Levin, 1989; Laroche et al., 1990). Phospholipids were mixed with buffer (0.15M Na Tris-acetate buffer, pH 7.2) or buffer containing Lfcin at a molar ratio of lipid to peptide of 60:1. The mixture was rehydrated in pre-warmed buffer for 1 hour at 72 °C. The solution was then agitated with a vortex mixer, heated for 10 minutes, agitated again, and cooled down below the gel to liquid-crystalline phase transition temperature by incubating at -18 °C for 10 minutes. This cycle was repeated at least 3 times to ensure uniform packing of different racemates of the phospholipids in the bilayer. The samples were vortexed again, transferred to glass capillary tubes and concentrated in a hematocrit centrifuge for 5 minutes, then aged overnight at 4 °C to improve the homogeneity of the size distribution (Avanti Polar Lipid). Incorporation of Lfcin into the liposomes was inferred by the absence of Lfcin in the supernatant, as confirmed by protein assay using bicinchoninic acid.

4.2.3. Raman Spectroscopy

Raman spectra of each sample were measured on a JASCO NR-1100 Raman spectrometer (JASCO Inc., Tokyo, Japan) with excitation at 488 nm from an argon ion laser (Coherent Innova 70C series, Coherent Laser Group, Santa Clara, CA). Wavenumber was calibrated everyday using the 1050 cm^{-1} band of a standard potassium nitrate solution. Capillary tubes containing the samples were held inside the constant temperature measuring accessory (model RT-1C, JASCO Inc.) and equilibrated for at least 5 minutes at the desired temperature prior to spectral data collection. Spectra were collected in order of ascending temperature, with spectral data from at least 6 scans averaged for each sample at each temperature.

4.2.4. Raman Spectral Analysis

OMNIC Version 6.0a (Thermo Nicolet Corporation) and GRAMS/32 Version 4.14 (Spectral Notebase, Galactic Industries Corporation) were used to process the spectral data obtained in the present study. The spectra were baseline corrected (2-point system with anchors near the ends of each spectrum), smoothed (Savitsky-Golay function with a second order polynomial function with 5 points), and offset (minimum point at zero). Peak positions, heights, areas, widths at half height of peaks near 2850, 2880, and 2935 cm^{-1} were recorded and compared. Curve fitting of the three peaks near 2850, 2880, and 2935 cm^{-1} was performed. Properties of the fitted peaks were also measured. Typical coefficients of variation for replicate spectra of selected samples were less than 10%. The statistical method described by Badii and Howell (2003) was used to detect differences between treatments at the 5% significance level.

4.3. Results

The C-H stretching region of DPPC liposomes in the presence of Lfcin at various representative temperatures from $-10\text{ }^{\circ}\text{C}$ to $60\text{ }^{\circ}\text{C}$ are shown in **Figure 4.1**. A gradual broadening of the peak near 2880 cm^{-1} was observed with increasing temperature of the system. At temperatures below $40\text{ }^{\circ}\text{C}$, the peak near 2880 cm^{-1} remained very distinct and had a higher intensity than the peak near 2850 cm^{-1} . At temperatures above $40\text{ }^{\circ}\text{C}$, the peak near 2880 cm^{-1} widened, decreased in intensity, and gradually shifted to higher wavenumber. The peak near 2935 cm^{-1} also increased in relative intensity as temperature rose. Similar temperature dependent changes of the spectra were observed in the absence of Lfcin.

A more detailed analysis of the effects of the temperature dependence of the acyl chain packing characteristics and phase transition cooperativities on the various Raman spectroscopic features can be achieved through analyzing physical properties of peaks near 2850 , 2880 , and 2935 cm^{-1} . Preliminary studies showed that ratios of peak-height, peak-area, and peak-width at mid-height illustrated similar trends. Hence, only peak-height intensity ratios of peaks near 2850 , 2880 , and 2935 cm^{-1} , commonly used parameters in the literature (Snyder et al., 1980 and 1982; Devlin and Levin, 1989; Vincent et al., 1991 and 1993), are shown in **Figures 4.2**, **4.3**, and **4.4** for DPPC & POPC, DPPG & POPG, and DPPE & POPE, respectively. Statistical differences between peak-height intensity ratios were confirmed by a statistical method described by Badii and Howell (2003) at 5% significance level.

The intensity ratio I_{2850}/I_{2880} of DPPC liposomes gradually increased over the temperature range tested, with a broad transition between $20\text{ }^{\circ}\text{C}$ and $60\text{ }^{\circ}\text{C}$ (**Figure 4.2a**). The presence of Lfcin in the liposomes resulted in lower I_{2850}/I_{2880} ratios throughout the temperature range while exhibiting generally similar temperature dependent behaviour as the spectra without Lfcin. The presence of Lfcin increased the temperature at which the transition was observed; in other words, an increase in the intensity ratio was primarily between 20 and 40 , and at $50\text{ }^{\circ}\text{C}$ for DPPC with Lfcin, whereas DPPC without Lfcin showed an increase in the ratio starting already at $5\text{ }^{\circ}\text{C}$ and more pronounced at 10 , $15\text{ }^{\circ}\text{C}$, and had almost reached a plateau by 20 - $30\text{ }^{\circ}\text{C}$.

The I_{2935}/I_{2880} ratio depicted a sharper change as function of temperature increases in the terminal $-\text{CH}_3$ group than the I_{2850}/I_{2880} ratio (**Figure 4.2b**). In the absence of Lfcin, a sharp change in I_{2935}/I_{2880} ratio of DPPC liposomes occurred at approximately $38\text{ }^{\circ}\text{C}$. A minor increase in the I_{2935}/I_{2880} ratio was also detected at above $0\text{ }^{\circ}\text{C}$. The presence of Lfcin in DPPC liposomes resulted in a general lowering in I_{2935}/I_{2880} ratio over the temperature range tested and broadening of the transition stage. Addition of the Lfcin to DPPC liposomes caused the I_{2935}/I_{2880} ratio to increase from around $20\text{ }^{\circ}\text{C}$ to $50\text{ }^{\circ}\text{C}$ and delay the transition temperature to $40\text{ }^{\circ}\text{C}$. Furthermore, the presence of Lfcin in DPPC liposomes also led to the disappearance of the transition near $0\text{ }^{\circ}\text{C}$.

POPC liposomes experienced a very mild change over the temperature range tested as indicated by the I_{2850}/I_{2880} ratio (**Figure 4.2c**). A gentle upward shift in the I_{2850}/I_{2880} ratio was observed as temperature increased. Nevertheless, a transition near 0 °C was exhibited by the I_{2935}/I_{2880} ratio (**Figure 4.2d**). The presence of Lfcin had little effect on the thermal behaviour of POPC.

The I_{2850}/I_{2880} ratio of DPPG exhibited a gradual increase as temperature increased (**Figure 4.3a**). The ratio increased steadily at temperature below 25 °C and increased more rapidly between 25 and 40 °C, and then reached a plateau above 40 °C. The addition of Lfcin to the DPPG system had little effect as indicated by the I_{2850}/I_{2880} ratio. Sharper changes of the temperature dependent behaviour of DPPG were observed using the I_{2935}/I_{2880} ratio (**Figure 4.3b**). In the absence of Lfcin, DPPG liposomes demonstrated an increase in the I_{2935}/I_{2880} ratio from approximately 0.6 to 1.0 between 30 and 40 °C. The addition of Lfcin to the DPPG system also led to an increase of the I_{2935}/I_{2880} ratio starting at around 30 °C. However, the I_{2935}/I_{2880} ratio only increased to approximately 0.8 at near 40 °C in the presence of Lfcin.

Changes in temperature had no marked effect on the C-H stretching intensity ratios of POPG in either the absence or the presence of Lfcin (**Figures 4.3c** and **4.3d**). The addition of Lfcin to POPG significantly lowered the I_{2850}/I_{2880} ratio from approximately 1.0 to 0.7 over the temperature range investigated (**Figure 4.3c**), but had no effect on the I_{2935}/I_{2880} ratio (**Figure 4.3d**).

The I_{2850}/I_{2880} ratio of DPPE remained steady at approximately 0.4 at temperature below 32 °C in the absence of Lfcin with the appearance of a small hump near 20 °C (**Figure 4.4a**). The I_{2850}/I_{2880} ratio increased to 0.8 between 30 °C and 60 °C, and fluctuated between 0.8 and 1.0 at temperatures above 60 °C. The presence of Lfcin in DPPE liposomes led to an overall increase in the I_{2850}/I_{2880} ratio, particularly at temperature below 40 °C. A hump was also observed between 0 °C and 20 °C. The I_{2935}/I_{2880} ratio of the DPPE liposomes in either the absence or the presence of Lfcin remained stable at around 0.4 at temperature below 40 °C (**Figure 4.4b**). At about 40 °C, the ratio increased. In the absence of Lfcin, the ratio increased to above 0.8; however, with the addition of Lfcin to the system, the ratio started to rise at 42 °C and only reached to approximately 0.7.

POPE exhibited very little response to temperature changes. Only gradual increases were observed in both the I_{2850}/I_{2880} and the I_{2935}/I_{2880} ratios (**Figures 4.4c** and **4.4d**). The presence of Lfcin led to little changes in the thermal behaviour of POPE liposomes.

4.4. Discussion

4.4.1. Temperature-induced Changes in Raman Spectra of Model Membranes

The two dominant Raman features at 2850 and 2880 cm^{-1} are assigned, respectively, to the symmetric and the asymmetric C-H stretching modes for the coupled methylene moieties of the hydrocarbon chains in the bilayer interior (Lewis and McElhane, 2002). The band around 2935 cm^{-1} mainly arises from the symmetric C-H stretching mode of terminal methyl groups in the hydrophobic center of the bilayer (Devlin and Levin, 1989). The I_{2850}/I_{2880} ratio directly monitors acyl chain disorder/order arising from lateral chain-chain interactions, while the I_{2935}/I_{2880} ratio also furnishes an index of the degree of interchain disorder/order (Bunow and Levin, 1977). Increases in I_{2935}/I_{2880} ratio also indicate increases in the number of *gauche* conformations along the lipid chains (Huang et al., 1982). In other words, increases in I_{2850}/I_{2880} and I_{2935}/I_{2880} ratios reflect the loosening or increased fluidity and mobility of the phospholipid chains. As observed in the Raman spectra for all the phospholipids in the present study, these I_{2850}/I_{2880} and I_{2935}/I_{2880} ratios increased as temperature increased, indicating a loosening effect.

The thermal behaviours of the phospholipids observed in the Raman spectra are in agreement with those previously reported. Bonora et al. (2003) reported that DPPC exhibited two endothermic transitions in the 25-50 $^{\circ}\text{C}$ temperature range: a broad pre-transition, with a low enthalpy change at about 35 $^{\circ}\text{C}$ and a major, sharp transition at about 41.7 $^{\circ}\text{C}$. Raman spectra of planar supported lipid bilayers of DPPC showed large thermal changes over the range of 25 to 50 $^{\circ}\text{C}$ as indicated by the I_{2850}/I_{2880} ratio. A broad and gradual increase in the I_{2850}/I_{2880} ratio of the DPPC lipid bilayers between 20 and 60 $^{\circ}\text{C}$ and a sharp increase in the I_{2935}/I_{2880} ratio at around 40 $^{\circ}\text{C}$ were detected. Lee and Bain (2005) reported that the spectra of POPC showed only small changes over the range of 14 to 41 $^{\circ}\text{C}$. Similar results were observed in the present study.

In comparison, it was previously reported that dimyristoyl PE exhibited only one main sharp transition near 49.9 $^{\circ}\text{C}$ in the thermal range of 30-60 $^{\circ}\text{C}$ (Bonora et al., 2003). The I_{2850}/I_{2880} ratios in the present study showed that DPPE has a transition temperature at approximately 42 $^{\circ}\text{C}$, whereas the I_{2935}/I_{2880} ratios indicated a transition temperature of DPPE at 50 $^{\circ}\text{C}$. Furthermore, the I_{2850}/I_{2880} ratios indicated a pre-transition stage between 0 and 20 $^{\circ}\text{C}$ in DPPE liposome.

The origin of the pre-transition thermal behaviour observed in liposomes is not very well established; it has been proposed to arise from the conversion of a lamellar gel phase (L_{β}) to a rippled gel phase (P_{β}). When the phospholipid bilayer is heated, increased rotational motion of the glycerophospholipids occurs, especially about the C-C bonds of the acyl chains, causing the acyl chains to melt and to initiate the first stage of the transition to the liquid state through the conversion of L_{β} to P_{β} . As the temperature is further increased, the main transition arises from the conversion of the P_{β} gel phase to a lamellar liquid-crystal L_{α} phase. Further temperature increases lead to more

extensive disordering of the acyl chains and rearrangements into the nonlamellar, cubic and hexagonal phases.

The I_{2850}/I_{2880} and I_{2935}/I_{2880} ratios observed in the present study supported these phenomena; the transition temperatures indicated by the I_{2850}/I_{2880} ratios of DPPC, DPPG, and DPPE liposomes were lower than those indicated by the I_{2935}/I_{2880} ratios. For instance, the I_{2850}/I_{2880} ratios of DPPC began to increase at around 10 °C and indicated a transition temperature at around 20 °C (**Figure 4.2a**), whereas the I_{2935}/I_{2880} ratios remained stable at temperatures between 10 and 20 °C, started to increase at about 25 °C, and showed a transition temperature near 40 °C (**Figure 4.2b**). Similar results could be detected in DPPG (**Figures 4.3a** and **4.3b**) and DPPE (**Figure 4.4a** and **4.4b**) liposomes. This indicated that as temperature increased, the lateral chain-chain interactions began to increase, increasing distance among chains in the hydrophobic interior. Intra-chain trans/gauche isomerizations became possible only after further increases in temperatures when the P_{β} gel phase was ready to be converted to a lamellar liquid-crystal L_{α} phase.

The lamellar (or liquid crystalline) state of phospholipids is considered to be the biologically active state of the membrane. In the lamellar state, the lipid molecules are melted and trans-gauche isomerizations are able to propagate freely up and down the acyl chains; however, rotation of the first 8 to 10 carbons in the acyl chains is restricted. Distortions caused by acyl chains prevent a perfect packing order from being established and contribute to the level of membrane fluidity observed. With the lamellar state, a variety of acyl chain organizations can be accommodated, allowing for a gradient of phase states to occur within the membrane. Upon transition to the gel state, the lipid chains become stiff and the frequency of these rotations is reduced. Upon increasing membrane disturbance, transition to the cubic and inverted hexagonal (H_{II}) phases may also occur (Denich et al. 2003). However, a greater severity of disturbance is required to change the bilayer towards H_{II} phase than is needed to cause gel-to-liquid-crystalline transition.

The size and charge of the head groups may affect the packing of glycerophospholipids in the bilayer. Comparison between DPPC and DPPE liposomes shows that DPPE has a higher transition temperature than DPPC. The I_{2935}/I_{2880} ratios of DPPC began to rise at around 35 °C and showed a transition temperature at around 40 °C (**Figure 4.2b**), while the I_{2935}/I_{2880} ratios of DPPE began to rise at around 40 °C and continued to increase above 60 °C (**Figure 4.4b**). This indicates that DPPE molecules pack more tightly than DPPC molecules. The structures of the two molecules are similar, differing only by their terminal functional groups. DPPC has a $N(CH_3)_3^+$ head group and DPPE has NH_3^+ as its headgroup. Since both head groups carry a positive charge, the differences in head group size would account for the differences in their thermal behaviour. Molecules of DPPE have a smaller polar head group, meaning that charge delocalization occurs over a smaller area. This creates a stronger charge on the DPPE head group and allows for a more stable membrane structure

to exist as compared with membranes composed of DPPC molecules. The smaller head group allows DPPE to interact with adjacent head groups through intermolecular interactions. More energy would therefore be needed to disturb the acyl chains in DPPE liposomes than those in DPPC liposomes.

DPPG has a neutral, $\text{CH}_2\text{CH}(\text{OH})\text{CH}_2\text{OH}$, head group, and therefore a overall negative charge contributed from the phosphate group. The glycerol moiety is similar in size to the positively-charged choline head group of DPPC, which is a zwitterion carrying no net charge. Results from the present study showed that the I_{2935}/I_{2880} ratios of both DPPC and DPPG liposomes began to increase at approximately 35 °C and exhibited a gel to liquid-crystalline transition near 40 °C (**Figures 4.2b** and **4.3b**, respectively). However, at lower temperatures, the I_{2850}/I_{2880} ratios of DPPG were about 0.9 (**Figure 4.3a**), whereas the I_{2850}/I_{2880} ratios of DPPC were about 0.7 (**Figure 4.2a**). An opposite trend was observed in the I_{2935}/I_{2880} ratios of DPPG and DPPC. At low temperatures, DPPG had I_{2935}/I_{2880} ratios near 0.4 (**Figure 4.3b**) and DPPC had I_{2935}/I_{2880} ratios near 0.5 (**Figure 4.2b**). This indicated that the charge of the head group had an impact on the structural properties of the gel phase of phospholipids. The overall negativity of the DPPG headgroup might have caused a disturbance in the acyl chains, leading to the higher I_{2850}/I_{2880} ratios as observed (**Figure 4.3a**). The disturbance near the surface of the phospholipids bilayer could have led to a more tightly packed hydrophobic centre, leading to more ordered intra-chain packaging and lower I_{2935}/I_{2880} ratios in the DPPG liposomes at low temperatures.

Results from the present study showed that the negatively charged headgroup had an effect on the packing properties of phospholipid liposomes at low temperatures. However, the overall thermal dependence of the gel to liquid-crystalline phase transition was little affected by the charge of the headgroup. In contrast, the size of the headgroup could significantly affect the phase transition of phospholipid liposomes. The small head groups of PE allow strong hydrophobic interaction among its acyl chains, forming a more stable structure.

All three phospholipids containing unsaturated fatty acids tested in the present study exhibited gradual increases in I_{2850}/I_{2880} and I_{2935}/I_{2880} ratios over the temperature range examined. Phase transition was observed in POPC near 0 °C as indicated by the I_{2935}/I_{2880} ratios (**Figure 4.2d**). I_{2935}/I_{2880} ratios of POPE also indicated a gradual phase transition between 0 and 10 °C (**Figure 4.4d**). These results are in agreement with those reported (Caffrey and Hogan, 1992). POPC, POPG, and POPE had lower transition temperatures than their saturated counterparts due to the presence of the cis-double bond in the oleoyl hydrocarbon chains. The cis-double bond introduces a kink in the acyl chains which hinders close packing, de-stabilizes the liposomes, and causes the liposomes to remain in a liquid-crystalline phase even at low temperatures. Since the majority of the temperature range examined in the present study was higher than the transition temperatures of the phospholipids

studied, only the thermal behaviour of the liquid crystalline phase of these phospholipids was observed. The introduction of heat at above the transition temperatures continued to induce lateral chain-chain interactions and disorder interchain structure.

4.4.2. Effects of Lactoferricin on Model Membranes

The results of the present study showed that Lfcin exhibited different effects on the thermal behaviour of phospholipids depending on the headgroup and acyl chain composition. **Figures 4.2a** and **4.2b** indicated that the presence of Lfcin in DPPC liposomes led to an overall decrease in both the I_{2850}/I_{2880} and I_{2935}/I_{2880} ratios, indicating that both the intermolecular and intramolecular interactions of DPPC became more ordered in the presence of Lfcin over the temperature range examined. In other words, DPPC, a common phospholipid found in mammalian cells, became more ordered in the presence of Lfcin. Similar effects have not been reported for other cationic peptides. Melittin, for instance, led to the conformational disorder of DMPC as examined by Raman spectroscopy (Dasseux et al., 1984). The Raman spectra showed decreases in CH_2 groups in the trans conformation and intermolecular order of the chains, without significant changes in the CH_2 groups trans/gauche ratio. Acyl chain symmetry was also lowered in the presence of melittin. Similar results were reported for natural sphingomyelin. In contrast, in the present study, Lfcin increased the order of both the intermolecular and intramolecular movement of the acyl chains in DPPC liposomes. This could be due to the presence of hydrophobic amino acids in Lfcin, which might have been incorporated into the hydrophobic interior of the phospholipid bilayer, increasing the order of the acyl chains. However, the exact mechanism is not known.

In contrast to its effects on DPPC liposomes, Lfcin affected the DPPG liposomes only at temperatures above the transition temperatures. **Figure 4.3a** indicates that the presence of Lfcin lowered the I_{2850}/I_{2880} ratio from 1.1 to 1.0 at temperatures above 38 °C, while **Figure 4.3b** indicates that the I_{2935}/I_{2880} ratios at above 38 °C were also lowered to 0.8 in the presence of Lfcin. These changes in the I_{2850}/I_{2880} and I_{2935}/I_{2880} ratios indicated that Lfcin restricted both inter- and intra-chain interactions of DPPG's acyl chains above transition temperature. At low temperature, the interaction of the negatively charged head groups of PG with the positively charged amino acid residues on Lfcin appear to have restricted the position of Lfcin near the polar head group layer surface, and thereby inhibited the interaction of Lfcin with the hydrophobic core of the lipid bilayer. In contrast, at temperatures above the transition temperature, electrostatic repulsion among the charged head groups seems to have been minimized and hydrophobic attraction between the acyl chains and hydrophobic amino acids was strengthened, leading to the lowering of both I_{2850}/I_{2880} and I_{2935}/I_{2880} ratios. Dumas et al. (1999) stated that neutral and polar head groups may regulate membrane proteins through electrostatic interactions. For example, the head groups of phosphatidylglycerol, phosphatidic acid, phosphatidylserine, and phosphatidylinositol are acidic and may interact with positively charged amino acid residues (Epanand, 1998). Nevertheless, effects of temperatures on the

electrostatic interactions between acidic head groups and positively charged peptides/proteins have not been reported in the literature.

The influence of Lfcin on DPPE liposomes also differed from those observed for DPPC and DPPG. The addition of Lfcin increased the intermolecular fluidity of the DPPE acyl chains and lowered the transition temperature of DPPE as indicated by changes in the I_{2850}/I_{2880} ratios (**Figure 4.4a**). DPPE is characterized by a cone-shaped molecular geometry and possesses a positive spontaneous curvature. DPPE are prone to adopt an inverse hexagonal (H_{II}) phase and exhibit the largest hydrophobic cross-section (Lohner and Prenner, 1999). Hence, this could have allowed greater interactions between the hydrophobic amino acids of Lfcin and the acyl chains and led to the formation of peptide/lipid pores or nonlamellar lipid structures (Lohner and Prenner, 1999). Both these mechanisms will destabilize the acyl chains and result in massive membrane perturbation (Lohner and Prenner, 1999).

Vogel et al. (2002) reported that at high Lfcin to lipids ratios (10:1), the characteristic melting transitions of DPPC and DPPE in multilamellar liposomes were not affected by further addition of the Lfcin. In contrast, for DPPG, the researchers noted that a broad pre-transition around 32 °C disappeared. When more peptide was added to DPPG liposomes, the peak for the main transition also shifted to a slightly higher temperature. These results show that the peptide interacted more strongly with the overall negatively charged PG headgroup than the zwitterionic PC or PE. Results from fluorescence spectrophotometry also showed that lactoferricin peptides bound more tightly and penetrated somewhat more deeply into vesicles containing 40% negatively charged PG headgroup (Vogel et al., 2002). It was estimated that the Trp aromatic rings resided close to the glycerol portion of the phospholipids (Schibli et al., 2002).

Vogel et al. (2002) suggested that DPPE can undergo a transition from a bilayer to a hexagonal phase at around 43.5 °C. Perturbation of the bilayer structure by the antimicrobial peptide magainin through an effect called positive membrane curvature leads to an increase in the transition temperature (Matsuzaki et al., 1997 and 1998). It was shown that Lfcin and other antimicrobial peptides including tritrypticin (Schibli et al., 2002) and indolicidin (Selsted et al., 1992) are capable of perturbing the regular bilayer structure, perhaps promoting the formation of a pore structure with the lipids having positive curvature around the rim of the pore in the direction of the bilayer normal. It is possible that the membrane-destabilizing effects of Lfcin may allow it to spontaneously cross bacterial membranes.

Unsaturated phospholipids, POPC and POPE, were relatively unaffected by the presence of Lfcin (**Figures 4.2c, 4.2d, 4.4c, and 4.4d**). However, the addition of Lfcin to POPG liposomes decreased the I_{2850}/I_{2880} ratio over the range of temperatures tested. In the absence of Lfcin, POPG liposomes had a I_{2850}/I_{2880} ratio around 1.0, while in the presence of Lfcin, the ratio dropped to around

0.7 (**Figure 4.3c**). Similar observations were reported in the presence of V4, an amphipathic cationic peptide, in POPC, POPG, and POPE (Yu et al., 2005). Fluorescence correlation spectrophotometry showed that V4 had a higher affinity for POPG than for POPC and POPE. These results indicated that electrostatic interaction is the major driving force for the binding process in phospholipid liposomes containing unsaturated acyl chains. The I_{2935}/I_{2880} ratios of POPG, however, were not affected by the presence of Lfcin (**Figure 4.3d**). Results from a ^2H NMR experiment (Thennarasu et al., 2005) also showed that the effect of a lipopeptide, MSI-843, on POPC was maximum for CD_2 groups closer to the head group region and decreased along the acyl chain towards a minimum for the other end of the chain. In the present study, positively charged amino acids on Lfcin interacted with the anionic head groups on the surface of the lipid bilayer of POPG. Once Lfcin molecules were anchored on the surface of the POPG liposomes, hydrophobic amino acids on Lfcin were allowed to interact with the hydrophobic acyl chains near the head group of the acyl chains.

Results from the present study showed that Lfcin can interact with phospholipids and affect the thermal stability of the system. However, depending on the charge and size of the head groups of the phospholipids and the saturation level of the acyl chains, the effects could vary. Lohner and Prenner (1999) suggested in a review that charge-charge interactions, membrane curvature strain and hydrophobic mismatch between peptides and lipids are important parameters in determining the mechanism of membrane perturbation. Depending on the molecular properties of both lipid and peptide, antimicrobial peptides could cause membrane thinning, pore formation, promotion of nonlamellar lipid structures, or bilayer disruption. Results from this study showed that Lfcin, an amphipathic cationic peptide, was particularly effective for disrupting PG containing micelles, a negatively charged phospholipid. A better understanding of the mutual dependence of these parameters will help to elucidate the molecular mechanism of membrane damage by antimicrobial peptides and their target membrane specificity, keys for the rational design of novel types of peptide antibiotics.

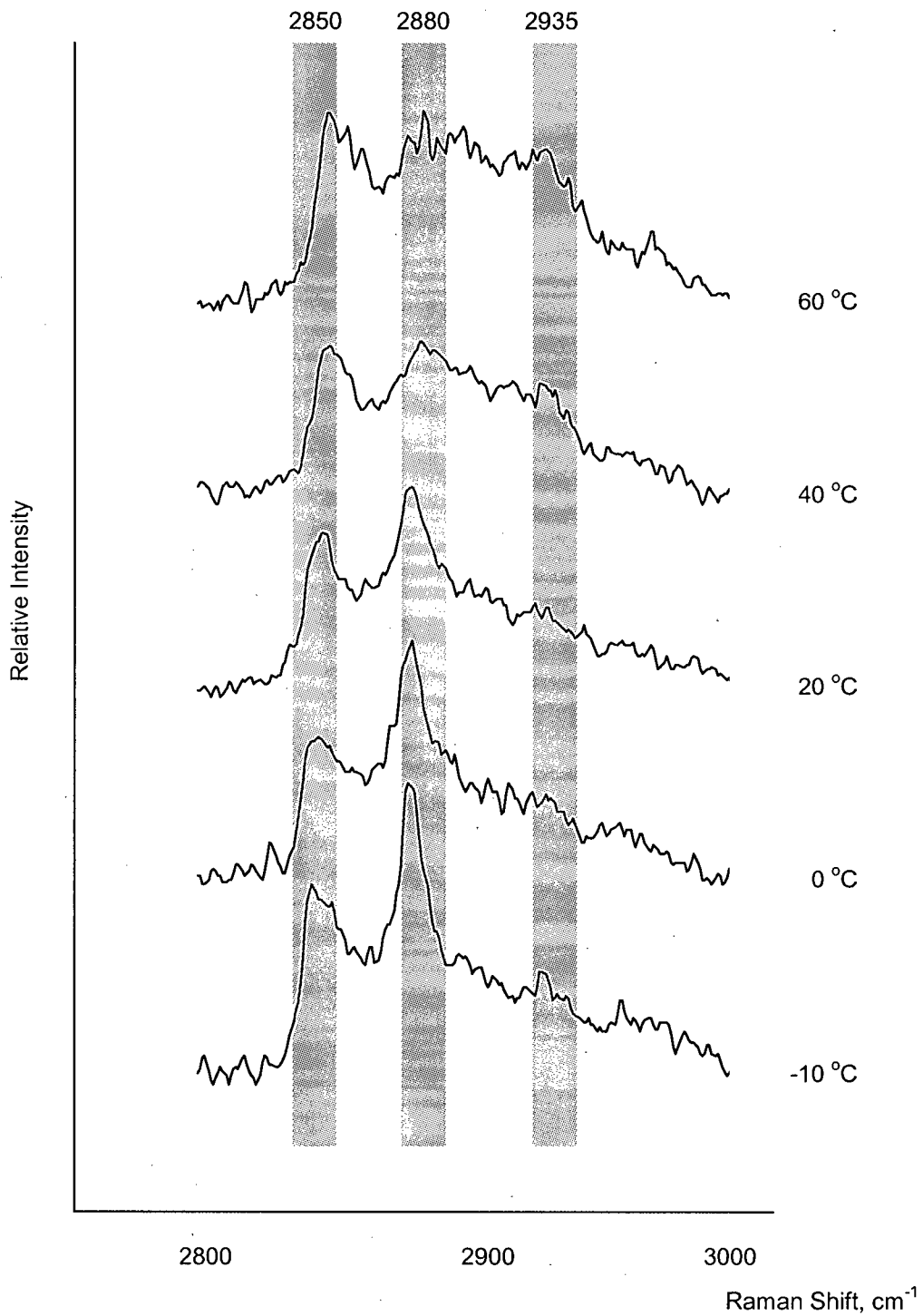


Figure 4.1. Raman spectra of dipalmitoylphosphatidylcholine (DPPC) liposomes in the presence of lactoferricin showing changes in the major peaks near 2850, 2880, and 2935 cm^{-1} as a function of temperature.

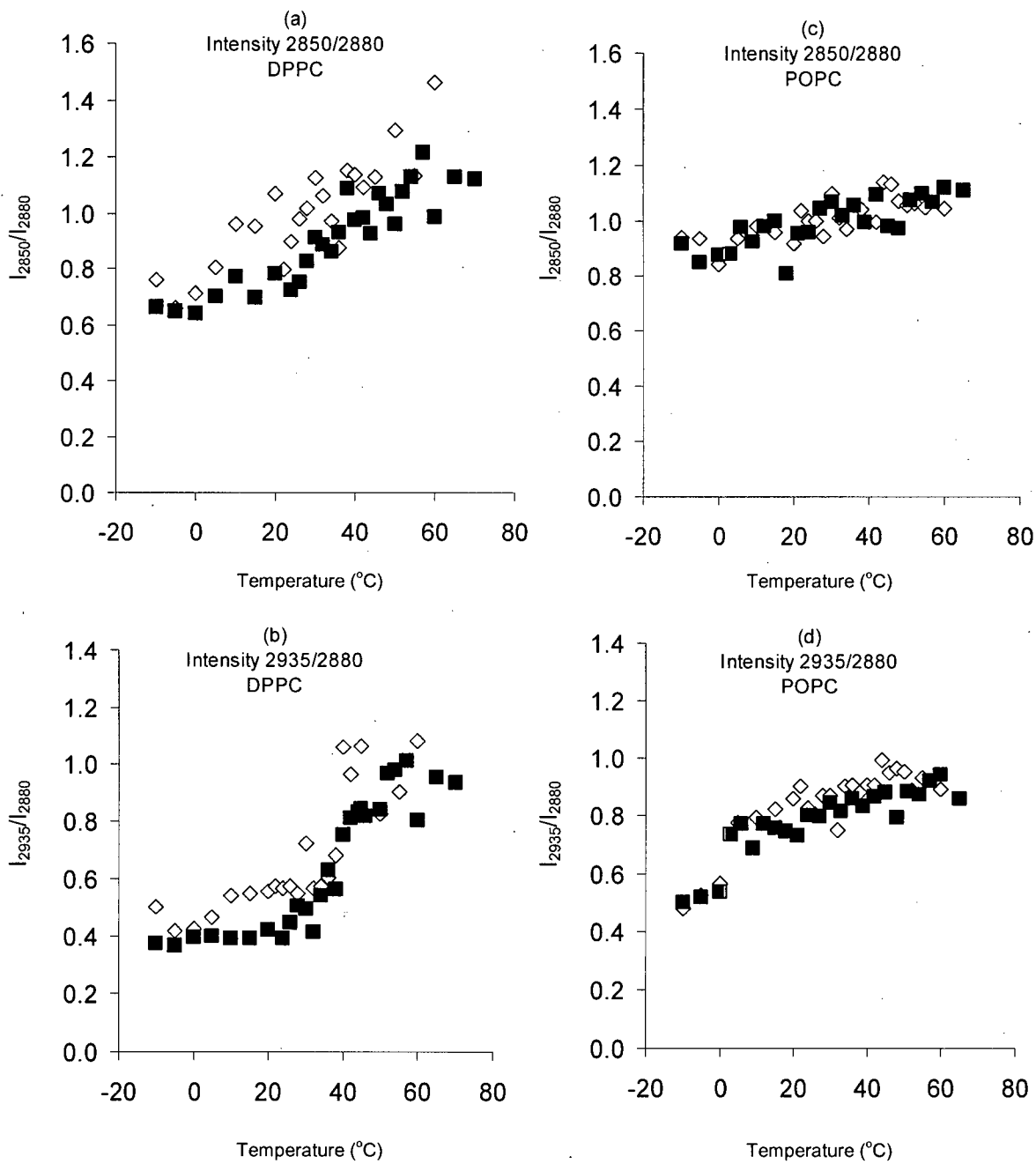


Figure 4.2. I_{2850}/I_{2880} ratio of DPPC (a), I_{2935}/I_{2880} ratio of DPPC (b), I_{2850}/I_{2880} ratio of POPC (c), and I_{2935}/I_{2880} ratio of POPC (d) in the absence (◇) or presence (■) of Lfcin measured between -10 °C and 70 °C by Raman spectroscopy.

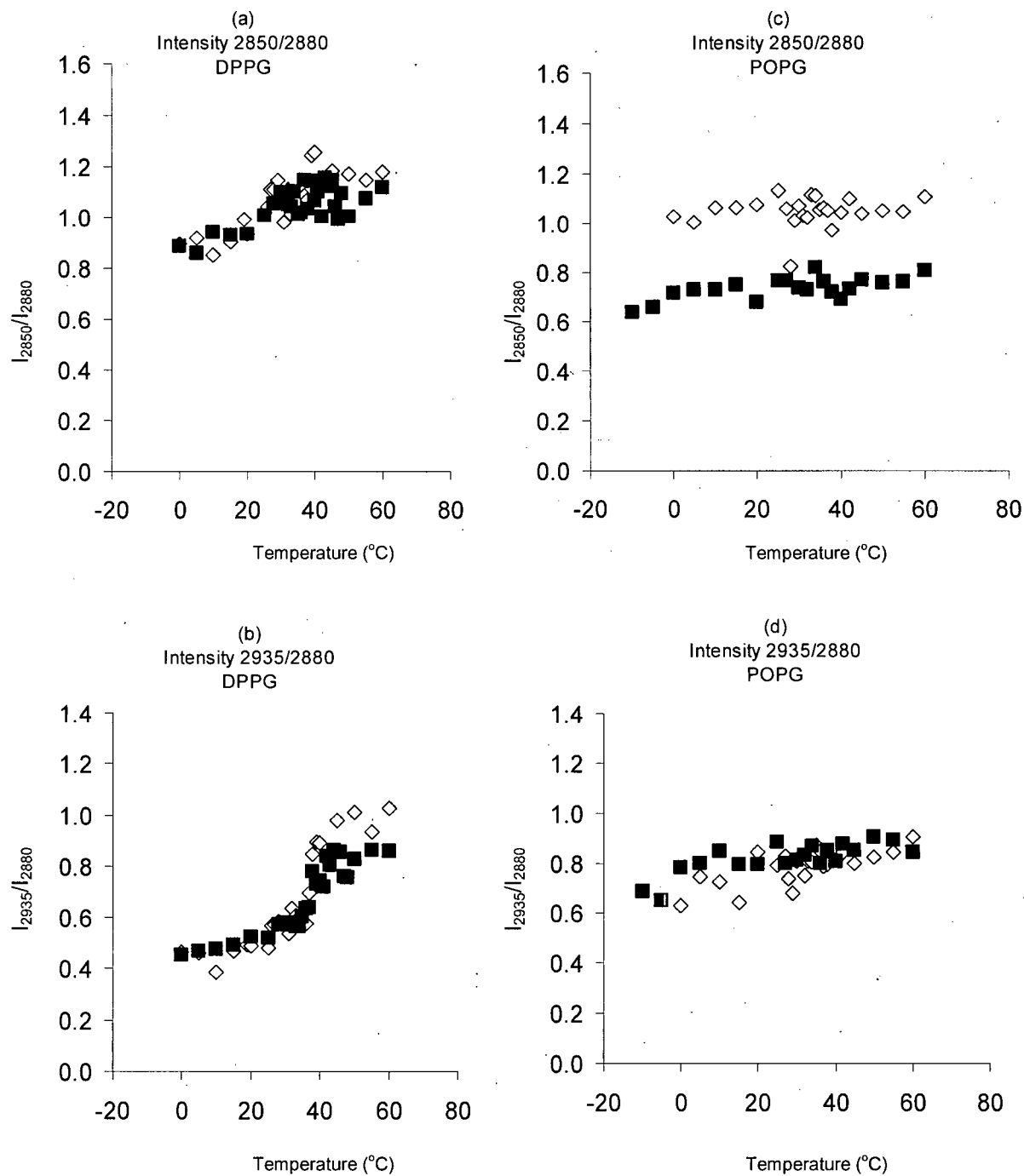


Figure 4.3. I_{2850}/I_{2880} ratio of DPPG (a), I_{2935}/I_{2880} ratio of DPPG (b), I_{2850}/I_{2880} ratio of POPG (c), and I_{2935}/I_{2880} ratio of POPG (d) in the absence (◇) or presence (■) of Lfcin measured between -10 °C and 70 °C by Raman spectroscopy.

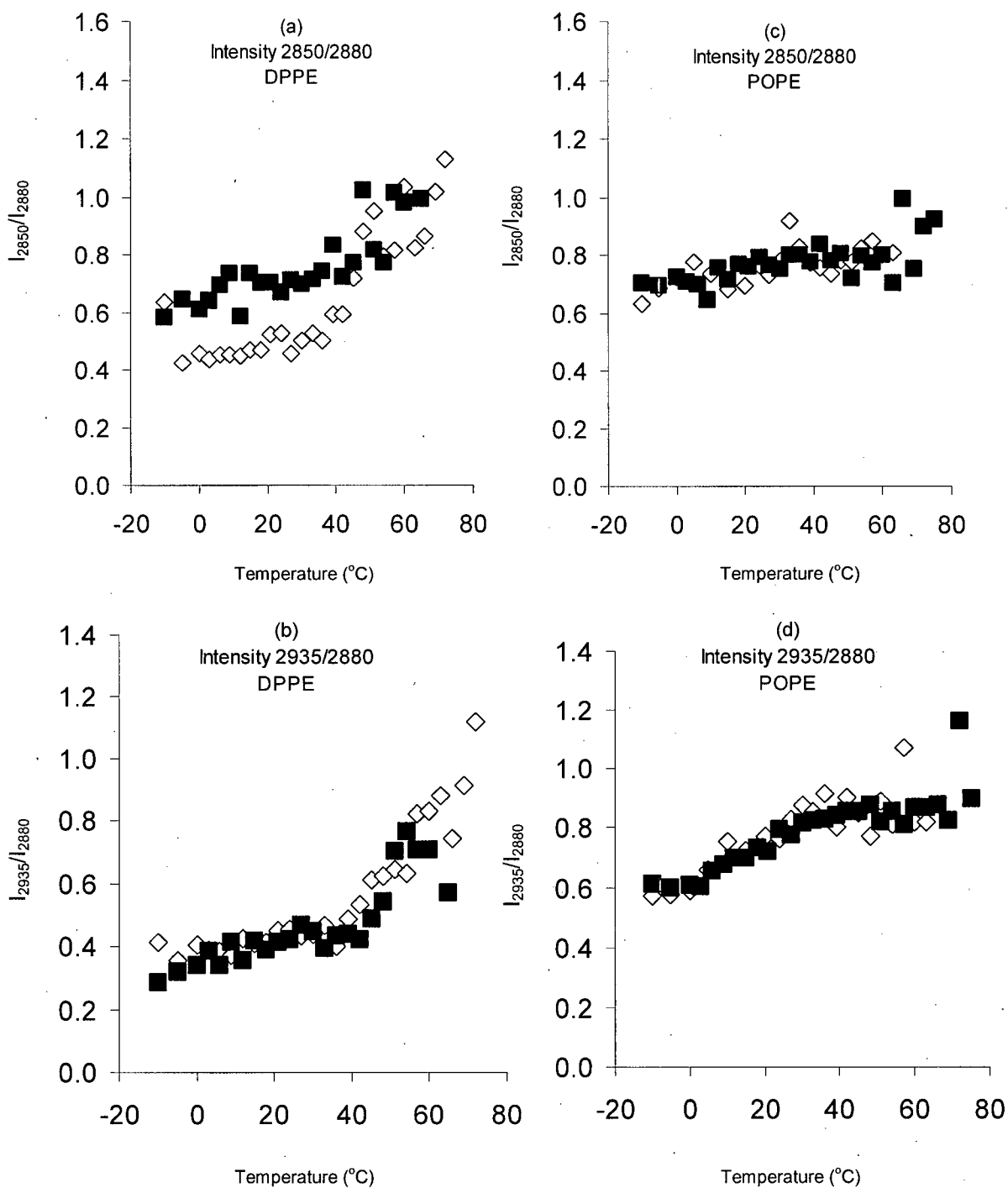


Figure 4.4. I_{2850}/I_{2880} ratio of DPPE (a), I_{2935}/I_{2880} ratio of DPPE (b), I_{2850}/I_{2880} ratio of POPE (c), and I_{2935}/I_{2880} ratio of POPE (d) in the absence (◇) or presence (■) of Lfcin measured between -10 °C and 70 °C by Raman spectroscopy.

4.5. References

- Badii, F.; Howell, N. K. Elucidation of the effect of formaldehyde and lipids on frozen stored cod collagen by FT-Raman spectroscopy and differential scanning calorimetry. *J. Agric. Food Chem.* **2003**, *26*, 1440-1446.
- Bonora, S.; Torreggiani, A.; Fini, G. DSC and Raman study on the interaction between polychlorinated biphenyls (PCB) and phospholipid liposomes. *Thermochimica Acta* **2003**, *408*, 55-65.
- Bouchard, M.; Auger, M. Solvent history dependence of gramicidin-lipid interactions: a Raman and infrared spectroscopic study. *Biophys. J.* **1993**, *65*, 2484-2492.
- Bunow, M. R.; Levin, I. W. Comment on the carbon-hydrogen stretching region of vibrational Raman spectra of phospholipids. *Biochim. Biophys. Acta* **1977**, *487*, 388-394.
- Caffrey, M.; Hogan, J. LIPIDAT: a database of lipid phase transition temperatures and enthalpy changes. DMPC data subset analysis. *Chem. Phys. Lipids* **1992**, *61*, 1-109.
- Choung, S.-Y.; Kobayashi, T.; Takemoto, K.; Ishitsuka, H.; Inoue, K. Interaction of a cyclic peptide, Ro09-0198, with phosphatidylethanolamine in liposomal membranes. *Biochim. Biophys. Acta* **1988**, *940*, 180-187.
- Dasseux, J. L.; Faucon, J.-F.; Lafleur, M.; Pezolet, M.; Dufourcq, J. A restatement of melittin-induced effects on the thermotropism of zwitterionic phospholipids. *Biochim. Biophys. Acta* **1984**, *775*, 37-50.
- Denich, T. J.; Beaudette, L. A.; Lee, H.; Trevors, J. T. Effect of selected environmental and physico-chemical factors on bacterial cytoplasmic membranes. *J. Microbiol. Methods* **2003**, *52*, 149-182.
- Devlin, M. T.; Levin, I. W. Raman spectroscopic studies of the packing properties of mixed dihexadecyl- and dipalmitoylphosphatidylcholine bilayer dispersion. *Biochemistry* **1989**, *28*, 8912-8920.
- Dumas, F.; Lebrun, M. C.; Tocanne, J. F. Is the protein/lipid hydrophobic matching principle relevant to membrane organization and functions? *FEBS Lett.* **1999**, *458*, 271-277.
- Epanand, R. M. Lipid polymorphism and protein-lipid interactions. *Biochim. Biophys. Acta* **1998**, *1376*, 353-368.
- Epanand, R. M.; Vogel, H. J. Diversity of antimicrobial peptides and their mechanisms of action. *Biochim. Biophys. Acta* **1999**, *1462*, 11-28.
- Gaber, B. P.; Peticolas, W. L. On the quantitative interpretation of biomembrane structure by Raman spectroscopy. *Biochim. Biophys. Acta* **1977**, *465*, 260-274.
- Herbig, M. E.; Fromm, U.; Leuenberger, J.; Krauss, U.; Beck-Simkinger, A. G.; Merkle, H. P. Bilayer interaction and localization of cell penetrating peptides with model membranes: a comparative study of human calcitonin (hCT)-derived peptide with pVEC and pAntp(43-58). *Biochim. Biophys. Acta* **2005**, *1712*, 197-211.

- Huang, C.-H.; Lapidus, J. R.; Levin, I. W. Phase-transition behaviour of saturated, symmetric chain phospholipid bilayer dispersions determined by Raman spectroscopy: Correlation between spectral and thermodynamic parameters. *J. Am. Chem. Soc.* **1982**, *104*, 5926-5930.
- Kang, J. H.; Lee, M. K.; Kim, K. L.; Hahm, K. S. Structure-biological activity relationships of 11-residue highly basic peptide segment of bovine lactoferrin. *Int. J. Pept. Protein Res.* **1996**, *48*, 357-363.
- Kanyshkova, T. G.; Semenov, D. V.; Buneva, V. N.; Nevinsky, G. A.. Human milk lactoferrin binds two DNA molecules with different affinities. *FEBS Lett.* **1999**, *451*, 235-237.
- Lafleur, M.; Faucon, J. F.; Dufourcq, J.; Pezolet, M. Perturbation of binary phospholipid mixtures by melittin: a fluorescence and Raman spectroscopy study. *Biochim. Biophys. Acta.* **1989**, *980*, 85-92.
- Laroche, G.; Carrier, D.; Pézolet, M. Study of the effect of poly(L-lysine) on phosphatidic acid and phosphatidylcholine/phosphatidic acid bilayers by Raman spectroscopy. *Biochemistry* **1988**, *27*, 6220-6228.
- Laroche, G.; Dufourc, E. J.; Pezolet, M.; Dufourcq, J. Coupled changes between lipid order and polypeptide conformation at the membrane surface. A ²H NMR and Raman study of polylysine-phosphatidic acid systems. *Biochemistry* **1990**, *29*, 6460-6465.
- Lee, C.; Bain, C. D. Raman spectra of planar supported lipid bilayers. *Biochim. Biophys. Acta* **2005**, *1711*, 59-71.
- Lewis, R. N. A. H.; McElhaney, R. N. Vibrational spectroscopy of lipids. In. *Handbook of Vibrational Spectroscopy*, Vol. 5, Chalmers, J. M. and Griffiths, P. R. (Eds), Wiley, Chichester, UK, 2002, pp. 3447-3464.
- Lohner, K.; Prenner, E. J. Differential scanning calorimetry and X-ray diffraction studies of the specificity of the interaction of antimicrobial peptides with membrane-mimetic systems." *Biochim. Biophys. Acta* **1999**, *1462*, 141-156.
- Matsuzaki, K.; Sugishita, K.-I.; Harada, M.; Fujii, N.; Miyajima, K. Interactions of an antimicrobial peptide, magainin 2, with outer and inner membranes of Gram-negative bacteria. *Biochim. Biophys. Acta* **1997**, *1327*, 119-130.
- Matsuzaki, K.; Sugishita, K.-I.; Ishibe, N.; Ueha, M.; Nakata, S.; Miyajima, K.; Epand, R. M. Relationship of membrane curvature to the formation of pores by magainin 2. *Biochemistry* **1998**, *37*, 11856-11863.
- Neville, F.; Cahuzac, M.; Konovalov, O.; Ishitsuka, Y.; Lee, K. Y. F.; Kuzmenko, I.; Kale, G. M.; Gidalevitz, D. Lipid headgroup discrimination by antimicrobial peptide LL-37: Insight into mechanism of action. *Biophys. J.* **2006**, *90*, 1275-1287.
- Opekarová, M.; Tanner, W. Specific lipid requirements of membrane proteins – a putative bottleneck in heterologous expression. *Biochim. Biophys. Acta* **2003**, *1610*, 11-22.
- Schibli, D. J.; Epand, R. F.; Vogel, H. J.; Epand, R. M. Tryptophan-rich antimicrobial peptides: comparative properties and membrane interactions. *Biochem. Cell Biol.* **2002**, *80*, 667-677.
- Selsted, M. E.; Novotny, M. J.; Morris, W. L.; Tang, Y. Q.; Smith, W.; Cullor, J. S. Indolicidin, a novel bactericidal tridecapeptide amide from neutrophils. *J. Biol. Chem.* **1992**, *267*, 4292-4295.

- Snyder, R.; Scherer, J.; Gaber, B. Effects of chain packing and chain mobility on the Raman spectra of biomembranes. *Biochim. Biophys. Acta* **1980**, *601*, 47-53.
- Snyder, R.; Strauss, H.; Elliger, C. C-H stretching modes and the structure of n-alkyl chains. I. Long, disordered chains. *J. Chem. Phys.* **1982**, *86*, 5145-5150.
- Susi, H.; Sampugna, J.; Hampson, J. W.; Ard, J. S. Laser-Raman investigation of phospholipid-polypeptide interactions in model membranes. *Biochemistry* **1979**, *18*, 297-301.
- Thennarasu, S.; Lee, D.-K.; Tan, A.; Prasad Kari, U.; Ramamoorthy, A. Antimicrobial activity and membrane selective interactions of a synthetic lipopeptide MSI-843. *Biochim. Biophys. Acta* **2005**, *1711*, 49-58.
- Vincent, J. S.; Revak, S. D.; Cochrane, C. G.; Levin, I. W. Raman spectroscopic studies of model human pulmonary surfactant systems: phospholipid interactions with peptide paradigms for the surfactant protein SP-B. *Biochemistry* **1991**, *30*, 8395-8401.
- Vincent, J. S.; Revak, S. D.; Cochrane, C. D.; Levin, I. W. Interactions of model human pulmonary surfactants with a mixed phospholipid bilayer assembly: Raman spectroscopic studies. *Biochemistry* **1993**, *32*, 8228-8238.
- Vogel, H. J.; Schibli, D. J.; Jing, W.; Lohmeier-Vogel, E. M.; Epan, R.F.; Epan, R. M. Towards a structure-function analysis of bovine lactoferricin and related tryptophan- and arginine-containing peptides. *Biochem. Cell Biol.* **2002**, *80*, 49-63.
- Yeagle, P. L. The Lipids of Cell Membranes. In. *The Membranes of Cells*. **1993**. New York, Academic Press Inc.: pp. 22-28.
- Yu, L.; Ding, J. L.; Ho, B.; Wohland, T. Investigation of a novel artificial antimicrobial peptide by fluorescence correlation spectroscopy: An amphipathic cationic pattern is sufficient for selective binding to bacterial type membranes and antimicrobial activity. *Biochim. Biophys. Acta* **2005**, *1716*, 29-39.

CHAPTER 5. RAMAN SPECTROSCOPIC STUDY OF THE EFFECTS OF LACTOFERRICIN DERIVATIVES ON PHOSPHOLIPID LIPOSOMES⁴

5.1. Introduction

Lactoferrin (LF) is an iron-binding protein that is present in milk (Sørensen and Sørensen, 1939) and exhibits a wide range of antimicrobial activities. It has been shown that pepsin hydrolysate of LF has higher antimicrobial potency than undigested LF. A 25-residue peptide named lactoferricin (Lfcin), released from the amino-terminal region of LF during peptic digestion, has been identified as being responsible for the antimicrobial properties (Bellamy et al., 1992). The peptide is highly basic, containing many Arg and Lys. Furthermore, a number of Trp and Phe are also present in Lfcin. Studies have also shown that fragments, such as ¹⁷FKCRR WQWRM KKLGA PSITC VRRAF⁴¹ (Bellamy et al., 1992), ¹⁷FKCRR WQWRM KKLGA³¹ (Rekdal et al., 1999; Strøm et al., 2000), ²⁰RRWQW MKKLG³⁰ (Kang et al., 1996), and ²⁰RRWQWR²⁵-NH₂ (Tomita et al., 1994) of Lfcin possess similar antimicrobial activity.

The presence of hydrophobic and positively charged amino acids has been reported to be particularly important for the bioactivity of Lfcin. QSAR analyses (Lejon et al., 2001; Strøm et al., 2000) of Lfcin revealed that net charge, charge asymmetry, and micelle affinity of Lfcin were the most important structural parameters affecting their antimicrobial activity. Using principal component similarity analysis followed by artificial neural network, helix propensity and net charge of the peptides were demonstrated to have a significant effect on the antimicrobial activity of Lfcin and its derivatives against *Escherichia coli* (Chapter 3).

Franaud et al. (2004) showed that the replacement of Trp by Ala (W22A or W24A) led to a decrease in antimicrobial activity against wild-type *E. coli* and LPS mutant strains. An alanine-scan experiment on Lfcin (Strøm et al., 2000) revealed that the presence of Trp22 or Trp24 was mandatory for antimicrobial activity. A loss of antibacterial activity against *S. aureus* was observed when Phe replaced the Trp residues (Haug and Svendsen, 2001).

Aside from the hydrophobic Trp residues, cationic Arg residues also play an important role in the bioactivity of Lfcin. Even "conservative" replacements of Arg with Lys produce peptides of much lower antimicrobial potency (Strøm et al., 2000). Strøm et al. (2001) identified the key amino acids in Lfcin by synthesizing a series of Lfcin derivatives in which amino acids were successively replaced with alaine (Ala). Similar effects have been observed for other Trp- or Arg-rich antimicrobial peptides. For example, Blondelle et al. (1995), Blondelle and Houghton (1996), and Blondelle and Lohner (2000) found that only Trp/Arg-rich hexapeptides were potent antimicrobials, while hexapeptides

⁴ A version of this chapter will be submitted for publication. Chan, J. C. K., and Li-Chan, E. C. Y. Raman spectroscopic study of the effects of lactoferricin derivatives on phospholipid liposomes. *Biochimica et Biophysica Acta (BBA) – Biomembranes*.

composed of Phe/Arg, Tyr/Arg, Trp/Lys, or Tyr/Lys and Phe/Lys exhibited much lower antimicrobial activities.

Early studies suggested that binding to the microbial membrane surfaces was important for the action of Lfcin (Bellamy et al., 1993). However, it is not clear exactly where and how Lfcin interacts with bacterial and host membranes of different compositions. Phosphatidylglycerol (PG) and phosphatidylethanolamine (PE) are the major components of bacterial membranes (Opekarová and Tanner, 2003). In contrast, erythrocyte membranes and most other eukaryotic membranes are generally made up of phosphatidylcholine (PC). The positively charged choline ($(\text{CH}_3)_3\text{N}^+\text{CH}_2\text{CH}_2-$) on PC and ethanolamine ($\text{H}_3\text{N}^+\text{CH}_2\text{CH}_2-$) on PE, together with the negatively charged phosphate moiety, form zwitterions leading to overall neutral phospholipids. In contrast, PG carries a glycerol ($\text{CH}_2\text{OHCHOHCH}_2\text{OH}-$) on its polar head, forming overall negatively charged phospholipids.

Raman spectroscopy is a very useful tool to examine the microenvironment of C-H groups in the fatty acyl hydrocarbon chains of phospholipids. Results from Raman spectroscopic study reported in **Chapter 4** indicated that Lfcin affected the thermal behaviour of PC, and destabilized the acyl chains and decreased the degree of order of PE. Furthermore, negatively charged PG may have interacted with the positive residues on Lfcin through electrostatic force and facilitated the interaction of hydrophobic fatty acyl chains with the hydrophobic amino acid residues on Lfcin.

The objective of the present study was to examine the influence of insertion or replacement of tryptophan and arginine residues in a 15-residue fragment of Lfcin, on the effects of these derivatives on the thermal transition profiles of phospholipids using Raman spectroscopy in the C-H stretching region. The effect of a 6-residue peptide sequence containing the active core of Lfcin was also investigated.

5.2. Materials and Methods

5.2.1. Materials

Sodium salts of DPPC, DPPG, and DPPE were obtained from Avanti Polar Lipids (Alabaster, AL) in lyophilized powder forms. Lactoferricin derivatives, FKCRW WQWRW KKLGA (Lfcin₁₅), FKCAA WQWAM KKLGA (Lfcin₁₅R-), FKCRW AQARM KKLGA (Lfcin₁₅W-), FKCRW WQWRW KKLGA (Lfcin₁₅W+), and RRWQW R-NH₂ (LfcinCore), were purchased from Sigma-Genosys (The Woodlands, Texas) (**Table 5.1**). HPLC, mass spectrometry, and amino acid analyses were performed by Sigma-Genosys to confirm that the Lfcin derivatives had the expected masses and amino acid compositions. All samples were used without further purification. Other chemicals used were of reagent grade quality.

5.2.2. Preparation of Liposomes

As described in Section 4.2.2.

5.2.3. Raman Spectroscopy

As described in Section 4.2.3.

5.2.4. Raman Spectral Analysis

As described in Section 4.2.4.

5.2.5. Properties of Lactoferricin Derivatives

Structural properties of the lactoferricin derivatives were calculated. Molecular weight, pI, and hydropathicity index of the peptides were determined using the ProtParam tool available on <http://ca.expasy.org/tools/protparam.html> (Kyte and Doolittle, 1982). Helix and charge pattern similarities of residues 4 to 10 of the derivatives were calculated using the Homology Similarity Analysis (HSA) described in **Chapter 3**. Lfcin₁₅ was used as the reference peptide in HSA.

5.3. Results

5.3.1. Effects of Lactoferricin Derivatives on DPPC Liposomes

Raman spectroscopy in the C-H stretching region was used to investigate the effects of Lfcin derivatives on temperature transitions of DPPC, DPPG, and DPPE. Analyses of the effects of temperature dependence of the acyl chain packing characteristics and phase transition cooperativities on the various Raman spectroscopic features can be achieved through peak-height intensity ratios of peaks near 2850 cm⁻¹ (I_{2850}), 2880 cm⁻¹ (I_{2880}), and 2935 cm⁻¹ (I_{2935}). The I_{2850}/I_{2880} ratio provides insight into the intermolecular chain-chain interactions among the acyl chains in the hydrophobic core of the phospholipid bilayer, while the I_{2935}/I_{2880} ratio indicates the degree of disorder and order of the acyl chains as well as the presence of intrachain *trans/gauche* isomerizations (Huang et al., 1982). The I_{2850}/I_{2880} and I_{2935}/I_{2880} ratios of the Raman spectra of DPPC, DPPG, and DPPE as a function of temperature are shown in **Figures 5.1, 5.2, and 5.3**, respectively.

The intensity ratio, I_{2850}/I_{2880} , of DPPC liposomes gradually increased over the temperature range tested (**Figure 5.1a**). In the absence of Lfcin (open square symbols), a broad gel-to-liquid crystalline phase transition was detected between 30 °C and 50 °C, with a pre-transition stage at about 15 °C to 20 °C (**Figure 5.1a**). With the presence of Lfcin₁₅ in the liposomes (**Figure 5.1ai**), I_{2850}/I_{2880} ratios were lowered throughout the temperature range while exhibiting similar behaviour as the spectra without Lfcin. The presence of Lfcin₁₅ in the liposomes led to a decrease in the transition temperature at around 38 °C. The transition was also sharper in the presence of Lfcin than that without Lfcin, and a smaller pre-transition stage was seen between 15 °C and 20 °C. The intensity

ratio, I_{2935}/I_{2880} , showed a slightly different trend (**Figure 5.1b**). The I_{2935}/I_{2880} ratios for both DPPC liposomes with and without Lfcin₁₅ increased gradually at temperature above 20 °C, although the presence of Lfcin₁₅ attenuated the extent of this increase (**Figure 5.1bi**).

Effects of Lfcin₁₅ derivatives were less obvious when Arg was replaced with Ala (**Figures 5.1aii and 5.1bii**). The presence of Lfcin₁₅R- led to a slight decrease in the I_{2850}/I_{2880} ratio at temperatures below 15 °C, and thermal transition of the DPPC liposome was observed to be initiated at a lower temperature near 32 °C (**Figure 5.1aii**). The I_{2935}/I_{2880} ratio was not affected by the presence of Lfcin₁₅R- (**Figure 5.1bii**).

The addition of Lfcin₁₅W- to the DPPC liposomes led to a decrease in I_{2850}/I_{2880} ratio at temperatures below 15 °C (**Figure 5.1aiii**). The thermal behaviour of DPPC was unaffected by Lfcin₁₅W- at higher temperature as shown by the I_{2850}/I_{2880} ratio. However, differences in the I_{2935}/I_{2880} ratios were observed (**Figure 5.1biii**). In the absence of Lfcin derivatives, DPPC exhibited I_{2935}/I_{2880} ratios near 0.4 at temperature below 20 °C, which gradually increased to 0.6 between 20 and 40 °C and continued to increase to 0.8 between 40 and 70 °C. The presence of Lfcin₁₅W- in DPPC liposomes resulted in a very steady I_{2935}/I_{2880} ratio at 0.2 at temperatures below 40 °C. A sharp increase in the I_{2935}/I_{2880} ratio occurred between 40 and 55 °C and the ratio reached 0.8 at temperatures above 55 °C (**Figure 5.1biii**).

Lfcin₁₅W+ exhibited little effect on the thermal behaviour of DPPC as indicated by both I_{2850}/I_{2880} and I_{2935}/I_{2880} ratios (**Figures 5.1aiv and 1biv**). The addition of LfcinCore to the DPPC liposomes lowered the I_{2850}/I_{2880} ratio at temperatures below 30 °C from 0.8 to 0.7 (**Figure 5.1av**). The I_{2935}/I_{2880} ratio of DPPC liposomes was unaffected by LfcinCore at temperatures below 40 °C, but at temperatures above 40 °C, LfcinCore lowered the ratio from 0.8 to 0.6.

5.3.2. Effects of Lactoferricin Derivatives on DPPG Liposomes

DPPG exhibited higher ratios than those of DPPC (**Figure 5.2**). In the absence of any Lfcin derivatives (open diamond symbols), the I_{2850}/I_{2880} ratio of DPPG liposomes increased from 0.7 at temperatures below 0 °C to about 1.0 between 10 and 40 °C. A sharp increase in the ratio from 1.0 to 1.4 was observed around 40 °C. A similar pattern was observed in the I_{2935}/I_{2880} ratio (**Figure 5.2bi**); a sharper and narrower increase in the I_{2935}/I_{2880} ratio occurred at around 38 °C.

The presence of Lfcin₁₅ had no observable effect on the thermal behaviour of DPPG liposomes at temperature below 40 °C as shown by the I_{2850}/I_{2880} ratio (**Figure 5.2ai**) and at temperatures below 30 °C as indicated by the I_{2935}/I_{2880} ratio (**Figure 5.2bi**). The I_{2850}/I_{2880} ratio of DPPG in the presence of Lfcin₁₅ fluctuated between 0.8 and 1.2 between 20 and 70 °C (**Figure 5.2ai**). The I_{2935}/I_{2880} ratio remained steady at around 0.4 to 0.6 between 0 and 40 °C in the presence of Lfcin₁₅ (**Figure 5.2bi**) and increased to 0.7 at around 42 °C. The presence of Lfcin₁₅ in DPPG

delayed the shift in I_{2935}/I_{2880} ratio from 38 °C to 40 °C and led to a smaller change in the I_{2935}/I_{2880} ratio.

When the R in the Lfcin₁₅ was replaced with A, the effects of Lfcin₁₅ on the thermal behaviour of DPPG liposomes diminished (**Figures 5.2aii and 5.2bii**). Lfcin₁₅R- caused a slight decrease of the I_{2850}/I_{2880} ratio at temperatures above 40 °C. The most noticeable effect of Lfcin₁₅R- occurred between 40 and 50 °C as indicated by the I_{2935}/I_{2880} ratio. Lfcin₁₅R- caused a major decrease of the I_{2935}/I_{2880} ratio between 40 and 50 °C. In addition, Lfcin₁₅R- also lowered the I_{2935}/I_{2880} ratio at temperatures below 10 °C (**Figure 5.2bii**).

The thermal stability of DPPG was increased by the presence of Lfcin₁₅W- (**Figure 5.2aiii**). The I_{2850}/I_{2880} ratio exhibited a very gradual increase from 0.6 to 0.8 between 0 and 65 °C. The I_{2935}/I_{2880} ratio also exhibited a gradual increase from 0.2 to 0.6 between 15 and 40 °C.

Effects of Lfcin₁₅W+ and LfcinCore on the I_{2850}/I_{2880} ratio of DPPG liposomes were very similar. The I_{2850}/I_{2880} ratio of DPPG fluctuated in a very narrow range in the presence of these two Lfcin derivatives (**Figures 5.2aiv and 5.2av**). However, Lfcin₁₅W+ and LfcinCore caused different effects on the DPPG liposomes as indicated by the I_{2935}/I_{2880} ratio (**Figures 5.2biv and 5.2bv**). Lfcin₁₅W+ had no effect on DPPG liposomes below 25 °C and the ratio remained steady at 0.4. The ratio experienced a small shift from 0.4 to 0.8 between 26 and 30 °C and remained stable at 0.8 at higher temperatures. Comparing to the thermal behaviour of DPPG in the absence of Lfcin derivatives, Lfcin₁₅W+ caused a smaller shift at lower temperature (**Figure 5.2biv**). In contrast, the presence of LfcinCore led to a very steady and significant increase in the I_{2935}/I_{2880} ratio of DPPG liposomes from 5 to 60 °C (**Figure 5.2bv**).

5.3.3. Effects of Lactoferricin Derivatives on DPPE Liposomes

As indicated by the I_{2850}/I_{2880} and the I_{2935}/I_{2880} ratios, DPPE liposomes exhibited very little response to temperature changes between -10 and 60 °C (open circle symbols in **Figures 5.3ai and 5.3bi**). Sharp increases in both ratios only occurred at temperatures around 60 °C. The intensity ratios of DPPE were also lower than those of DPPC and DPPG.

The addition of Lfcin₁₅ derivatives caused a general upward shift of the I_{2850}/I_{2880} ratio of DPPE. The presence of Lfcin₁₅ or Lfcin₁₅W- in DPPE led to increases in the I_{2850}/I_{2880} ratio (**Figures 5.3ai and 5.3aiii**, respectively). The ratios also demonstrated very gradual increases between -10 and 50 °C, and moderate increases at temperatures between 50 and 70 °C. In comparison, Lfcin₁₅R- had less effect on the I_{2850}/I_{2880} ratio of DPPE below 40 °C, but led to significant increase in the ratios starting at around 42 °C (**Figure 5.3aii**). LfcinCore had a similar effect on DPPE liposomes and caused a sharp increase in the I_{2850}/I_{2880} ratio at around 38 °C (**Figure 5.3av**). Among all Lfcin derivatives, Lfcin₁₅W+ was the only exception. Unlike other derivatives that increased the I_{2850}/I_{2880}

ratio of DPPE, Lfcin₁₅W+ caused a significant decrease in the ratio over the temperature range tested, with little change as a function of increasing temperature until a sharp increase was observed near 52 °C (**Figure 5.3aiv**).

The I₂₉₃₅/I₂₈₈₀ ratio of DPPE was unaffected by the presence of any Lfcin derivatives in the conditions studied in the present experiment (**Figure 5.3b**).

5.4. Discussion

5.4.1. Effects of Arginine on Lactoferricin on the Thermal Behaviour of Phospholipid Liposomes

The presence of Lfcin₁₅ affected the thermal transition behaviour of DPPC, DPPG, and DPPE. Replacing the positively charged Arg amino acid in Lfcin₁₅ with Ala (Lfcin₁₅R-) reduced the impact of Lfcin₁₅ on DPPC and DPPE. The thermal behaviour of the acyl chains of DPPG was mildly affected by Lfcin₁₅R-, while Lfcin₁₅R- caused a higher gel-to-liquid crystalline phase transition temperature at the methyl ends of DPPG.

The presence of positively charged amino acids, especially R, has been demonstrated to be a key factor in many cationic antimicrobial peptides including Lfcin (Strøm et al., 2001). However, the discussion on the exact role of R in facilitating the antimicrobial function is inconclusive. Results from **Chapter 4** showed that Lfcin had the most impact on DPPG possibly due to the interactions between the negatively charged head groups on PG and the positively charged amino acid side chains on Lfcin. Results from the present study showed that when Arg was replaced with Ala, Lfcin₁₅R- no longer exhibited the same effects exerted by Lfcin₁₅ on DPPG (**Figures 5.2ii**). This indicates that Arg may be important for the anchoring of Lfcin on the polar head group of PG and facilitating further hydrophobic interactions between the acyl chains and hydrophobic amino acids on Lfcin.

Lfcin₁₅R- also decreased the intermolecular chain-chain interactions of DPPE (**Figure 5.3ii**). Such a result is quite unexpected based on results reported in **Chapter 4**. However, a closer look at the structural properties (**Table 5.1**) of Lfcin₁₅R- shows that although the helix propensity of Lfcin₁₅R- was similar to that of Lfcin₁₅, the replacement of Arg with Ala minimized the charge similarity of Lfcin₁₅R-, lowered its pI, but also increased its overall hydrophobicity. As discussed in **Chapter 4**, due to the positive curvature stress, DPPE often exists as hexagonal type II (cone shaped, H_{II}) and exposes its hydrophobic acyl chains. In the presence of the highly hydrophobic Lfcin₁₅R-, the acyl chains of DPPE were more readily disturbed, resulting in an increase in the I₂₈₅₀/I₂₈₈₀ ratio when at higher temperature.

Although the presence of arginine on Lfcin₁₅ seemed to play an important role in its interaction with pathogenic cell membranes, studies on other cationic antimicrobial peptides showed that the actual number of positive charges within the polypeptide chain was less significant. For

instance, temporins appeared to exhibit antibiotic action with only a single positively charged residue (Mangoni et al., 2000) and there was an optimal positive charge for the lytic activity of magainin 2 analogues (Blondelle and Houghten, 1992; Kiyota et al., 1996). The decrease in activity above a certain peptide charge was suggested to be the result of instability and reduced lifetime of the pore formed by the peptide chains in the membrane (Matsuzaki et al., 1997).

Investigation of synthetic pardaxin in model membranes by solid-state NMR showed a decrease in the ability of the peptide to disrupt lipid bilayers in the presence of acidic phospholipids (Hallock et al., 2002). The results suggested that preferential interactions between the positively charged residues of pardaxin and the anionic lipid headgroups had prevented the peptide from inserting into the acyl chain region of the bilayer and causing morphological changes in the membrane, a phenomenon observed for zwitterionic vesicles. Temporin L (Rinaldi et al., 2002) and melittin (Ladokhin and White, 2001) lost their lytic activities in the presence of negatively charged phospholipids (Rinaldi et al., 2002). Indeed, an oriented CD study revealed that melittin was able to adopt a transmembrane orientation only in zwitterionic bilayers (Ladokhin and White, 2001). In negatively charged membranes, the strong electrostatic interaction between the cationic peptide chain and the lipid headgroups seemed to suppress peptide reorientation that in turn hindered the formation of well-defined pores. In a recent surface plasmon resonance study of melittin, Papo and Shai reached similar conclusions (Papo and Shai, 2003). Results from the present study suggest that the replacement of Arg with Ala on Lfcin₁₅R- affected how Lfcin binds to negatively charged DPPG liposomes. The shift in the I_{2850}/I_{2880} and I_{2935}/I_{2880} ratios of DPPG in the presence of Lfcin₁₅R- likely indicated that the absence of Arg prevented the Lfcin derivative from interacting with the acyl chains as well as the methyl ends of the hydrophobic core of the DPPG bilayers.

5.4.2. Effects of Tryptophan on the Thermal Behaviour of Lactoferricin of Phospholipid Liposomes

Tryptophan has been shown to be a key amino acid in the antimicrobial activity of Lfcin (Strøm et al., 2001). It was suggested that the hydrophobic amino acid was needed to stabilize the peptide in the hydrophobic bilayer on bacterial membrane. Strøm et al. (2000) reported that the addition of Trp to Lfcin from human, caprine, murine, and porcine sources significantly improved the antimicrobial activity of these Lfcins. Haug and Svendsen (2001) demonstrated that the hydrophobic aromatic side chains of Trp were responsible for the antimicrobial activity. Furthermore, they reported that increasing the bulkiness of the side chains would further enhance the antimicrobial activity (Haug and Svendsen, 2001).

Results from the present study show that the presence or absence of Trp on Lfcin₁₅ had variable effects on different phospholipid liposomes. The absence of tryptophan (Lfcin₁₅W-) made little difference to the effect of Lfcin₁₅ on DPPC (**Figure 5.1iii**). Effects of Lfcin₁₅W- on DPPE were similar to those of Lfcin₁₅ (**Figures 5.3iii and 5.3i**). In contrast, Lfcin₁₅W- had a major impact on

DPPG, lowering both the I_{2850}/I_{2880} and I_{2935}/I_{2880} ratios throughout the temperature range tested (**Figure 5.2iii**). The insertion of two extra tryptophan residues on Lfcin₁₅ (Lfcin₁₅W+) had little effect on Lfcin₁₅'s effect on DPPC. Effects of Lfcin₁₅W+ on DPPC and DPPG were similar to those of Lfcin₁₅W- (**Figures 5.1iv** and **5.2iv**), but Lfcin₁₅W+ decreased the I_{2850}/I_{2880} ratio of DPPE in the temperature range tested (**Figure 5.3iv**).

The importance of Trp on the interaction of Lfcin with DPPG was therefore confirmed by the present study. Results depicted in **Figure 5.2iii** showed that Lfcin₁₅W- indeed increased the degree of order and decreased the formation of *gauche* conformations of the acyl chains of DPPG at high temperature. The replacement of Trp with Ala would be expected to decrease the bulkiness, and calculated hydrophobicity GRAVY values indicate that Lfcin₁₅W- was less hydrophobic than Lfcin₁₅ (**Table 5.1**). Furthermore, homology similarity analysis of Lfcin₁₅W- indicated that the helix propensity of Lfcin₁₅ was altered after the Trp was replaced. The results imply that the presence of Ala and absence of Trp created a peptide that would likely promote greater order of rather than destabilize the DPPG bilayer.

Interestingly, results presented here unexpectedly showed that the extra tryptophan residues on Lfcin₁₅W+ had the least effect on the thermal behaviour of DPPE. In fact, the insertion of two additional Trp minimized the disordering effects on DPPE exerted by Lfcin₁₅, Lfcin₁₅R-, Lfcin₁₅W-, and LfcinCore, and Lfcin₁₅W+ appeared to increase the intermolecular interactions and order of the acyl chains. These results seem to disagree with those reported in **Chapter 4** and **Section 5.4.1** where it was suggested that hydrophobicity and the presence of hydrophobic amino acids of Lfcin were responsible for the decrease in the degree of order of DPPE. However, Lfcin₁₅W+ behaved very differently and promoted the degree of order of DPPE in the present model as shown on **Figure 5.3av**. The increase in bulkiness of Lfcin₁₅W+ could have contributed to the promotion of the order of the acyl chains of DPPE. Furthermore, the present observations could be a result of the removal of the Arg and Met residues while adding two Trp to make Lfcin₁₅W+. Results presented in **Section 5.4.1** showed that the removal of Arg, Lfcin₁₅R-, had reduced the effect of Lfcin₁₅.

Hence, the presence of the appropriate number of Arg and Trp residues is critical in designing a peptide that would affect the thermal behaviour of DPPE. Increases in hydrophobicity alone without the presence of Arg would indeed minimize the effects of Lfcin on DPPE. Farnaud et al. (2004) also suggested that a balance of the number of tryptophan residues and positively charged amino acids are essential in the activities of CAPs. Tachi et al. (2002) reported that increasing peptide hydrophobicity may alter the leakage mechanism of magainin. Although increasing hydrophobicity generally increased the affinity of magainin peptides for zwitterionic phospholipids and erythrocytes, more hydrophobic analogues appeared to form less stable pores. Furthermore, while magainins are known to promote a positive membrane curvature, large increases in hydrophobicity

promoted the penetration of peptide chains into the lipid bilayer and expanded the hydrophobic core region. The increase in hydrophobicity imposed a negative curvature strain on the membrane, affecting pore formation rate, pore size, and pore stability (Tachi et al., 2002).

The location and distribution of the Arg and Trp residues along the peptide also play important roles in the final antimicrobial activity of the peptide. Tachi et al. (2002) suggested that the mode of action of magainin is dependent on the position of hydrophobic amino acids in the peptide sequence. Multiple regression analysis of thirteen model peptides suggested that the hydrophobic moment of the peptide chain and the positioning of the hydrophobic amino acids may be the parameters that have the most significant effect on the antimicrobial activity of lytic peptides (Pathak et al., 1995). Rearrangement of the sequence in the hydrophilic C-terminal region of melittin led to increased amphipathicity, which parallels the antimicrobial activity of the peptide (Subbalakshmi et al., 1999). Wieprecht et al. (1997) suggested that Arg residues in CAPs are responsible for the establishment of electrostatic interactions and binding affinity between the CAPs and bacterial membranes. The hydrophobic amino acids are then responsible for the interactions between the peptide chain and the lipid bilayer. This interdependence of both kinds of interactions, electrostatic and hydrophobic, for antimicrobial activity was confirmed by observations made in the present study.

5.4.3. Effects of Peptide Length on the Thermal Behaviour of Lactoferricin of Phospholipid Liposomes

As indicated by the I_{2850}/I_{2880} ratio, LfcinCore had similar effects on DPPE as those exerted by Lfcin₁₅ (**Figure 5.3v**). On the other hand, LfcinCore promoted the degree of order of the acyl chains of DPPG (**Figure 5.2v**).

Jing et al. (2003) reported that a hexapeptide Ac-RRWWRF-NH₂ had a large influence on the thermotropic phase behaviour of DPPG and had little effect on model membranes containing the zwitterionic DPPC. This behaviour is consistent with its biological activity and with its affinity to these membranes as determined by titration calorimetry, implying that peptide-lipid interactions play an important role in this process. Jing et al. (2003) suggested that the amphipathic structure may allow this peptide to penetrate deeper into the interfacial region of negatively charged membranes, leading to local membrane destabilization. However, Hunter et al. (2004) showed that fragments from human (RAWVARW-NH₂) and chicken (IVSDGNGMNAWVAWR-NH₂) lysozyme bound strongly to the interface of a bacterial membrane and did not interact with the hydrophobic acyl chains in the phospholipid bilayer. RAWVARW-NH₂ is too short to span the membrane and form channels. Hunter et al. (2004) proposed that its antimicrobial activity arises from the ability to either immediately alter the membrane characteristics and/or traverse the membrane spontaneously and act on intracellular targets.

LfcinCore is too short to span the phospholipid bilayer; hence, its action on DPPG phospholipid bilayer is limited to the region near the negatively charged head groups on the bilayer interface. This indicated that changes on the bilayer surface could affect the packing of the acyl chains in the hydrophobic core. In the present study, LfcinCore stabilized the DPPG acyl chains especially at temperatures above the transition temperature. In fact, the stabilization was so strong that the conversion of a lamellar gel phase (L_{β}) to a liquid-crystal (L_{α}) phase was not detected in the temperature range investigated (**Figure 5.2v**). Knowledge about the importance of electrostatic interactions of Arg and the role of Trp residues as a membrane interface anchor will provide insight into the future design of potent antimicrobial peptidomimetics.

5.4.4. Proposed Antimicrobial Actions

Results from the present study suggest a few key characteristics of the actions of Lfcin and its derivatives on phospholipid bilayers. In general, Lfcin and its derivatives exerted less effect on DPPC, a major phospholipid in mammalian cells, than DPPG and DPPE, major phospholipids in bacterial membranes. Results presented here are consistent with other observations reported in the literature. For example, as monitored by differential scanning calorimetry (DSC), the thermal transition behaviours of DPPC and DPPE were not affected by the addition of Lfcin at high concentration. In contrast, a broad pre-transition around 32 °C disappears when Lfcin was added to DPPG. When more Lfcin is added, the peak for the main transition also shifts to a slightly higher temperature (Vogel et al. 2002). These results show that Lfcin interacts more strongly with the overall negatively charged PG headgroup than the zwitterionic PC or PE headgroups (Liu and Deber, 1997). Fluorescence spectroscopy study of lactoferricin B and some of its shorter fragments have shown that Lfcin and its derivatives bind more tightly and penetrate somewhat deeper into vesicles containing 40% negatively charged PG headgroups (Schibli et al., 1999). This also explains why cationic antimicrobial peptides such as Lfcin typically prefer to bind to bacterial membranes rather than to those of the host.

In the present study, changes in the amino acid composition of Lfcin₁₅ had little effect on how Lfcin and its derivative affected DPPE, with the exception of Lfcin₁₅W+ (**Figure 5.3**). The replacement of Arg (Lfcin₁₅R-) and Trp (Lfcin₁₅W-) with Ala had little effect on how Lfcin₁₅ interacted with DPPE (**Figure 5.3ii and iii**). However, the addition of two Trp residues with the removal of an Arg and a Met in Lfcin₁₅W+ minimized the effects observed in other Lfcin derivatives (**Figure 5.3iv**). This indicated that the presence of both Arg and Trp is important in the action of Lfcin. Furthermore, the presence of two bulky Trp might in fact hinder the electrostatic interactions between Arg and the negatively charged phospholipid head groups on the membrane interface, weakening the anchoring of Lfcin₁₅W+ on DPPE membrane and minimizing the effect of Lfcin derivatives on DPPE.

Interactions between DPPG and Lfcin derivatives observed in the present study provided a wealth of information towards the understanding of how Lfcin interacts with DPPG. The replacement of Arg with Ala in Lfcin₁₅R- did not affect how Lfcin₁₅ interacted with DPPG (**Figure 5.2ii**). The absence of Trp, Lfcin₁₅W-, altered the thermal behaviour of DPPG and increased its degree of order throughout the temperature range investigated (**Figure 5.2iii**). On the contrary, the addition of Trp with simultaneous removal of one Arg, Lfcin₁₅W+, showed the same effects on DPPG (**Figure 5.2iv**). Acyl chains of DPPG became more ordered in the presence of LfcinCore (**Figure 5.2v**).

Removing Trp from Lfcin₁₅, Lfcin₁₅W-, stabilized the DPPG, indicating that the presence of Trp was important to destabilize the DPPG (**Figure 5.2iii**). Nevertheless, the presence of too many Trp without the appropriate support from Arg would not destabilize DPPG (**Figure 5.2iv**). This indicates that the presence of too many bulky Trp could hinder the electrostatic interactions between the cationic amino acids and the negatively charged membrane, minimizing the ability of Lfcin to disrupt DPPG. The importance of the electrostatic interaction on the surface of the phospholipid bilayer is further supported by the actions of LfcinCore (**Figure 5.2v**). Since LfcinCore is too short to span across the phospholipid bilayer, the increases in the degree of order of the DPPG acyl chains in the hydrophobic core were likely the result of the action of the LfcinCore near the negatively charged headgroups. All of these pieces of evidence show the interdependence of the electrostatic and hydrophobic groups in the interactions of Lfcin with phospholipid. The presence of both electrostatic and hydrophobic interactions is needed in the design of antimicrobial peptides.

Although the presence of both electrostatic and hydrophobic actions are essential in the disruption of the degree of order of DPPG acyl chains, it is important to understand that increasing the number of Arg and Trp alone will not lead to the creation of a more "powerful" antimicrobial peptide. For instance, the addition of Trp in Lfcin₁₅W+ indeed led to the stabilization of DPPG (**Figure 5.2iv**). On the contrary, the removal of Arg in Lfcin₁₅R- had no effect on the behaviour of Lfcin₁₅ on DPPG. In the present study, Lfcin₁₅R- was designed by replacing Arg with Ala, creating a weak cationic peptide (pI = 9.79) with strong hydrophobicity (GRAVY = 0.053) (**Table 5.1**). Results from these two Lfcin derivatives indicate that the design of an antimicrobial peptide requires a delicate balance of the number of cationic and hydrophobic amino acids in the peptide.

Other structural properties of the peptides are important to their antimicrobial functions. Results presented in **Chapter 4** indicated that the helix propensity and charge property in selected segments of Lfcin derivatives were particularly important for the prediction of their antimicrobial property against *E. coli*. HSA analysis of the Lfcin derivatives used in the present study showed that the helix propensity of Lfcin₁₅ was altered when Trp was replaced by Ala (Lfcin₁₅W-). Charge property of Lfcin₁₅ was also changed when Arg was replaced by Ala (Lfcin₁₅R-) (**Table 5.1**). These

changes might be responsible for the effects of Lfcin derivatives on model bacterial membranes observed in the present study.

Other structural properties have also been found to be important for the bioactivity of peptides. For instance, the presence of a β -fold is more essential than the number of cationic charges for protegrin-1 (Mani et al., 2005) and polyphemusin I (Powers et al., 2004). The importance of the β -hairpin fold may result from the fact that it places the hydrophobic and charged residues in these peptides in an amphipathic fashion, in order to promote the insertion of the peptides into the lipid bilayers without permeabilizing the membrane. The number of charges is a secondary factor that regulates the strength of the interaction between the anionic membrane and the cationic peptides (Mani et al., 2005).

Raman spectra of phospholipid liposomes with and without the presence of Lfcin derivatives observed in the present study indicated that Lfcin and its derivatives exerted less effect on DPPC, a major phospholipid in mammalian cells, than on DPPG and DPPE, major phospholipids in bacterial cells. Although the presence of both electrostatic and hydrophobic interactions is needed to establish interactions between cationic antimicrobial peptides and phospholipid membranes, the presence of positively charged and hydrophobic amino acids is not the only necessary characteristic in determining the actions of Lfcin and its derivatives on DPPG and DPPE. Other structural properties, such as the total number of cationic and hydrophobic amino acids, their overall location and distribution along the peptides, and secondary structures are also important in determining the overall antimicrobial properties of cationic antimicrobial peptides.

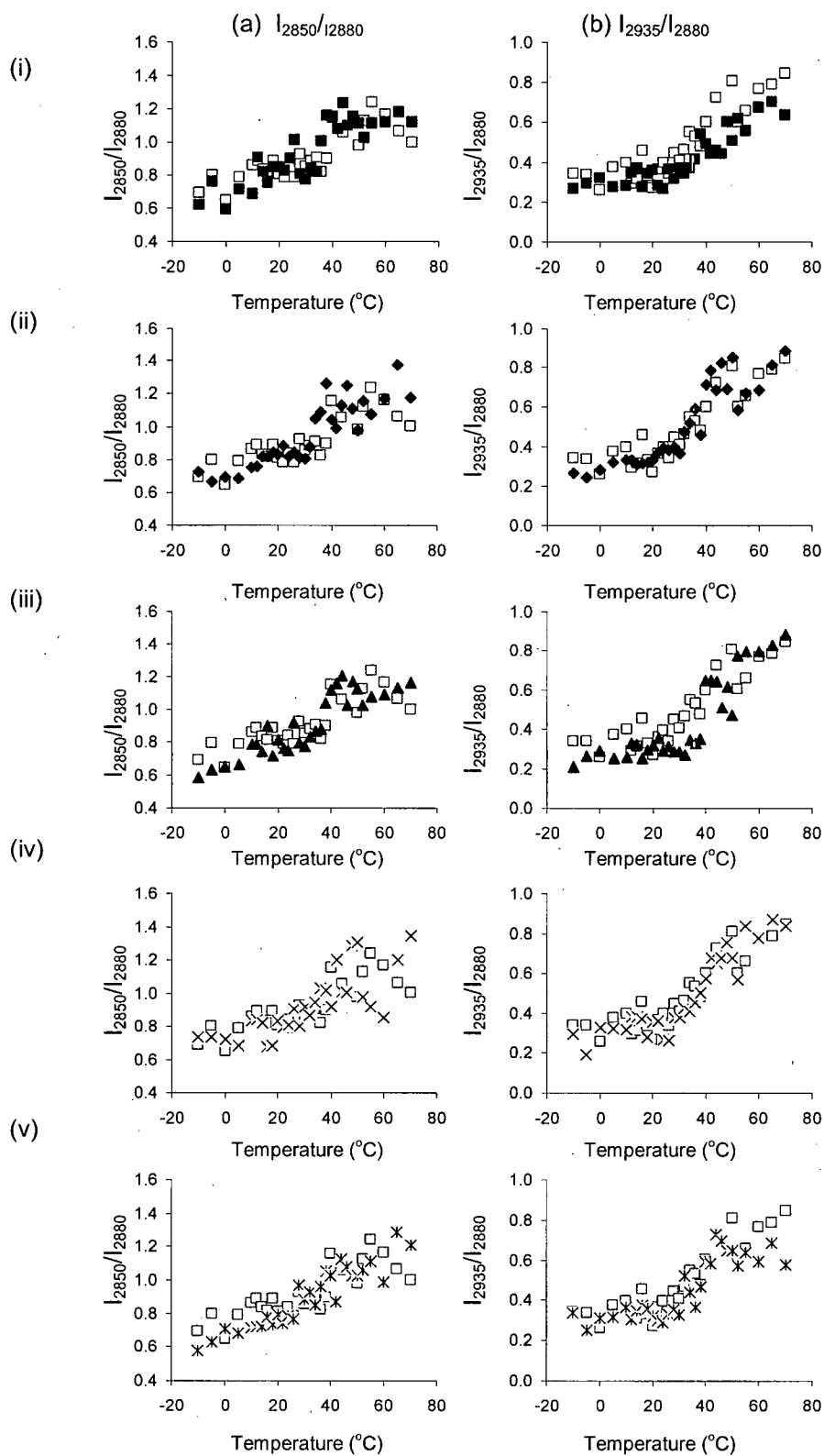


Figure 5.1. Thermal behaviours of DPPC as indicated by I_{2850}/I_{2880} (a) and I_{2935}/I_{2880} (b) in the absence of lactoferricin (Lfcin, □), the presence of Lfcin₁₅ (i, ■), Lfcin₁₅R- (ii, ◆), Lfcin₁₅W- (iii, ▲), Lfcin₁₅W+ (iv, ✕), and LfcinCore (v, *) measured between -10 °C and 70 °C by Raman spectroscopy.

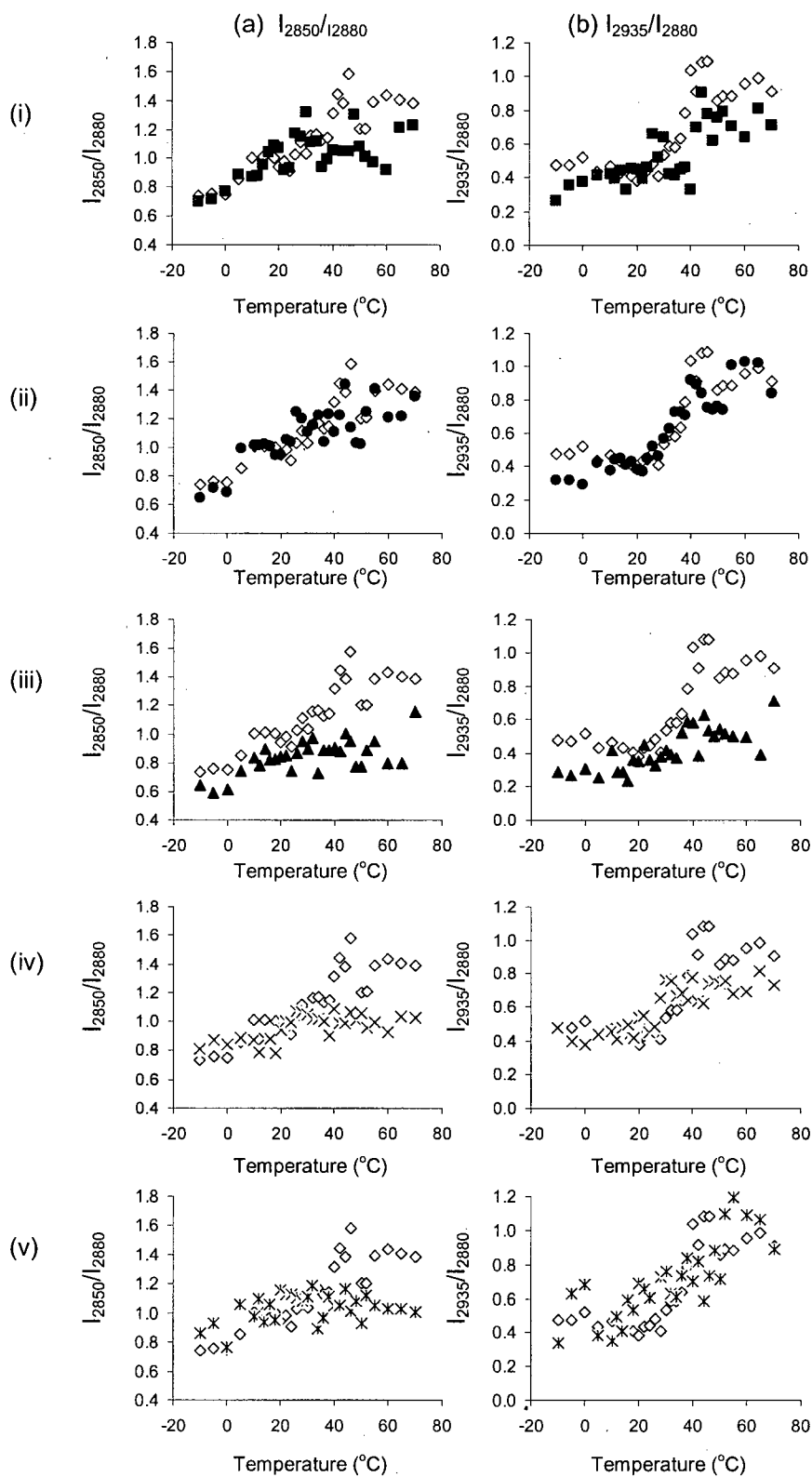


Figure 5.2. Thermal behaviours of DPPG as indicated by I_{2850}/I_{2880} (a) and I_{2935}/I_{2880} (b) in the absence of lactoferrin (Lfcin, ◇), the presence of Lfcin₁₅ (i, ■), Lfcin₁₅R- (ii, ●), Lfcin₁₅W- (iii, ▲), Lfcin₁₅W+ (iv, ✕), and LfcinCore (v, ✱) measured between -10 °C and 70 °C by Raman spectroscopy.

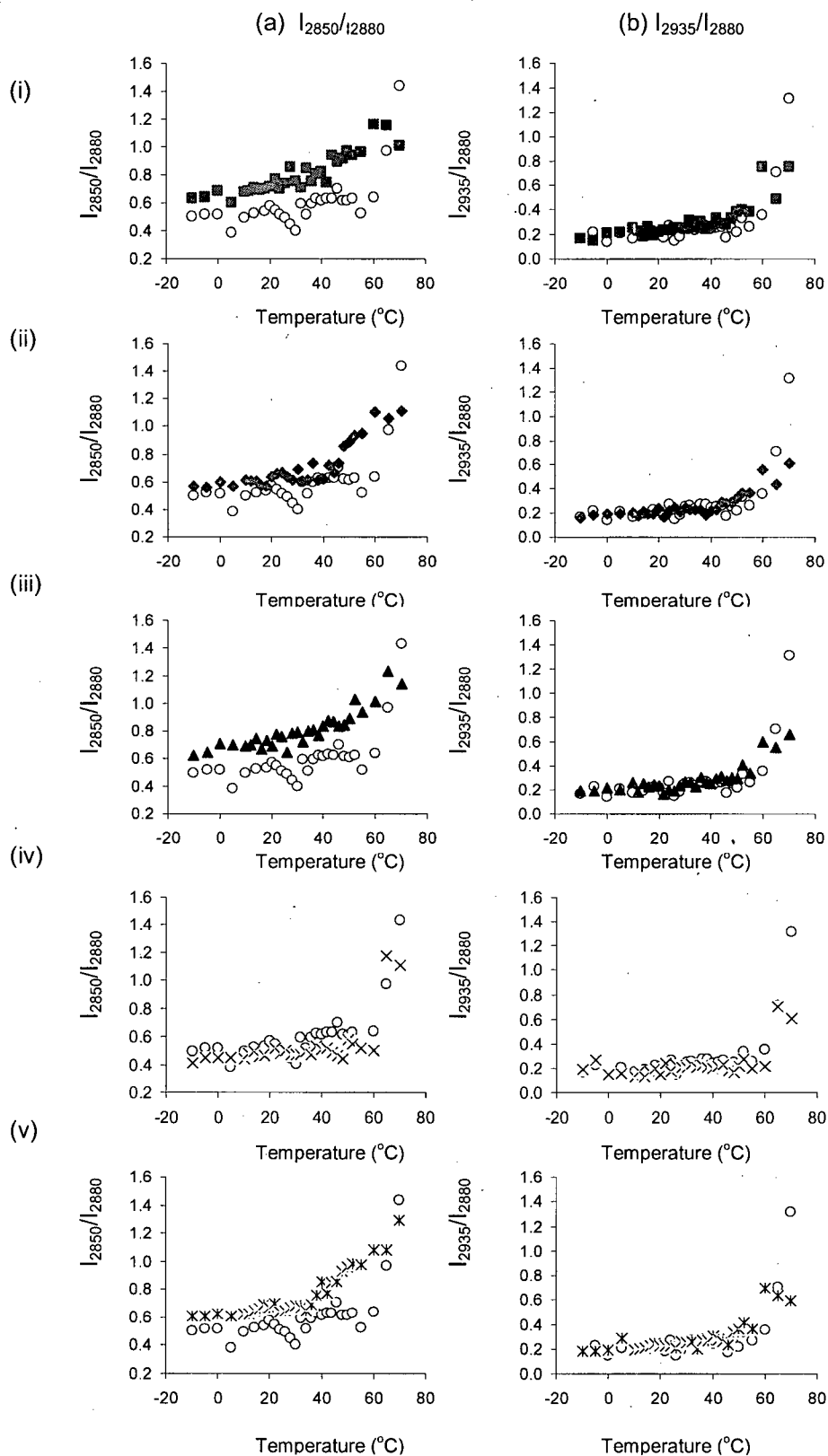


Figure 5.3. Thermal behaviours of DPPE as indicated by I_{2850}/I_{2880} (a) and I_{2935}/I_{2880} (b) in the absence of lactoferricin (Lfcin, O), the presence of Lfcin₁₅ (i, ■), Lfcin₁₅R- (ii, ◆), Lfcin₁₅W- (iii, ▲), Lfcin₁₅W+ (iv, ✕), and LfcinCore (v, *) measured between -10 °C and 70 °C by Raman spectroscopy.

Table 5.1. Structural properties of lactoferricin derivatives used in the study.

	Code	MW ¹	pI ¹	GRAVY ^{1,2}	Helix Similarity ³	Charge Similarity ³
FKCRR WQWRM KKLGA	Lfcin ₁₅	1994.46	11.74	-1.207	1.000	1.00
FKCAA WQWAM KKLGA	Lfcin ₁₅ R-	1739.13	9.79	0.053	0.883	0.00
FKCRR AQARM KKLGA	Lfcin ₁₅ W-	1764.19	11.74	-0.847	-0.948	1.00
FKCWR WQWRW KKLGA	Lfcin ₁₅ W+	2079.50	11.11	-1.153	0.463	0.73
RR WQWR	LfcinCore	987.13	12.30	-3.133		

¹ ProtParam Tool: <http://ca.expasy.org/tools/protparam.html>

² GRAVY: Grand average of hydropathicity index: positive GRAVY (hydrophobic), negative GRAVY (hydrophilic).

³ Homology Similarity Analysis: Helix and charge similarity of residues 4 to 10. Lfcin₁₅ was used as the reference peptide.

5.5. References

- Bellamy, W.; Takase, M.; Yamauchi, K.; Wakabayashi, H.; Kawase, K.; Tomita, M. Identification of the bactericidal domain of lactoferrin. *Biochim. Biophys. Acta* **1992**, *1121*, 130-136.
- Bellamy, W.; Wakabayashi, H.; Takase, M.; Kawase, K.; Shimamura, S.; Tomita, M. Killing of *Candida albicans* by lactoferricin B, a potent antimicrobial peptide derived from the N-terminal region of bovine lactoferrin. *Med. Microbiol. Immunol.* **1993**, *182*, 97-105.
- Blondelle, S. E.; Houghten, R. A. Design of model amphipathic peptides having potent antimicrobial activities. *Biochemistry* **1992**, *31*, 12688-12694.
- Blondelle, S. E.; Takahashi, E.; Dinh, K. T.; Houghten, R.A. The antimicrobial activity of hexapeptides derived from synthetic combinatorial libraries. *J. Appl. Bacteriol.* **1995**, *78*, 39-46.
- Blondelle, S. E.; Houghten, R. A. Novel antimicrobial compounds identified using synthetic combinatorial library technology. *Trends Biotechnol.* **1996**, *14*, 60-65.
- Blondelle, S. E.; Lohner, K. Combinatorial libraries: A tool to design antimicrobial and antifungal peptide analogues having lytic specificities for structure-activity relationship studies. *Pept. Sci.* **2000**, *55*, 74-87.
- Devlin, M. T.; Levin, I. W. Raman spectroscopic studies of the packing properties of mixed dihexadecyl- and dipalmitoylphosphatidylcholine bilayer dispersion. *Biochemistry* **1989**, *28*, 8912-8920.
- Farnaud, S.; Spiller, C.; Moriarty, L. C.; Patel, A.; Gant, V.; Odell, E. W.; Evans, R. W. Interactions of lactoferricin-derived peptides with LPS and antimicrobial activity. *FEMS Microbiol. Lett.* **2004**, *233*, 193-199.
- Hallock, K. J.; Lee, D. K.; Omnaas, J.; Mosberg, H. I.; Ramamoorthy, A. Membrane composition determines pardaxin's mechanism of lipid bilayer disruption. *Biophys. J.* **2002**, *83*, 1004-1013.
- Haug, B. E.; Svendsen, J. S. The role of tryptophan in the antibacterial activity of a 15-residue bovine lactoferricin peptide. *J. Pept. Sci.* **2001**, *7*, 190-196.
- Huang, C.-H.; Lapidus, J. R.; Levin, I. W. Phase-transition behaviour of saturated, symmetric chain phospholipid bilayer dispersions determined by Raman spectroscopy: Correlation between spectral and thermodynamic parameters. *J. Am. Chem. Soc.* **1982**, *104*, 5926-5930.
- Hunter, H. N.; Jing, W.; Schibli, D. J.; Trinh, T.; Park, I. Y.; Kim, S. C.; Vogel, H. J. The interactions of antimicrobial peptides derived from lysozyme with model membrane systems. *Biochim. Biophys. Acta* **2004**, *1688*, 175-189.
- Jing, W.; Hunter, H. N.; Hagel, J.; Vogel, H. J. The structure of the antimicrobial peptide Ac-RRWRF-NH₂ bound to micelles and its interactions with phospholipid bilayers. *J. Pept. Res.* **2003**, *61*, 219.
- Kang, J. H.; Lee, M. K.; Kim, K. L.; Hahm, K.-S. Structure-biological activity relationships of 11-residue highly basic peptide segment of bovine lactoferrin. *Int. J. Pept. Protein Res.* **1996**, *48*, 357-363.

- Kiyota, T.; Lee, S.; Sugihara, G. Design and synthesis of amphiphilic α -helical model peptides with systematically varied hydrophobic-hydrophilic balance and their interaction with lipid- and bio-membranes. *Biochemistry* **1996**, *35*, 13196-13204.
- Kyte, J.; Doolittle, R. F. A simple method for displaying the hydropathic character of a protein. *J. Mol. Biol.* **1982**, *157*, 105-32.
- Ladokhin, A. S.; White, S. H. 'Detergent-like' permeabilization of anionic lipid vesicles by melittin. *Biochim. Biophys. Acta* **2001**, *1514*, 253-260.
- Laroche, G.; Carrier, D.; Pézolet, M. Study of the effect of poly(L-lysine) on phosphatidic acid and phosphatidylcholine/phosphatidic acid bilayers by Raman spectroscopy. *Biochemistry* **1988**, *27*, 6220-6228.
- Laroche, G.; Dufourc, E. J.; Pezolet, M.; Dufourcq, J. Coupled changes between lipid order and polypeptide conformation at the membrane surface. A 2H NMR and Raman study of polylysine-phosphatidic acid systems. *Biochemistry* **1990**, *29*, 6460-6465.
- Lejon, T.; Strøm, M. B.; Svendsen, J. S. Is information about peptide sequence necessary in multivariate analysis? *Chemometrics Intelligent Lab. Sys.* **2001**, *57*, 93-95.
- Liu, L. P.; Deber, C. M. Anionic phospholipids modulate peptide insertion into membranes. *Biochemistry* **1997**, *36*, 5476-5482.
- Mangoni, M. L.; Rinaldi, A. C.; Di Giulio, A.; Mignogna, G.; Bozzi, A.; Barra, D.; Simmaco, M. Structure-function relationships of temporins, small antimicrobial peptides from amphibian skin. *Eur. J. Biochem.* **2000**, *267*, 1447-1454.
- Mani, R.; Waring, A. J.; Lehrer, R. I.; Hong, M. Membrane-disruptive abilities of β -hairpin antimicrobial peptides correlate with conformation and activity: A 31P and 1H NMR study. *Biochim. Biophys. Acta* **2005**, *1717*, 11-18.
- Matsuzaki, K.; Nakamura, A.; Murase, O.; Sugishita, K.-I.; Fujii, N.; Miyajima, K. Modulation of magainin 2-lipid bilayer interactions by peptide charge. *Biochemistry* **1997**, *36*, 2104-2111.
- Opekarová, M.; Tanner, W. Specific lipid requirements of membrane proteins—a putative bottleneck in heterologous expression. *Biochim. Biophys. Acta* **2003**, *1610*, 11-22.
- Papo, N.; Shai, Y. Exploring peptide membrane interaction using surface plasmon resonance: differentiation between pore formation versus membrane disruption by lytic peptides. *Biochemistry* **2003**, *42*, 458-466.
- Pathak, N.; Salas-Auvert, R.; Ruche, G.; Janna, M. H.; McCarthy, D.; Harrison, R. G. Comparison of the effects of hydrophobicity, amphiphilicity, and alpha-helicity on the activities of antimicrobial peptides. *Proteins* **1995**, *22*, 182-186.
- Powers, J.-P. S.; Rozek, A.; Hancock, R. E. W. Structure-activity relationships for the β -hairpin cationic antimicrobial peptide polyphemusin I. *Biochim. Biophys. Acta* **2004**, *1698*, 239-250.
- Rekdal, Ø.; Andersen, J.; Vorland, L. H.; Svendsen, J. S. Construction and synthesis of lactoferricin derivatives with enhanced antibacterial activity. *J. Pept. Sci.* **1999**, *5*, 32-45.
- Rinaldi, A. C.; Mangoni, M. L.; Rufo, A.; Luzi, C.; Barra, D.; Zhao, H.; Kinnunen, P. K.; Bozzi, A.; Di Giulio, A.; Simmaco, M. Temporin L: antimicrobial, haemolytic and cytotoxic activities, and effects on membrane permeabilization in lipid vesicles. *Biochem. J.* **2002**, *368*, 91-100.

- Schibli, D. J.; Hwang, P. M.; Vogel, H. J. The structure of the antimicrobial active center of lactoferricin B bound to sodium dodecyl sulfate micelles. *FEBS Lett.* **1999**, *446*, 213-217.
- Sørensen, M.; Sørensen, S. P. L. The proteins in whey. *Compt. Rend. Lab. Carlsberg* **1939**, *23*, 55-99.
- Strøm, M. B.; Rekal, Ø.; Svendsen, J. S. Antibacterial activity of 15-residue lactoferricin derivatives. *J. Pept. Res.* **2000**, *56*, 265-274.
- Strøm, M. B.; Rekdal, Ø.; Stensen, W.; Svendsen, J. S. Increased antibacterial activity of 15-residue murine lactoferricin derivatives. *J. Pept. Res.* **2001**, *57*, 127-139.
- Subbalakshmi, C.; Nagaraj, R.; Sitaram, N. Biological activities of C-terminal 15-residue synthetic fragment of melittin: design of an analog with improved antibacterial activity. *FEBS Lett.* **1999**, *448*, 62-66.
- Tachi, T.; Epand, R. F.; Epand, R. M.; Matsuzaki, K. Position-dependent hydrophobicity of the antimicrobial magainin peptide affects the mode of peptide-lipid interactions and selective toxicity. *Biochemistry* **2002**, *41*, 10723-10731.
- Tomita, M.; Takase, M.; Bellamy, W.; Shimamura, S. A review: The active peptide of lactoferrin. *Acta Paediatr. Jpn.* **1994**, *36*, 585-591.
- Vogel, H. J.; Schibli, D. J.; Jing, W.; Lohmeier-Vogel, E. M.; Epand, R. F.; Epand, R. M. Towards a structure-function analysis of bovine lactoferricin and related tryptophan- and arginine-containing peptides. *Biochem. Cell Biol.* **2002**, *80*, 49-63.
- Wieprecht, T.; Dathe, M.; Beyermann, M.; Krause, E.; Maloy, W. L.; MacDonald, D. L.; Bienert, M. Peptide hydrophobicity controls the activity and selectivity of magainin 2 amide in interaction with membranes. *Biochemistry* **1997**, *36*, 6124-6132.

CHAPTER 6. CONCLUSION

6.1. Review of Results as Related to Working Hypotheses

The fractionation procedure described in Chapter 2 resulted in the production of two peptides with masses of 3196 and 3124 Da from peptic digest of food-grade lactoferrin, which corresponded to the 26- and 25-amino acid peptides, lactoferricin (Lfcin), FKCRWQWRM KKLGA PSITC VRRAF (A). An industrial grade cation exchange resin with stepwise salt gradient elution was used in the procedure. A fraction eluted using 2.0 M NaCl contained predominantly two peptides containing the Lfcin sequence. Based on the competitive displacement concept, a 2-step process using industrial grade cation exchange resin led to 35% recovery of Lfcin and also produced other cationic peptides. Putative sequences of cationic peptides in other eluted fractions included FKNKS RSFQ, WRMKK LGAPS ITCVR RA, and GAPSI TCVRR AFALE CIRAI AEKKA. Iron saturation level of LF had no effect on the production of Lfcin. Nevertheless, the digestion of LF containing lower iron content led to the production of a higher quantity of low molecular weight cationic peptides.

Homology sequence analysis (HSA) was performed on Lfcin and 71 Lfcin derivatives followed by multivariate data analysis using techniques including principal component similarity and artificial neural network to examine structure-function relationship of Lfcin and its derivatives. Results presented in Chapter 3 showed that helical property of position 4 to 9 in the Lfcin sequence was the most important in determining the antimicrobial activity of Lfcin against *E. coli*, followed by cationic charge property at positions 4 to 9 and 1 to 3.

Raman spectra presented in Chapter 4 showed that the effects of Lfcin on phospholipid liposomes depend on the saturation of the acyl chain and the properties of the head groups. Lfcin had little effect on POPC and POPE, i.e., phospholipids with unsaturated acyl chains and zwitterion head groups. On the contrary, Lfcin lowered the lateral chain-chain interaction along the acyl chains of POPG with negatively charged head groups. The presence of Lfcin in DPPC liposomes restricted the lateral chain-chain interaction along the acyl chain throughout the temperature range examined, and shifted the main transition temperature from 38 °C (in the absence of Lfcin) to 40 °C. Lfcin had little effect on DPPG liposomes at temperatures below the transition temperature, but increased the order of the acyl chain terminal methyl group in the hydrophobic core of the phospholipid bilayer at temperatures above the transition temperature (~ 40 °C). In contrast, mobility of the acyl chains in DPPE was increased in the presence of Lfcin at temperatures below 32 °C.

Based on results obtained in Chapters 3 and 4 and data reported in the literature (Farnaud et al., 2004; Strøm et al., 2000 and 2001), synthetic Lfcin 15-mer derivatives with special features were designed for investigation of their interactions with phospholipid liposomes. Results in Chapter 5

indicated that the removal of cationic R residues from Lfcin₁₅ led to a peptide with low charge homology similarity and decreased its effects on negatively charged DPPG, a phospholipid that makes up 20 to 25 % of the phospholipids in *E. coli*. This is in agreement with results reported in Chapter 3 that the charge properties in positions 1 to 3 and 4 to 9 were important in determining Lfcin derivatives' antimicrobial activity against *E. coli*. The removal of hydrophobic Trp residues from Lfcin₁₅ increased the degree of order of DPPG. This indicated that the presence of Trp in Lfcin₁₅ was needed for the disruption of DPPG. Moreover, as determined by HSA, replacing Trp by Ala in Lfcin₁₅ caused a major change in the helix propensity of the peptide. Changes in the helical structure of Lfcin derivatives may have affected how Lfcin affected DPPG liposomes. DPPE, a highly ordered phospholipid, was disturbed in the presence of Lfcin and its derivatives. Nevertheless, the addition of Trp and removal of Arg from Lfcin₁₅ minimized the effects of Lfcin₁₅ on the thermal behaviours of DPPE.

6.2. Strengths and Significance of Results to the Field of Study

Lactoferricin is a peptide with antimicrobial activity against a wide range of microorganisms. It is also one of the very few antimicrobial peptides originating from a human food source (Chan and Li-Chan, 2006). The fractionation strategy presented in Chapter 2 can be easily adapted for the large-scale production of Lfcin, hence facilitating the usage of Lfcin for human health.

Homology similarity analysis and principal component similarity analysis in conjunction with artificial neural network provided an effective strategy to predict the antimicrobial activity of peptides of interest. This approach allows for a rapid screening of bioactive peptides without the expensive costs associated with conducting bioassays.

Results from Chapters 4 and 5 of this thesis demonstrated the effects of Lfcin and its derivatives on model phospholipid liposomes and allowed further understanding of the interaction between antimicrobial peptides and phospholipid membranes. Although Lfcin has been the subject of intense research in the last two decades, very few studies have been conducted to elucidate the molecular mechanism of Lfcin on its targeted microorganisms. The use of Raman spectroscopy provides an insight on how Lfcin may interact with phospholipid bilayers during its entry to bacterial cell. Such understanding could facilitate the design of Lfcin derivatives or other CAPs that exhibit effective antimicrobial action, without the undesirable interactions with mammalian membranes that can lead to hemolysis (Kang et al., 1996).

6.3. Recommendations for Future Studies

To further expand the potential applications of food-grade bovine lactoferrin, it is recommended that a more detailed analysis of the peptides produced during peptic digestion is

needed. Since the identification of Lfcin as an antimicrobial peptide by Tomita and colleagues in 1991 (Tomita et al., 1991), Lfcin has been the centre of research attention in the past decade. Numerous studies have been conducted to examine its bioactivity (e.g. Gifford et al., 2005 and Mader et al., 2005). Results presented in Chapter 2 indicated that many cationic peptides were produced during the purification of Lfcin. It is highly possible that some of these peptides would carry health promoting properties. A systematic procedure should be developed to screen for their bioactivities and allow for the production of additional value-added products from food-grade bovine lactoferrin.

Results from the present study showed that Lfcin, an amphipathic cationic peptide, was particularly effective against PG, an anionic phospholipid. A better understanding of the mutual dependence of these parameters will help to elucidate the molecular mechanism of membrane damage by antimicrobial peptides and their target membrane specificity. Future studies should also include the use of liposomes composed of phospholipids extracted from bacteria of interest. Such studies would allow direct comparison of results from bioassays and those from spectroscopic studies and facilitate the understanding of peptide-phospholipid interactions. Interactions between phospholipids of epithelial cells along the digestive tract and Lfcin should be investigated to understand how Lfcin affect the protective properties of phospholipids in human body. Raman spectroscopic analysis of phospholipids also facilitated the development of using liposomes as a delivering medium for antimicrobial peptides, an essential key for the rational design of novel peptide antibiotics.

6.4. References

- Chan, J. C. K.; Li-Chan, E. C. Y. Antimicrobial Peptides. In *Nutraceutical Proteins and Peptides in Health and Disease*. (Eds. Y. Mine and F. Shahidi.) **2006**. Boca Raton: CRC/Taylor and Francis, pp. 99-136.
- Farnaud, S.; Spiller, C.; Moriarty, L. C.; Patel, A.; Gant, V.; Odell, E. W.; Evans, R. W. Interactions of lactoferricin-derived peptides with LPS and antimicrobial activity. *FEMS Microbiol. Lett.* **2004**, 233, 193-199.
- Gifford, J. L.; Hunter, H. N.; Vogel, H. J. Lactoferricin: a lactoferrin-derived peptide with antimicrobial, antiviral, antitumor and immunological properties. *Cell Mol. Life Sci.* **2005**, 62, 2588-2598.
- Kang, J. H.; Lee, M. K.; Kim, K. L.; Hahm, K.-S. Structure-biological activity relationships of 11-residue highly basic peptide segment of bovine lactoferrin. *Int. J. Pept. Protein Res.* **1996**, 48, 357-363.
- Mader, J. S.; Salsman, J.; Conrad, D. M.; Hoskin, D. W. Bovine lactoferricin selectively induces apoptosis in human leukemia and carcinoma cell lines. *Mol. Cancer Ther.* **2005**, 4, 612-624.
- Strøm, M. B.; Rekal, Ø.; Svendsen, J. S. Antibacterial activity of 15-residue lactoferricin derivatives. *J. Pept. Res.* **2000**, 56, 265-274.
- Strøm, M. B.; Rekdal, Ø.; Stensen, W.; Svendsen, J. S. Increased antibacterial activity of 15-residue murine lactoferricin derivatives. *J. Pept. Res.* **2001**, 57, 127-139.
- Tomita, M.; Bellamy, W.; Takase, M.; Yamauchi, K.; Wakabayashi, H.; Kawase, K. Potent antibacterial peptides generated by pepsin digestion of bovine lactoferrin. *J. Dairy Sci.* **1991**, 74, 4137-4142.